



**COLOUR IMAGE SEGMENTATION USING PERCEPTUAL COLOUR
DIFFERENCE SALIENCY ALGORITHM**

By

TAIWO, TUNMIKE BUKOLA

(21557473)

Submitted in fulfilment of the requirements of the
MASTERS DEGREE IN INFORMATION AND COMMUNICATION TECHNOLOGY
in the
DEPARTMENT OF INFORMATION TECHNOLOGY
in the
FACULTY OF ACCOUNTING AND INFORMATICS
at
DURBAN UNIVERSITY OF TECHNOLOGY

July 2017

DECLARATION

I, Taiwo, Tunmike Bukola hereby declares that this dissertation is my own work and has not been previously submitted in any form to any other university or institution of higher learning by other persons or myself. I further declare that all the sources of information used in this dissertation have been acknowledged.

Taiwo, Tunmike Bukola

Date

Approved for final submission

Supervisor: _____

Professor O. O. Olugbara

PhD (Computer Science)

Date

Co-Supervisor: _____

Dr. Delene Heukelman

DTech (Information Technology)

Date

DEDICATION

This dissertation is dedicated to my family for their support, encouragement and motivation throughout the period of this study.

ACKNOWLEDGEMENTS

First and foremost, my profound appreciation goes to the Almighty Jehovah, the giver of life and wisdom, for His limitless love, inspiration and strength throughout the period of this study. I return to Him all the glory, honour and adoration.

I am particularly grateful to my supervisor, Prof. Oludayo Olugbara. A humble genius in image processing research field, his mentorship on both professional and personal levels was tremendous. Since the beginning of this study, he has always been there not only as my supervisor, but a father and guardian. I wouldn't be writing this today if I had a different supervisor. I really appreciate all the valuable time he spent in helping me with programming and new concepts with reference to my research work. I was fortunate to work with such a kind and encouraging professor over the years.

I would also like to sincerely thank my co-supervisor, Dr. Delene Heukelman for her constructive and thoughtful suggestions. Your advice and direction was invaluable and you always made time to read through my work.

I would also like to express my gratitude to Mrs. O. S. Olugbara for the role she played throughout the journey.

I would like to thank all friends in and out of the ICT and Society Research group, who made any sort of support and motivation into this dissertation.

The support from Postgraduate Research and Support, Durban University of Technology in offering me scholarship to pursue this degree is gratefully acknowledged.

Last, but definitely not the least, I wish to express my deepest gratitude, love and affection to my family. They deserve a special mention for their love, support, prayers, encouragement, motivation and dedication to make this degree a success. I appreciate you all.

TABLE OF CONTENTS

DECLARATION	ii
DEDICATION	iii
ACKNOWLEDGEMENTS	iv
TABLE OF CONTENTS.....	v
LIST OF FIGURES	viii
LIST OF TABLES.....	x
Abstract.....	xi
CHAPTER ONE.....	1
INTRODUCTION	1
1.1 Research problem statement	4
1.2 Research question	4
1.3 Research Aim and Objectives	5
1.4 Research Methodology	5
1.5 Research Contributions.....	6
1.6 Dissertation Synopsis.....	7
Chapter TWO.....	8
LITERATURE REVIEW	8
2.1 Image Segmentation.....	8
2.1.1 Region based Image Segmentation Methods	9
2.1.3 Pixel based Image Segmentation methods.....	10
2.2 Histogram thresholding algorithms.....	11
2.2.1 Otsu thresholding algorithm.....	13
2.2.2 Multilevel Thresholding algorithms.....	13
2.2.3 Nature Inspired Optimization Algorithms	16
2.3 Cluster Analysis	18
2.3.1 K-means clustering algorithm.....	20
2.3.2 Fuzzy C-means Algorithm	22
2.4 Improvements of clustering algorithms	23
2.4.1 Improved Variants of K-means algorithm	24
2.4.2 Improved Variants of the Fuzzy C-means Algorithm.....	28
2.5 Colour Image Segmentation Methods.....	34
2.5.2 Colour Based Saliency Segmentation Methods	35
2.5.3 Image Segmentation Based on Different Colour Models	42

2.6 Image Segmentation Performance Evaluation	49
2.6.1 Benchmark Data sets.....	49
2.6.2 Image segmentation Evaluation Methods	50
2.7 Chapter summary	53
CHAPTER THREE	54
METHODOLOGY OF THE STUDY	54
3.1 Image Datasets Acquisition	54
3.1.2 ISBI 2016 Challenge Dataset.....	55
3.1.3 Pedro Hispano Hospital Dataset	57
3.1.4 Microsoft Research Asia Dataset.....	59
3.1.5 Extended Complex Scene Saliency Dataset.....	60
3.2.1 Colour Image Transformation.....	61
3.2.2 Luminance Image enhancement.....	63
3.2.3 Salient Pixel Computation	64
3.2.4 Image Artefact filtering.....	69
3.3 Algorithmic Implementation of the PCDS Algorithm.....	70
3.4 Chapter Summary	71
CHAPTER FOUR.....	71
EVALUATION EXPERIMENTS, RESULTS AND INTERPRETATIONS	72
4.1 Analysis of Performance Evaluation.....	72
4.1.1 Comparison with State-of-the-art Saliency and Non-Saliency Segmentation Algorithms	73
4.2 Qualitative Analysis of Experimental Results	73
4.2.1 Qualitative Analysis of Saliency Results with Images from ISBI 2016 Challenge Dataset	73
4.2.2 Comparison of Non-Saliency Results with Images from ISBI 2016 Challenge dataset without Image Artefact Filtering.....	76
4.2.3 Comparison of Saliency Results with Images from PH2 Dataset.....	80
4.2.4 Comparison of Non-Saliency Segmentation Results with Images from PH2 dataset without Image Artefact Filtering.....	82
4.2.5 Qualitative Analysis of Saliency Results on MSRA Dataset.....	84
4.2.6 Qualitative Analysis of Non-Saliency Results on MSRA Dataset without Image Artefact Filtering.....	89
4.2.7 Qualitative Analysis of Saliency Results on ECSSD.....	92
4.2.8 Qualitative Analysis of Non-Saliency Results With Images on ECSSD without Image Artefact Filtering.....	95
4.3 Quantitative Analysis of Binary Segmentation Results	98

4.3.1 Evaluation Metrics	100
4.3.1.1 Precision.....	100
4.3.1.2 F-measure.....	100
4.3.1.3 Error Rate.....	101
4.3.1.4 Dice	101
4.3.2 Quantitative Analysis of Precision Scores	101
4.3.3 Quantitative Analysis of F-measure Scores	104
4.3.4 Quantitative Analysis of Error Scores	106
4.3.5 Quantitative Analysis of Dice Scores	109
4.4 Chapter conclusion.....	111
CHAPTER 5	112
DISCUSSION AND CONCLUSIONS	112
5.1 Summary	112
5.2 Future Work.....	114
5.3 Conclusion	115
References.....	116

LIST OF FIGURES

Figure 2.1: Image segmentation evaluation methods (Zhang, Fritts and Goldman 2008; Zuva et al. 2011).....	52
Figure 3.1 Melanoma skin lesion images selected from the ISBI 2016 challenge dataset	57
Figure 3.2 Melanoma skin lesion images selected from the PH2 dataset	58
Fig 3.3 Natural images selected from the MSRA dataset.....	60
Fig 3.4 Natural images selected from ECSSD	61
Figure 3.5: Enhancement of luminance channel using the adaptive gamma correction. (a) Original image, (b) ground truth, (c) enhanced saliency segmentation using exponential gamma function, (d) enhanced saliency segmentation using the product of logarithmic and exponential gamma functions.	64
Fig. 3.5 Selection of background and object pixels. (a) input image, (b) ellipsoidal patch in yellow font contains background pixels and portion of object pixels in red font are covered by the rectangular patch, (c) input image, (d) ellipsoidal patch in yellow font contains background pixels and portion of object pixels in red font are fully covered by the rectangular patch.....	65
Fig 4.1: Qualitative illustration of saliency segmentation results obtained using four benchmark saliency segmentation algorithms and PCDS segmentation algorithm on the melanoma skin lesion images from ISBI 2016 challenge dataset.	76
Fig 4.2: Qualitative illustration of binary segmentation results obtained using four state-of-the-art non-saliency image segmentation algorithms and the PCDS segmentation algorithm on melanoma skin lesion images from the ISBI challenge dataset.....	80
Fig 4.3: Qualitative illustration of saliency segmentation results obtained using four benchmark salient segmentation algorithms and PCDS segmentation algorithm on PH2 dataset	82
Fig 4.4: Qualitative illustration of binary segmentation results obtained using four state-of-the-art non-saliency image segmentation algorithms and the PCDS segmentation algorithm on PH2 dataset.	84
Fig 4.5: Qualitative illustration of saliency segmentation results obtained using four saliency segmentation algorithms and PCDS segmentation algorithm on MSRA dataset.	87
Fig 4.6: Qualitative illustration of binary segmentation results obtained using four state-of-the-art image segmentation algorithms and our default thresholding technique on MSRA dataset.....	92

Fig 4.7: Qualitative illustration of saliency segmentation results obtained using four benchmark salient object segmentation algorithm and the proposed PCDS segmentation algorithm on ECSSD.94

Fig 4.8: Qualitative illustration of binary segmentation results obtained using four state-of-the-art non-saliency image segmentation algorithms and PCDS segmentation algorithm on ECSSD.98

LIST OF TABLES

Table 2.1 Nature inspired metaheuristic algorithm for multilevel image segmentation (Prakasam and Savarimuthu 2016).	17
Table 2.2 Summary of pixel based image segmentation algorithms.	32
Table 2.3 Summary of Colour Image Segmentation Methods Based on Different Colour Models.	46
Table 4.1: Precision scores of saliency and non-saliency image segmentation algorithms on ISBI 2016, PH2, MSRA and ECSS data sets.	103
Table 4.2: F-measure scores of saliency and non-saliency image segmentation algorithms on ISBI 2016 challenge, PH2, MSRA and ECSS data sets	106
Table 4.3: Error scores of saliency and non-saliency image segmentation algorithms on ISBI 2016 challenge, PH2, MSRA and ECSS data sets.....	109
Table 4.4: Dice scores of saliency and non-saliency image segmentation algorithms on ISBI 2016 challenge, PH2, MSRA and ECSS data sets.....	111

Abstract

The topic of colour image segmentation has been and still is a hot issue in areas such as computer vision and image processing because of its wide range of practical applications. The urge has led to the development of numerous colour image segmentation algorithms to extract salient objects from colour images. However, because of the diverse imaging conditions in varying application domains, accuracy and robustness of several state-of-the-art colour image segmentation algorithms still leave room for further improvement. This dissertation reports on the development of a new image segmentation algorithm based on perceptual colour difference saliency along with binary morphological operations. The algorithm consists of four essential processing stages which are colour image transformation, luminance image enhancement, salient pixel computation and image artefact filtering. The input RGB colour image is first transformed into the CIE L*a*b colour image to achieve perceptual saliency and obtain the best possible calibration of the transformation model. The luminance channel of the transformed colour image is then enhanced using an adaptive gamma correction function to alleviate the adverse effects of illumination variation, low contrast and improve the image quality significantly. The salient objects in the input colour image are then determined by calculating saliency at each pixel in order to preserve spatial information. The computed saliency map is then filtered using the morphological operations to eliminate undesired factors that are likely present in the colour image.

A series of experiments was performed to evaluate the effectiveness of the new perceptual colour difference saliency algorithm for colour image segmentation. This was accomplished by testing the algorithm on a large set of a hundred and ninety images acquired from four distinct publicly available benchmarks corpora. The accuracy of the developed colour image segmentation algorithm was quantified using four widely used statistical evaluation metrics in terms of precision, F-measure, error and Dice. Promising results were obtained despite the fact that the experimental images were selected from four different corpora and in varying imaging conditions. The results have indeed demonstrated that the performance of the newly developed colour image segmentation algorithm is consistent with an improved performance compared to a number of other saliency and non-saliency state-of-the-art image segmentation algorithms.

CHAPTER ONE

INTRODUCTION

The automatic image segmentation which is also known as automatic image detection is an important step in image processing to extract useful information from images without human assistance. It is the process of partitioning an image into homogenous and disjoint sets sharing similar properties into regions. The goal of image segmentation is to simplify an image for meaningful analysis and interpretation. For several decades, researchers have devoted enormous time to develop diverse segmentation algorithms to segment greyscale images - that is images with intensity values ranging from 0 to 255 inclusive because for many years digital cameras were not widely available to capture colour images. However, in reality colour is an important cue of the natural world and it has been acknowledged that the human eye has the capacity to discern thousands of colour shades, but only two shades of grey. Therefore, in addition to the intensity of an image, colour is an intrinsic property of an image that are generally believed to convey more useful information than greyscale images to enhance the image analysis process.

The human perception of colour is a combination of tristimuli red (R), green (G) and blue (B) referred to as primary colours. The RGB colour model is one of the most widely used in colour image acquisition, storage and display. Moreover, as time goes on, other colour models have been generated based on the RGB colour model by performing either linear or nonlinear colour transformations. The purpose of a colour model is to facilitate the specifications of colour in a standardized way. Therefore, a colour model is an abstract mathematical representation that describes the way colours are being represented as tuples by numbers. Colour image segmentation partitions image pixels that possess distinct colour features in an input image into homogeneous regions in such a way that each cluster defines a class of image pixels with similar colour properties.

For several decades, researchers proposed that one of the easiest approaches to process colour images is to extend existing greyscale image segmentation algorithms to segment colour images. Subsequently, colour image segmentation approaches are as a result of extending several existing well developed image segmentation algorithms for greyscale images to colour images based on different colour models. The algorithms are applied to each component of the colour models and results are merged to obtain a final segmentation result.

However, processing colour images are more complex than greyscale images. This is because for colour images with RGB colour representation, the colour of a pixel is a mixture of three primitive colours which are red, green and blue instead of the single intensity value of a pixel in a greyscale image. The computational complexity caused by a processing colour images, complex background, varying views and illuminations are amongst the factors that make colour image segmentation more difficult. Nonetheless, as improvement in computers with more processing power and speed continue to increase, it has become a lot easier to deal with the great amount of size and information in colour images. As a result of this, there has been a shift in current image processing research from processing greyscale images to colour images in recent years to segment colour images as the demand continues to increase.

Colour image segmentation has attracted a lot of attention of researchers and has become an active research field in diverse application domains, but not limited to:

1. Face detection and recognition (Chaves-González *et al.*, 2010, Uçar 2014).
2. Fingerprint recognition system (Baek 2016, Wang *et al.*, 2016).
3. Fire detection in video sequences (Celik *et al.*, 2007; Celik and Demirel 2009).
4. Geographical imaging (Campos *et al.*, 2010; Kamruzzaman *et al.*, 2016).
5. Irrigation management (Paraskevopoulos and Singels 2014; García-Mateos *et al.*, 2015).
6. Lung cancer classification (Taher *et al.*, 2013; Adetiba and Olugbara, 2015a; Adetiba and Olugbara, 2015b).
7. Product image based recommendation assistant technology (Olugbara, *et al.* 2010; Olugbara and Ndlovu, 2014; Oyewole *et al.*, 2015).
8. Magnetic resonance imaging (MRI) (De and Bhattacharyya 2016; Kather *et al.*, 2017).
9. Object classification and recognition (Bu *et al.*, 2016).
10. Pest monitoring and detection (Bodhe and Mukherji 2013; Omrani *et al.*, 2014).
11. Real time robotic vision system (Zhang *et al.*, 2013; Tsai and Liu 2015).
12. Shopping assistant system for mobile users (Olugbara *et al.*, 2010; Gershon *et al.*, 2015).
13. Skin lesion segmentation (Damilola *et al.*, 2013; Pennisi *et al.*, 2016; Zortea *et al.*, 2017).

14. Sport technology (Hung *et al.*, 2011; Zhang *et al.*, 2015).
15. Video surveillance (Lu *et al.*, 2014; Foggia *et al.*, 2015).
16. Parking assistance system (Al-Kharusi and Al-Bahadly 2014; Bonde *et al.*, 2014).
17. Video assistant referee (D’Orazio *et al.*, 2009).

It can be observed that the application of colour image segmentation cuts across several disciplines like medicine, security, agriculture, sport technology and many more. In recent years, the application of colour image segmentation in medical applications has attracted significant interest in image processing research to assist in early detection, prognosis, operation plans and therapeutics. Consequently, medical image segmentation has emerged a challenging and promising area of image processing research to aid in the development of computer aided detection and diagnosis systems to assist medical practitioners in the accurate clinical diagnosis and analysis. In sport technology, video sport analysis has attracted wide applications to monitor sport activities during gaming events such as the players’ motion detection and tracking, goal analysis, verification of referee decisions during a game. Even in real time robotic vision system for sport activities, for example, the *Robocop* games held in a field are officially defined as “*a square with green carpets and white walls in which two teams of four or five completely black robots are trying to kick a red ball towards two goal posts coloured in blue and yellow, respectively*” (Noda *et al.* 1998).

In this scenario, colour vision is the essential tool for object recognition based on colour diversity. As increasing social security demand continues to increase over the years, the use of biometric features such as iris, voice, palm, signature and fingerprint, signature recognition systems has been employed for security reasons. In addition, video surveillance, face detection and recognition are being deployed in strategic locations to intelligently monitor human activities have attracted keen interest of researchers in colour image processing field in the last decades therefore it has become an important task. In agriculture, colour image segmentation applications have been extended to the agricultural sector to assist in the development of automated systems for agricultural purposes such as fruit grading and picking, crop yield estimation and production analysis, crop disease detection, irrigation management systems and harvesting robots.

1.1 Research problem statement

Image segmentation is an important problem in image processing and computer vision. The problem of image segmentation, which is the identification of different homogeneous regions in an image is a subject research activity in the last few decades. Consequently, many segmentation algorithms have been well developed for greyscale images. However, the problem of segmenting colour images has received less attention of scientists in image processing and computer vision fields. Until recently, colour image segmentation has become attractive in recent years because colour images are said to convey more useful information than greyscale images. However, the computational expensiveness of direct colour image segmentation is a major impediment in practical applications. It has become thrilling therefore to extend greyscale image segmentation algorithms such as thresholding and clustering to colour image segmentation.

Clustering algorithms are multidimensional extensions of thresholding algorithms that are amenable to colour image segmentation. However, the application and performance of clustering algorithms to the segmentation of colour images are highly affected by initialization of cluster centroids (Muthukannan and Merlin Moses 2010; Khattab et al., 2014; Rajaby et al., 2016). Furthermore, the performance of colour image segmentation critically depends on the choice of colour model as there is no one single colour model that is better than the others and most suitable for all images (Cheng *et al.* 2001; Hachouf and Mezhoud 2005; Kong *et al.*, 2014; Rajaby, Ahadi and Aghaeinia 2016). Moreover, the effectiveness of clustering algorithms and choice of colour model is dependent on the choice of distance metric to measure the difference between colours, the choice of distance metric has significant influence on the final segmentation result (Wang et al., 2016).

1.2 Research question

Colour image segmentation has been for many years and is still a challenging task in image processing and computer vision tasks that contains two critical issues. This study seeks to provide appropriate answers to the following research questions based on the identified research problems discussed in the previous section of this dissertation. In summary, the aforementioned difficulties faced in the segmenting colour images the researcher wishes to address the following research question:

What segmentation algorithm can be developed to improve the performance of colour image segmentation?

1.3 Research Aim and Objectives

The aim of this research is to investigate the effectiveness of perceptual colour difference saliency segmentation algorithm to improve the performance of colour image segmentation.

To achieve this particular aim, the following research objectives were set:

1. To comprehensively review relevant publications based on image segmentation algorithms.
2. To develop an image segmentation algorithm based on perceptual colour difference saliency segmentation.
3. To experimentally compare the performance of the developed image segmentation algorithm with existing state of the art segmentation algorithms using well known statistical evaluation metrics.

1.4 Research Methodology

The methodological steps taken towards the realization of the set aim and objectives of this study consist of three consecutive stages. The first stage addressed the first objective of this study by carrying out a comprehensive literature review with specific focus on the development of numerous image segmentation algorithms presented in the chapter two of this study. The second stage addresses the research objective two of this study. The methodology of the colour difference saliency segmentation algorithm consists of five stages: image dataset acquisition, colour image transformation, luminance image enhancement, salient pixel computation and image artefacts filtering.

At the initial phase of the second stage, the experimental images were selected from four publicly available benchmark image data sets, followed by resizing the default image size to a fixed dimension of 300 by 225 pixel resolution to ensure computational efficiency. Thereafter, the transformation of colour image was performed on the resized experimental images from the Adobe RGB colour image to CIE L*a*b colour image. At the luminance enhancement stage, the luminance channel of the transformed CIE L*a*b colour image was adaptively enhanced using an adaptive gamma correction to improve the image quality. Then, the salient pixels were computed using the mean value of the background colour feature estimated on an ellipsoidal patch drawn around the image borders and the mean value of the salient object colour feature. The computed mean values of the background and object pixels are therefore aggregated to create a greyscale saliency map which was converted to a binary

segmented image using a simple thresholding decision technique. At the final stage of the proposed approach, the resulting binary images are subjected to an image artefact filtering process to eliminate image artefacts that are present in the final segmented binary image.

The last stage addressed the third set objective of this study. The effectiveness of the perceptual colour difference saliency segmentation algorithm investigated in this study was demonstrated by experimentations. A series of experiments was conducted to evaluate the performance of the newly developed image segmentation algorithm against eight state-of-the-art saliency and non-saliency image segmentation algorithms using four statistical evaluation metrics

1.5 Research Contributions

The basic research question of what segmentation algorithm can be developed to improve the performance of colour image segmentation was targeted towards the development of a new image segmentation algorithm in this study. In order to back up the proposition that the investigated perceptual colour difference segmentation algorithm will improve the performance of colour image segmentation and in due course answer to the research question formulated in this study. The main contributions of the new perceptual colour difference saliency segmentation algorithm reported in this study have:

- (a) Demonstrated that the newly proposed segmentation algorithm can effectively segment salient object in an image through the aggregation of a colour feature of background pixels and colour feature of object pixels.
- (b) Demonstrated an improved way of using a simple thresholding decision technique that does not follow the conventional thresholding methods for bimodal thresholding of salient objects in an image.
- (c) Shown a detailed performance evaluation against state-of-the saliency and non-saliency segmentation algorithms to demonstrate the effectiveness of the proposed image segmentation algorithm.
- (d) Created as a means to evaluate the proposed segmentation algorithm both qualitatively and quantitatively on varying experimental images acquired from four publicly available benchmark data sets using four standard statistical evaluation metrics in terms of Precision, F-measure, Error and Dice.

1.6 Dissertation Synopsis

This dissertation is comprehensively organized into five major chapters. Chapter one introduces the basic background study of the research and discusses the need for colour image segmentation. In addition, the identified research problems which led to the research question, research aim and objectives and research contribution of the study are clearly described in this chapter.

Chapter two presents a comprehensive review of relevant publications based on image segmentation algorithms. Chapter three presents the major contribution of this study. In this chapter, step by step methodology carried out to achieve the set research aim and objectives proposed in this study are well described. Chapter four provides the qualitative and quantitative performance assessment of the proposed segmentation algorithm results and its comparison with other state of the art image segmentation algorithms already proposed in the literature. Chapter five concludes this dissertation with considerations of future work and conclusion.

CHAPTER TWO

LITERATURE REVIEW

This chapter presents a comprehensive review of related studies that influenced work done in this current study. For clarity of presentation, the chapter is divided into six major sections. The first section discusses the three major classifications of image segmentation methods. In the next two sections, emphasis was placed on pixel based image segmentation methods that include image thresholding and clustering algorithms and various improved variants published in the literature which is the major focus of segmentation algorithms incorporated into this research study. In the fourth and fifth sections, colour image segmentation methods, review of several existing colour models that have been applied to colour image segmentation and its extension to salient object segmentation are discussed. Finally, image segmentation performance assessment which includes benchmark data sets and image segmentation evaluation methods are presented.

2.1 Image Segmentation

Image segmentation plays a critical pre-processing role in practical applications such as image, video and computer vision applications (Peng, Zhang and Zhang 2011; Khattab *et al.* 2015). The final output obtained from an image segmentation process can be extended and applied to high-level methods which include feature extraction, semantic interpretation, image recognition and classification, image compression, content-based retrieval, medical imaging, traffic control systems, object location in satellite images, machine vision (Wang and Bu 2010; Alihodzic and Tuba 2014; Olugbara, Adetiba and Oyewole 2015). Image segmentation has been and still is an active area of image processing research for decades (Wang *et al.* 2015; Wang *et al.* 2016c). Over the past few decades, a number of inspiring image segmentation algorithms have been proposed to address the problem of image segmentation (McCann *et al.*, 2014). The proposed image segmentation algorithms have been applied and proven to be successful in various application areas. However, the development of a unified approach to image segmentation which can be applied to all classes of images is still a challenging task and an open problem in image processing (Peng and Li 2013). According to Haralick and Shapiro (1985), one of the desirable characteristics good image segmentation must have with reference to grey scale images is “*Regions of image*

segmentation must be uniform and homogeneous with respect to some characteristics such as intensity, colour, texture”.

As earlier stated, in the early years, a large number of the several existing image segmentation algorithms were developed for greyscale images. A comprehensive survey of existing image segmentation algorithms for greyscale images can be found in (Pal and Pal 1993; Skarbek *et al.* 1994; Cheng *et al.* 2001). Image segmentation methods can be appositely classified into region based, edge based and pixel based approaches on the basis of three essential properties of connectivity, discontinuity and similarity (Ikonomakis, Plataniotis and Venetsanopoulos 2000; Cheng *et al.* 2001; Chamorro-Martinez, Sanchez and Prados-Suarez 2003; Zhang, Fritts and Goldman 2008). Connectivity denotes that pixels belonging to the same region are grouped together. The discontinuity property entails that each region stands out to possess clear edges while similarity implies that pixels in an image belonging to the same region possess similar features. Image segmentation algorithms can be appositely classified as region-based, edge-based and pixel-based approaches based on these essential properties (Ikonomakis *et al.*, 2000; Cheng *et al.*, 2001).

2.1.1 Region based Image Segmentation Methods

Region based methods rely on the assumption that adjacent pixels in the same region share similar features such as intensity, colour or texture (Wang *et al.* 2015). They group image pixels into clusters and maintain connectivity among the pixels in the same cluster based on predefined criteria. Region growing is one of the popularly used image segmentation algorithm in this category (Okuboyejo *et al.*, 2013; Rouhi *et al.*, 2015; Wu *et al.*, 2016). The algorithm compares a pixel intensity of its neighbouring pixels until a predefined region criterion is met, then the pixel is said to belong to the same class as one or more of its neighbours. The procedure is repeated until no image pixel can be added to the region (Despotović *et al.*, 2015; Wang *et al.* 2016c). In addition to region growing, several region-based image segmentation methods have been proposed in the literature, including split and merge (Lughofer and Sayed-Mouchaweh 2015; Lei *et al.*, 2016), watershed transformations (Bhattacharjee and Saini 2015; Zheng and Hryciw 2016), graph cuts and random walks (Tian *et al.* 2013; Taubenböck *et al.* 2014; Li *et al.* 2016a; Dong *et al.*, 2016; Lee *et al.*, 2017). The efficiency of region based algorithms greatly depends on the application area and the input image has to be simple. However, they tend to over segment. Moreover, for difficult image scenes, they often fail to produce satisfactory segmentation results for images with

overlapping greyscales and suffer high mathematical and computational complexity (Li *et al.* 2016; Rajaby, Ahadi and Aghaeinia 2016).

2.1.2 Edge based Image Segmentation methods

Edge based methods are one of the widely used methods that have been applied to address the difficulties faced in addressing image segmentation (Wang *et al.* 2011). They aim at detecting discontinuities in image pixel intensity values, colour or texture. They locate image pixels that correspond to the edges of the objects seen in the image (Wang and Oliensis 2010; El-Sayed 2012). Examples include the Sobel edge operator (Martínez *et al.* 2015; Gonzalez *et al.* 2016), Laplacian of Gaussian operator (Anand, Tripathy and Kumar 2015; Chen, Yao and Chen 2016) and Canny edge operator (Wang *et al.* 2011; Seo, Hernández and Jo 2015; Ingle and Talmale 2016). Edge-based algorithms are usually suitable for simple and noise-free images (Wang *et al.* 2015). However, they have performance problems when images possess extra edges or when edges are not clearly defined (Wang *et al.* 2016c). Moreover, they are usually time-consuming and converting edges to regional boundaries is not a trivial task (Wang *et al.* 2015). These aforementioned limitations have a negative impact on segmentation results. Since region based image segmentation methods have several drawbacks, it was not considered as a potential choice for segmentation in this study.

2.1.3 Pixel based Image Segmentation methods

Pixel based image segmentation methods are the most basic, well-understood class of image segmentation methods and one of the most efficient ways of solving image segmentation problems because of their simplicity, low computational cost, and easy implementation (Dhanachandra, Manglem and Chanu 2015; Mansoor *et al.*, 2015). The commonly used pixel based methods include image thresholding and clustering algorithms (Le *et al.* 2013; Son and Tuan 2016). In these algorithms, similar image pixel intensities are grouped as belonging to a homogeneous cluster that corresponds to an object or a part of an object (Zhang, Fritts and Goldman 2008; Sevara *et al.* 2016). They are effective for both bi-level and multilevel image segmentation and do not require prior information about the input image. Pixel-based image segmentation algorithms have been reported not to consider spatial information during the segmentation process. This attribute makes image segmentation algorithms in this category susceptible to image noise. Moreover, image clustering algorithms are highly dependent on the initialization of initial cluster centres.

Pixel based image segmentation methods are further categorized into two main classes of algorithms (Le *et al.* 2013):

1. **Histogram thresholding algorithms:** an image histogram is computed from all the pixel intensities present in an input image. Thereafter, image pixels are classified into clusters formed by using peaks and valleys in the image histogram.
2. **Clustering based algorithms:** image pixels are grouped into clusters, by means of hard or soft clustering algorithms using characteristics such as intensity, colour, textures.

In order to propose a useful image segmentation algorithm that fit into this current study, it is important to note that our choice of image segmentation method was among the pixel-based image segmentation methods because of their long rich history, simplicity, robustness, computational efficiency. Hence, the next few sections of this dissertation will examine several existing pixel based image segmentation methods and their improvements proposed in the literature.

2.2 Histogram thresholding algorithms

Image thresholding algorithms are simple and popular image segmentation methods (Jumb, Sohani and Shrivastava 2014; Wang *et al.* 2015). The motivation behind the extensive use of image thresholding algorithms is due to its simplicity, robustness, fast execution speed, computational efficiency, real-time applicability and accuracy (Nakib, Oulhadj and Siarry 2007; Olugbara, Adetiba and Oyewole 2015; Wang *et al.* 2016c). However, they do not take into account spatial characteristics of an image (Despotović *et al.*, 2015). As a result of this, they are sensitive to noise and intensity homogeneities. Generally, image thresholding is carried out based on the information available in the global greyscale image histogram (Alihodzic and Tuba 2014; Kurban *et al.*, 2014). The process of thresholding an input image involves three stages; recognizing image histogram modes, finding the valleys between the identified modes and applying thresholds based on the valleys to the input image (Yang, Zhang and Wang 2014; Wang *et al.* 2016c).

Image thresholding algorithms aim at subdividing an input image into thresholds of two or more values using image pixel intensity values with a predefined threshold value T (Zuva *et al.* 2011). Image thresholding algorithms can be implemented either locally or globally (Feng *et al.* 2005). In local thresholding, an input image is divided into several sub regions and several threshold values are selected for each of the sub regions. However, the

size of the local image thresholding usually influences the segmentation performance (Lu *et al.*, 2013). On the other hand, for global image thresholding, a single threshold value is set for overall grey level information in the entire input image (Akay 2013). Sahoo, Soltani and Wong (1988), Lievers and Pilkey (2004) and Sezgin (2004) carried out a thorough survey of several existing image thresholding algorithms proposed in the literature. The outcome of their survey revealed that global image thresholding algorithms (Glasbey 1993) are one of the most popularly used to determine threshold values in the greyscale image histogram. The reason being that, the background and the object of interest areas in an image can be interpreted by taking its histogram with probabilities for each greyscale (Bhandari *et al.* 2014). Consequently, this work will only be focused on global thresholding which is directly relevant to the work reported in this study.

Global image thresholding algorithms can be classified as bi-level or multilevel thresholding (Hammouche, Diaf and Siarry 2010; Cuevas *et al.*, 2012; Bouaziz, Draa and Chikhi 2015). Bi-level thresholding algorithms classify image pixels into two clusters so that the first cluster contains pixel values above a threshold while the second cluster includes pixel values below the threshold (Kumar *et al.* 2013; Alihodzic and Tuba 2014; Jiang *et al.* 2015). This is based on the assumption that greyscale image histograms are bimodal. However, image histograms of real world images are usually multimodal, which limits the practical applications of bi-level image thresholding algorithms (Sathya and Kayalvizhi 2011; Liu *et al.*, 2015). Therefore, multilevel image thresholding algorithms generalize bi-level thresholding by segmenting an image into multiple clusters such that image pixels belonging to the same cluster have values within a specific range defined by several thresholds (Hammouche, Diaf and Siarry 2010; Liu *et al.*, 2015; Chen *et al.*, 2016). Furthermore, global thresholding algorithms can further be classified into parametric and non-parametric approaches (Delon *et al.* 2007; Abo-Eleneen 2011; Hussein, Sahran and Abdullah 2016). In parametric approaches, the grey level of each cluster has a probability density function generally assumed to obey a Gaussian distribution. Parametric approaches attempt to find an estimate of the parameters of distribution to best fit the histogram of the greyscale image. On the other hand, non-parametric approaches determine optimal thresholds that separate the grey level regions of an image by optimizing objective functions based on discriminating criteria (Dirami *et al.* 2013; Mala and Sridevi 2015; Tsai and Liu 2015; Hussein, Sahran and Abdullah 2016). Examples include Otsu's method that maximizes the between-class intensity variance in the grey level image (Otsu 1979), Kapur's method that maximizes entropy of foreground and background objects (Kapur, Sahoo and Wong 1985), cross entropy between

the images and its threshold version (Li and Lee 1993) and total misclassification error rate (Kittler and Illingworth 1986) usually optimized to determine the optimal threshold values.

2.2.1 Otsu thresholding algorithm

Sezgin (2004) studied several existing global thresholding techniques and he concluded that the Otsu method (Otsu 1975) is one of the most popularly used image thresholding methods for threshold selection in general images with regard to uniformity and shape measures (Arora *et al.* 2008; Horng 2011). The Otsu thresholding algorithm is a non-parametric and unsupervised approach for automatic threshold selection, based on the maximization of between class variance. The method has been applied to diverse application areas like pattern recognition (Bindu and Prasad 2012), document binarization (Zhang and Wu 2011; Moghaddam and Cheriet 2012) and computer vision (Xu *et al.* 2011). In some cases, the Otsu thresholding algorithm is used as a preprocessing technique to segment input images for further processing such as feature analysis and quantification (Liao, Chen and Chung 2001; Cai *et al.* 2014).

In the Otsu method, the threshold level of an input image is automatically determined by examining the statistics of the grey level image histogram that maximizes the between-class variance or minimizes the weighted within-class variance in a greyscale image (Wang and Bu 2010; Mizushima and Lu 2013). The method has been reported to give remarkable results for bi-level thresholding problems. However, in the case of remote sensing images or real life images, it does not guarantee satisfactory results (Huang, Lin and Hu 2011). To address these drawbacks, researchers have extended bi-level image thresholding algorithms to perform multilevel image thresholding (Rajinikanth and Couceiro 2015).

2.2.2 Multilevel Thresholding algorithms

Multilevel image segmentation has in recent years attracted the attention of researchers because of its practical applications. Several multilevel image segmentation algorithms have been proposed in the literature as an alternative to reduce the computational cost and speed up the maximization process of the conventional Otsu algorithm (Otsu 1979). Liao, Chen and Chung (2001), proposed a Fast Otsu's method, named the "recursive Otsu method" to improve the computational efficiency of the optimal threshold values of an input image for one-dimensional multilevel Otsu's thresholding. The proposed algorithm utilizes a look-up table acceleration approach to maximize a modified between-class variance instead of the

original Otsu's method. The proposed approach efficiently reduces the computational complexity which occurs during the exhaustive search process. Performance evaluation was carried out using the proposed algorithm with a recursive form of the between-class variance. The authors compared the experimental results obtained to that of the conventional Otsu's method. They reported that the experimental results of the proposed algorithm showed that the processing time required is less than 107 seconds, while that of the conventional Otsu's method with the recursive form takes approximately or more than six minutes. They also added that the proposed algorithm greatly improves the computational speed, twenty-two (22) times faster than the original Otsu's method, when the number of clusters is relatively small. However, the algorithm suffers from the problem of long processing time complexity and poor performance when the number of threshold increases ($M > 5$) (Huang and Wang 2009; Huang, Lin and Hu 2011).

Dong *et al.* (2008) presented an efficient iterative algorithm to find optimal thresholds that minimize a weighted sum-of-squared-error objective function. The proposed algorithm is an iterative improvement in minimizing the objective function. They applied the conventional Otsu's algorithm and the proposed iterative algorithm to several images of different natures. The authors observed that the two algorithms were equivalent and also produced identical thresholds. However, the proposed algorithm requires less computational time when compared to that of the Otsu's algorithm and that the proposed algorithm was more than 200 times faster than the Otsu's algorithm in the case of two thresholds.

Huang and Wang (2009) extended the fast Otsu's algorithm proposed by Liao, Chen and Chung (2001). They combined the fast Otsu's algorithm with a two-stage process, the Two-Stage Multilevel threshold Otsu method (TSMO). The proposed algorithm determines the multi-level thresholding in a two-stage approach. A simple and straightforward approach was proposed to further reduce the number of iterations required for computing the zeroth and first-order moments of a class. In this method, the histogram of an image consisting of L ($=256$) grey levels was partitioned into M_Z groups that contained N_Z ($=256/M_Z$) i.e. TSMO-16, TSMO-32 and TSMO-64 grey levels and estimates a set of thresholds for these sets in the first stage. The proposed TSMO method, then searches for each threshold within the set that contains each threshold in the second stage to minimize the computational complexity of the original Otsu's method by speeding up the search process of sets (or bin group). To evaluate the efficiency and accuracy of the proposed TSMO method, the results obtained were compared with those of the conventional and the recursive Otsu's methods qualitatively and

quantitatively. To quantitatively measure the accuracy of the proposed method, the misclassification and the relative error rate were utilized to compute the error in the final segmented images, likewise, to carry out the qualitative comparison, the authors visually compared the segmented results of the TSMO method versus the conventional and recursive Otsu methods using four grey-level test images. The proposed method outperformed the conventional Otsu's method, considerably reduces the number of iterations required in the exhaustive search process; for computing the between-class variance in an input image because the grey level in the histogram is decreased from 256 to 32 sets and also has the advantage of having a small variance in runtime for different test images. However, TSMO cannot always guarantee a satisfactory performance for many complex images and may yield a locally optimal solution (Olugbara, Adetiba and Oyewole 2015; Tsai and Liu 2015).

Huang, Lin and Hu (2011) proposed a modified two-stage multilevel Otsu (TSMO) based on a two stage Otsu's optimization approach for multilevel thresholding with automatic determination by valley estimation for image segmentation. The proposed method starts by computing the histogram of input grey levels statistically. Afterwards, the method of valley estimation is used to determine the number of clusters to ensure proper segmentation of the input image. The proposed improved TSMO method produced the same set of thresholds similar to the conventional Otsu's method, but minimizes the high computational complexity especially when the number of clusters is relatively high. To evaluate the accuracy of the proposed method, the results of the proposed method were compared with that of the Otsu's method and TSMO method using real-world images, experimental results showed that the computational speed of the proposed method is about 19000 times faster than the conventional Otsu method when the number of clusters is 7. These image segmentation algorithms considerably reduce the number of iterations required in the exhaustive search in multilevel thresholding, but they are still computationally expensive (Tsai and Liu 2015; Chen *et al.* 2016).

Generally, the proposed multilevel image algorithms in literature considerably reduce the number of iterations required in the exhaustive search for optimal thresholds. However, they have been reported to be computationally intensive and time-consuming due to the exhaustive search and increase in the number of desired thresholds. The reason for this is that they evaluate all possible solutions and because of this, their efficiency becomes very low (Zahara, Fan and Tsai 2005; Liu *et al.* 2015).

2.2.3 Nature Inspired Optimization Algorithms

The conventional multilevel thresholding image segmentation algorithms exhaustively search for the optimal thresholds to optimize objective functions, which as reported in literature, are computationally expensive. Meta-heuristic algorithms for finding optimal thresholds have gained the attention of researchers in this field to address multilevel thresholding problems since the computational time for finding multiple thresholds grow exponentially with the number of desired thresholds (Oliva *et al.* 2014).

The metaheuristic algorithms are popular and well-known global optimization schemes. According to Blum and Roli (2001) and Martí, Glover and Kochenberger (2003), meta-heuristics are a set of algorithmic concepts developed, which are used to define heuristic methods that can be applied to solve complex optimization problems (Alihodzic and Tuba 2014). Meta-heuristic algorithms in recent years have been proposed for multilevel image segmentation for finding optimal thresholds to address the computational time complexity of the conventional exhaustive search methods in the literature (Horng 2010; Liu *et al.* 2015). Compared to other methods designed specifically for particular types of optimization tasks, they are general-purpose algorithms and require no particular knowledge about the problem structure (Mesejo *et al.* 2016). These algorithms are a step away from local optima by exploring the search space often via randomization. They converge rapidly by exploiting regions and selecting the best solution by performing a fine tradeoff between exploration and exploitation (Hussein, Sahran and Abdullah 2016).

Several existing works were conducted using swarm algorithms, including the ant colony optimization (ACO) (Dorigo and Stützle 2003; Ye *et al.* 2005), Genetic Algorithms (GA) (Goldberg 1989; Tang *et al.* 2011), Bacterial Foraging Optimization (BFO) (Maitra and Chatterjee 2008; Sathya and Kayalvizhi 2011), Particle Swarm Optimization (PSO) (Eberhart and Kennedy 1995; Sathya and Kayalvizhi 2010; Akay 2013), Differential Evolution (DE) (Storn and Price 1997), Simulated Annealing (SA) (Kirkpatrick and Vecchi 1983), Darwinian Particle Swarm Optimization (DPSO) (Tillett *et al.* 2005). The Firefly Algorithm (FA) is one of the latest swarm intelligence algorithms (Horng and Liou 2011). These aforementioned metaheuristics algorithms for multilevel image segmentation use different objective functions such as the maximum entropy, Kapur's entropy, and the Otsu's method (Akay 2013).

Several existing metaheuristics algorithms for multilevel image segmentation have been applied to improve the exhaustive search problems. These proposed metaheuristic

algorithms have been able to find good solutions for difficult optimization problems and have shown promising performance in improving the efficiency of multilevel image segmentation algorithms., however, as the numbers of thresholds continue to increase, there is no guarantee that optimal solutions can be reached. There is no guarantee for them to be able to find the balance between the global search and local search; they may be trapped in local optimum points which often lead to inaccurate results and a slow convergence rate. In addition, the computational complexity of these proposed metaheuristic algorithms makes it difficult to apply in real-life situations (Zhang *et al.* 2014; Li *et al.* 2015; Olugbara, Adetiba and Oyewole 2015; Son and Tuan 2016). Table 2.1 presents some of the examples of proposed nature-inspired metaheuristic algorithms for multilevel image segmentation.

Table 2.1 Nature inspired metaheuristic algorithm for multilevel image segmentation (Prakasam and Savarimuthu 2016).

Authors	Algorithm	Approach
Hammouche, Diaf and Siarry (2008); Oghaz <i>et al.</i> (2015); Sun <i>et al.</i> (2016)	Genetic Algorithm (GA)	Imitates the process of natural selection
Gao <i>et al.</i> (2010); Lee, Leou and Hsiao (2012); Liu <i>et al.</i> (2015)	Particle Swarm Optimization (PSO)	Based on social behaviour of bird flocking and fish schooling
Mohan and Baskaran (2012); Taherdangkoo <i>et al.</i> (2013); Castillo <i>et al.</i> (2015)	Ant Colony Optimization	Based on the foraging behaviour of ants choosing a path leading from its nest to a food source
Li <i>et al.</i> (2015); Zhu and Kwong (2010); Cuevas <i>et al.</i> (2012)	Artificial Bee Colony	Inspired by the intelligent behaviour of honeybees
Fister, Yang and Brest (2013); Rajinikanth and Couceiro (2015); Chen <i>et al.</i> (2016)	Firefly Algorithm	Inspired by the flashing light patterns of tropic fireflies
Yang (2010); Alihodzic and Tuba (2014); (Ye <i>et al.</i> (2015)	Bat Algorithm	Inspired by the echolocation behaviour of micro bats.
Sathya and Kayalvizhi (2011); Maitra and Chatterjee (2008); Yang <i>et al.</i> (2016)	Bacterial colony optimization	Simulates some typical behaviours of <i>E.coli</i> bacteria using their whole life cycle.
Horng (2010); Jiang <i>et al.</i> (2014); Durgadevi, Hemalatha and Kaliappan (2014)	Honey bee mating optimization algorithm (HBMO)	Inspired by the process of mating in real honey bees.

2.3 Cluster Analysis

Cluster analysis, as an unsupervised technique for finding and classifying a given dataset into clusters, is predominant in many disciplines that involve analysis of multivariate data (Jain 2010). Clustering has a long and rich history in literature, even to date. A search via Google Scholar (2016) found 3, 020, 000 results using the words “*data clustering*” alone. These large statistics of literatures indicate the great significance of clustering in data analysis. Consciously or unconsciously, individuals tend to perform clustering on a regular basis. For example, clustering is performed when similar items are arranged in a group, such that the data items in the same group are similar to one another. In view of this, clustering is a process of assigning a set of unlabelled objects into subsets called clusters such that objects found in a particular cluster are more similar to each other than objects from different clusters (Tsai and Lin 2011). Clustering is a crucial task in science that has been applied to interdisciplinary fields which includes taxonomists, social scientists, psychologists, biologists, statistician, mathematicians, engineers, medical researchers, as well as computer scientists to data mining, computer vision, bioinformatics, crime analysis, pattern recognition, data compression, machine learning, document retrieval, industrial automation, image analysis, object recognition and statistical data analysis (Peng *et al.*, 2016; Liang *et al.*, 2016; Rujirapipat *et al.*, 2017; Oh *et al.*, 2017).

Clustering based image segmentation algorithms are multidimensional extensions of image thresholding algorithms (Zhang 2006). Image clustering is an unsupervised classification algorithm that groups similar image pixels into subgroups i.e. clusters (Tzortzis and Likas 2014; Lei *et al.* 2016; Tripathy and Mittal 2016). The division of image pixels into clusters is based on the principle of minimizing intra-cluster similarity and maximizing inter-class differences (Chebbout and Merouani 2012; Wolf and Kirschner 2013). Therefore, clustering algorithms require using a measure of similarity. Several similarity measures have been proposed in the literature which includes Euclidean distance, Manhattan distance, Minkowski distance and Mahalanobis distance (De Amorim and Mirkin 2012; Zhao, Li and Zhao 2015; Ferreira, de Carvalho and Simões 2016; Wang *et al.* 2016a). The Euclidean distance is one of the most commonly used similarity measures in the conventional clustering algorithms (Ferreira and De Carvalho 2014).

Image clustering is carried out either in a supervised or unsupervised way, using two main clustering algorithms: hierarchical clustering and partitional clustering algorithms (Bai *et al.* 2012; Alam, Dobbie and Rehman 2015). In hierarchical clustering algorithms just as the

name implies, a hierarchy of clusters is identified which result in a hierarchical tree (Leung, Zhang and Xu 2000; Khanmohammadi *et al.*, 2017). Clusters are created in either a top down approach (divisive) or a bottom up approach (agglomerative) (Wolf and Kirschner 2013; Ozturk, Hancer and Karaboga 2015). In the bottom up approach, each data point is considered a cluster and they are iteratively merged according to some criterion, whereas top down approach considers the whole dataset a cluster and iteratively split them into multiple clusters according to some evaluation criterion. Hierarchical clustering algorithms possess the following advantages: the number of desired clusters needs not to be specified in advance and they are not dependent on initial cluster centres. However, hierarchical clustering algorithms are static such that when image pixels are assigned to a cluster; it cannot be moved to a different cluster (Lei *et al.* 2016) and hierarchical clustering algorithms require high computational time (Ozturk, Hancer and Karaboga 2015).

Contrarily, partitional clustering algorithms divide image pixels into disjoint clusters, whereby the image pixels in a cluster are similar while significantly different from the other pixels in the other clusters (Osamor *et al.* 2012; Alam, Dobbie and Rehman 2015; Ferreira, de Carvalho and Simões 2016). They optimize a locally or globally defined criterion function to determine a pre-specified number of clusters, in most cases based on the squared error criterion. Partitional clustering algorithms are dynamic; image pixels assigned to a cluster can be moved from one cluster to another. In partitional clustering algorithms, the disadvantages of the hierarchical clustering algorithms are advantages of the partitional clustering algorithms (Jain, Duin and Mao 2000; Omran 2004). Partitional clustering algorithms are either hard clustering or soft clustering algorithms. In hard clustering algorithms, clusters are disjoint and non-overlapping in nature that is image pixels can only belong to a single cluster. In soft clustering algorithms, image pixels can belong to more than one cluster with a certain fuzzy membership degree (Osamor *et al.* 2012; Ferreira, de Carvalho and Simões 2016). The most well-known and widely used partitional clustering algorithms are K-means clustering algorithms (hard clustering) and Fuzzy C-means (soft clustering) (Zhang and Wang 2000; Isa, Salamah and Ngah 2009; Stetco, Zeng and Keane 2015). Partitional clustering algorithms are preferred in various research fields due to their capability to cluster large data sets, just like in the case of signal and image processing, data mining and pattern recognition (Das, Abraham and Konar 2008; Jain 2010).

2.3.1 K-means clustering algorithm

The K-means clustering algorithm is the main and one of the most widely used partitional clustering algorithms. The algorithm was proposed over 50 years ago and has a rich, diverse history as it was independently discovered in different scientific fields by Steinhaus (1956), Ball and Hall (1965) and MacQueen (1967), Lloyd (1982). A few years ago, the K-means algorithm was nominated to be one of the ten most influential data mining algorithms (Kumar and Wu 2009). Its popularity can be attributed to its simplicity, flexibility, efficiency, scalability in handling big data sets and easy to adapt to different application domains (Deelers and Auwatanamongkol 2007; Siddiqui and Mat Isa 2012; Lei *et al.* 2016; Serapião *et al.* 2016). The algorithm is a numerical, unsupervised, non-deterministic and iterative clustering algorithm for solving clustering problems, based on a simple iterative scheme, to find a local minimal solution (Lloyd 1982).

The K-means clustering algorithm partitions the input data into k classes by iteratively computing the mean intensity value for each cluster and segmenting the image by distributing each image pixel into clusters with the closest centroid (Despotović *et al.*, 2015). A cluster is demarcated by its cluster centre, or centroid. A centroid is the point whose coordinates is obtained by means of computing the average of each of the co-ordinates of the point of samples assigned to clusters (Ghosh and Dubey 2013). The K-Means algorithm begins by initializing the cluster centres; K centroids, then, the algorithm recurrently distributes image pixels to its corresponding closest centroid based on a similarity measure. Finally, the positions of centroids are recomputed until convergence (Ozturk, Hancer and Karaboga 2015). The criterion is based on minimizing the total mean-squared distance from each point in N to that point's closest centre in K (Güngör and Ünler 2007).

Let I be an input image with a resolution of $x \times y$, assuming the input image is to be clustered into k number of clusters. Let $p(x, y)$ be image pixels to be clustered with C_k representing the cluster centres. The K-Means algorithm is executed using the following steps below (Dhanachandra, Manglem and Chanu 2015):

Step 1 Initialization: select K initial cluster centroids randomly from a given n point. K = the number of desired clusters.

Step 2 Compute: for each pixel of an image, calculate the Euclidean distance d , between the centroids and for each pixel of the input image.

Step 3 **Partition**: assign image pixels in the input image to the closest cluster centroid.

Step 4 **Re-compute**: when image pixels have been assigned, calculate the mean of the pixel values for each cluster and update the cluster centres

Step 5 **Repeat** the step 3 and 4 until centroid values no longer change (until a convergence criterion is met).

The K-Means algorithm has been applied extensively to solve numerous clustering problems due to its easy implementation. However, the algorithm is not faultless; it suffers from a number of limitations. According to De Amorim (2012), the K-means algorithm is a greedy algorithm firstly because the quality of the final clustering results is highly dependent on its initial centroids, as it may converge to suboptimal solutions, if not properly chosen. Secondly, the algorithm lacks a universally agreed definition for the term “cluster”, whose number has to be known beforehand, which can be restrictive in practice, since the number of clusters in a dataset is generally unknown, especially in real-world applications which involve high dimensional and/or distributed data (Naldi and Campello 2015). Moreover, the algorithm’s dependency on the selection of the number of cluster centroids before implementation usually is a time-consuming process (Isa, Salamah and Ngah 2009; Lei *et al.* 2016). Since the initialization of the K-means affects the results of the final clustering, there have been a wide range of different techniques proposed for selecting the initial cluster centre which includes the Forgy method (Forgy, 1965) and the random partition method (Jancey, 1966).

Forgy method assigns each point to one of the K clusters uniformly at random. The centres are then given by the centroids of these initial clusters. It has been alluded that this method has no theoretical basis, as such random clusters possess no internal homogeneity (Anderberg, 1973). On the other hand, the random initialization of cluster centroids selects centres randomly from the data points and data points are distributed into the randomly selected cluster centres. This method causes convergence to the nearest or trapped into local minima due to its hill climbing approach (Güngör and Ünler 2007; Serapião *et al.* 2016). Consequently, trapped cluster centroids could represent the image pixels incorrectly, resulting in uneven results from different initializations of cluster centres (Bai *et al.* 2012; Dhanachandra, Manglem and Chanu 2015). Moreover, the image pixels isolated far away from the cluster centres may cause a shift in the position of the centres from their optimum location leading to a poor representation of data (Isa, Salamah and Ngah 2009).

2.3.2 Fuzzy C-means Algorithm

Fuzzy clustering algorithms were introduced to address the intrinsic difficulties faced in hard-clustering algorithms. Examples of proposed soft clustering algorithms include the Fuzzy C-Means (FCM), Gustafon-Kessel, Gaussian mixture decomposition and fuzzy C-varieties. The most popularly used fuzzy clustering algorithm is the Fuzzy C-means (FCM) algorithm (Siddiqui and Mat Isa 2012; Nilima, Dhanesh and Anjali 2013).

Fuzzy set theory was first proposed by Zadeh (1965), whilst Ruspini (1969) proposed an objective function-based fuzzy clustering by using fuzzy c-partitions, the root concepts of fuzzy partition. He established the basis of extending Hard C-means (HCM) clustering algorithms to fuzzy concepts. Dunn (1973), proposed an extension of the hard mean clustering algorithms to preliminary concepts of fuzzy partition. Later, in 1981, Bezdek (James 1981) added the fuzzy factor and proposed the Fuzzy C-means (FCM) algorithm. The fuzzy clustering, based on the objective function, is popularly known as the Fuzzy c-means clustering (FCM) algorithm (James 1981). The FCM clustering algorithm has been widely studied in literature for its application to image segmentation (Suganya and Shanthi 2012; Liu *et al.* 2016b). This concept introduces the fuzzy concepts that image pixels can belong to more than one cluster concurrently with a certain fuzzy membership degree (Yu *et al.* 2010; Tan, Isa and Lim 2013; Olugbara, Adetiba and Oyewole 2015). It has been reported to be useful in applications where uncertainty and limited spatial resolutions are present. For example, in satellite images (Despotović *et al.* 2010).

The classical Fuzzy C-means (FCM) algorithm was originally developed and proposed by Dunn (1973). Subsequently, the algorithm was further improved by James (1981) with an objective function. The FCM algorithm is the most conventional and popularly used among fuzzy clustering approaches (Rajaby, Ahadi and Aghaeinia 2016). This is due to the introduction of fuzziness for the belongings of each image pixel (CAI, Chen and Zhang 2007). It considers every pixel intensity values in an image to have an affiliation relationship with each cluster centre (Liu *et al.* 2016b). The algorithm is an unsupervised and effective algorithm which does not require prior knowledge and retains more information from the original image (Cai, Chen and Zhang 2007; Zhao, Jiao and Liu 2013). The FCM algorithm can be minimized by the following objective function (Esme and Karlik 2016):

$$J_m = \sum_{i=1}^C \sum_{j=1}^N u_{ij}^m \|x_j - c_i\|^2 \quad (2.1)$$

where N represents the number of image pixels to be partitioned into C clusters, u_{ij}^m is the fuzzy membership function of the image pixel to the x_j belonging to the j th cluster, m is the weighting exponent that controls the fuzziness of the resulting partition manually provided by the user. $\|x_j - c_i\|$ is the similarity measure that is the Euclidean distance between x_j and the i th cluster centre c_i .

In accordance with the concept of fuzzy logic, each image pixel can only have a membership value between 0 and 1, they can belong to more than one cluster with a certain fuzzy membership degree (Wang and Bu 2010; Zhao *et al.*, 2011; Feng *et al.*, 2013). The FCM algorithm aims to minimize a fuzzy version of the least-square error criterion, the algorithm is influenced by the existence of the uncertainty of the data set (Ji *et al.* 2012). As a result of this, the FCM algorithm improves partitioning performance compared to hard clustering algorithms (Ozturk, Hancer and Karaboga 2015). However, FCM suffers a lower convergence speed to local minima (Fan, Zhen and Xie 2003). Like several standard unsupervised clustering algorithms, the conventional FCM algorithm does not consider any spatial information in the image (Chuang *et al.* 2006; Jiang *et al.* 2016).

As a result of this, the FCM algorithm is highly sensitive to image noise, outliers and other imaging artefacts (Liao, Lin and Li 2008; Ji *et al.* 2012; Zhao, Jiao and Liu 2013). Furthermore, the FCM algorithm is highly dependent on the initialization of the cluster centres (Tan, Lim and Isa 2013). Thus, image segmentation results produced by the FCM clustering algorithm depend on the initialization strategy, which could generate poor final cluster centroids that could incorrectly represent the clusters (Kim, Lee and Lee 2004; Siddiqui and Mat Isa 2012; Tan, Isa and Lim 2013). Moreover, the FCM algorithm computes the membership degree to a point proportional to its proximity to the cluster representatives, consequently, computational time of the FCM algorithm is highly dependent on the image size (Stetco, Zeng and Keane 2015).

2.4 Improvements of clustering algorithms

In this section, several improved variants of K-means and Fuzzy c-means clustering algorithms proposed by researchers to improve the performance of these image clustering algorithms published in the literature are reported. The section discusses some of the most

important and commonly used initialization techniques for the K-means clustering and Fuzzy C-means clustering algorithms.

2.4.1 Improved Variants of K-means algorithm

Different strategies have been proposed in the literature to address the problem of determining initial cluster centroids in the K-means algorithm. Zhang, Hsu and Dayal (1999) proposed the *K*-Harmonic means algorithm (*KHM*). The proposed algorithm was based on soft membership that uses the harmonic averages of the distances from each data point to the clusters as components of its performance function. The proposed algorithm was reported to have improved the quality of the segmentation results compared to that of the K-means algorithm. However, it does not solve the convergence problem to local optima. Mashor (2000) presented a modified version of the K-Means clustering algorithm, called, the “Moving K-Means” (MKM) clustering algorithm to address the listed shortcomings of the K-Means algorithm. The author proposed a fitness concept to ensure that each cluster has a significant number of members and final fitness values before the new position of the cluster is calculated. He reported that the main objective of the proposed MKM algorithm was to preserve the fitness value among all the similar clusters: the lower variance cluster or the cluster with lower fitness value is moved towards the active region. The proposed MKM algorithm was proven to minimize the issue of dead centres and centre redundancy problems as well as reducing the initialization problem often encountered by the effect of a trapped centre of local minima and may converge to an optimum location. However, the MKM algorithm suffered major limitations; it does not reduce the intra-cluster variance and images are sensitive to noise (Isa, Salamah and Ngah 2009; Siddiqui and Isa 2011).

Yuan *et al.* (2004), in an attempt to address the problem of K-means, proposed a modified version of K-means titled the standard K-means algorithm. The proposed algorithm alternated between assigning data points to the nearest centroid and moving each centroid to the mean of its assigned data points; the centroids obtained by the algorithm were consistent with the distribution of data. Hence, the algorithm was reported to have produced clusters with better accuracy, compared to the conventional K-means algorithm. However, the proposed algorithm did not improve the computational efficiency of the K-means algorithm in terms of computational complexity.

In 2006, Fahim *et al.*, (2006) proposed an enhanced variant of the K-Means algorithm to improve the distribution of data points to suitable clusters. In their approach, the authors introduced two *distance* functions. The first distance function uses a similar approach to that of the conventional K-Means algorithm, based on Euclidean distance value, while the second distance function finds the nearest centre for each data point by computing the distances from the centre of the current centroid and the distance from the newly assigned centroid in the previous iterations. If the result of the distances is smaller compared to the previous one, the pixel remains in the cluster, otherwise it is moved to the next cluster. The distances between image pixels and all the centroids are computed per iteration. The authors reported that the proposed algorithm reduced the number of iterations required compared to that of the conventional K-means algorithm. They observed that the algorithm proposed in their study improves the computational speed of the K-means algorithm by the magnitude in the total number of distance calculations and the overall time of computation. However, the algorithm suffers shortcomings; initial cluster centroids are selected randomly just like the conventional K-means algorithm, which makes the algorithm sensitive to the initialization of cluster centroids. This is an indication that there is no guarantee for the accuracy of the final clustering results (Nazeer and Sebastian 2009).

The K-Means++ careful seeding algorithm was introduced by Arthur and Vassilvitskii (2007) with the aim to propose a more robust selection of initial cluster centres to improve the K-means clustering results. In their method, the initial cluster centroid is selected randomly, after that, the next selected cluster centroid is proportional to the distance of the previously selected centroid in a probabilistic manner. The remaining object points are assigned into clusters based on the nearest distance to the initial cluster centroids. The major contribution of the proposed algorithm is the addition of “weight” to obtain efficient initial cluster clusters in step 1 of the conventional K-means algorithm. Previous authors reported that the proposed approach improves the convergence speed and does not increase the computational cost. Moreover, it yields an improvement in terms of performance and accuracy compared to the conventional K-Means with a lower potential. Despite all of these, the algorithm is not deterministic for multiple runs due to the randomization of initial centroids.

Nazeer and Sebastian (2009) proposed an iterative process to improve the selection of initial cluster centroids in the K-Means algorithm. The proposed algorithm combined two systematic approaches. At first, they selected k initial centroids based on relative distances

between data points. Next, they computed the clusters based on relative distance of each point from the initial cluster centroids. Subsequently, the resulting clusters are modified using a meta-heuristic approach to improve its efficiency based on Euclidean distance to find the distance between the centroids and data point. The authors reported that the proposed algorithm produced good clusters with reduced computational time. However, the value of k , which is the desired number of clusters, has to be speculated randomly before implementation. Also, the distance of each of the data points from all data points has to be calculated, in the case of a large set of data points; this may lead to a tremendous computational time complexity (Mahmud, Rahman and Akhtar 2012).

Isa, Salamah and Ngah (2009) presented three modified variants of moving the K-Means clustering algorithm called the fuzzy moving K-Means (FMKM), adaptive moving K-Means (AMKM) and adaptive fuzzy moving K-Means (AFMKM) algorithms to address the problem of initialization and sensitivity to noise. They introduced an integration of fuzzy concepts in the conventional K-means clustering algorithm called the fuzzy K-Means (FKM). The newly introduced FKM concept uses a fuzzy membership function to assign the pixel intensity values into clusters instead of Euclidean distance used in the conventional K-means algorithm. The first method, FMKM uses the concept of fuzzy logic that allows image pixel intensity values to be assigned simultaneously to more than one class of different degree of membership. Meanwhile, AMKM algorithm minimizes the problem of noise sensitivity by updating the moving member condition. Lastly, the proposed AFMKM algorithm combined the concepts of the FMKM and AMKM algorithms, sharing both of their characteristics. For performance evaluation, both qualitative and quantitative analyses were carried out. The authors reported that for the quantitative results, the introduced fuzzy concept in the FKM and FMKM algorithms outperformed the conventional K-Means and MKM algorithms and also require less computational time.

Sulaiman and Isa (2010) proposed another variant of the K-Means called the Adaptive Fuzzy-K-means clustering algorithm (AFKM). The proposed algorithm incorporates the fundamental theories of the conventional K-Means, MKM and Fuzzy C-means clustering algorithms. At the initial stage, all initial cluster centres were initialized to a certain value. Furthermore, to ensure a better clustering process, the authors introduced the fuzzy concept to allow each data point to be assigned to more than one class simultaneously by degrees of membership which determines the new position of the centre. To test the capability and suitability of the proposed algorithm, two conventional clustering algorithms were used as

their bases of comparison; MKM and Fuzzy C-means, since Fuzzy C-means and the proposed algorithm employ a similar fundamental concept for the clustering process and MKM has been proven to produce better segmentation performance when compared to the conventional KM clustering algorithm. The comparison was carried out both qualitatively and quantitatively. The authors reported that the proposed AFKM algorithm outperformed the clustering algorithms as the segmented images produced sharper and crispier with less noisy pixel segmentation results, while FCM and MKM results produced images corrupted with noise. However, the required computational time for the segmentation process is slightly higher than the conventional MKM clustering algorithm.

Siddiqui and Isa (2011) proposed an improved version of the moving K-Means algorithm (MKM) called enhanced moving K-means algorithm (EMKM). In the proposed EMKM algorithm, the authors enhanced the moving concept of the conventional moving K-Means and propose two variants of EMKM, EMKM-1 and EMKM-2. Before the implementation process, the initialization of cluster centre values, are randomly assigned, image pixels are then distributed to the nearest cluster, based on the minimum Euclidean distance. It was reported that the proposed variants of EMKM, EMKM-1 and EMKM-2 significantly maintain the segmentation variance difference between the clusters by assigning cluster members with values outside the range being assigned to the nearest clusters to ensure fitness value between clusters, by reducing the summation value of the Euclidean distance. The authors compared the efficiency of the proposed EMKM algorithms to the conventional algorithms, K-means and moving K-means algorithms. They reported that the proposed algorithm outperformed the other conventional clustering algorithms used in their study. However, initial cluster centres values were randomly assigned, which does not guarantee the final results.

Purohit and Joshi (2013), proposed another study to improve the K-Means algorithm. In the proposed algorithm, initial cluster centres were selected by calculating the Euclidean distance between each data point. Once this is done, the selected points are deleted from the set to form a new set. They carried out iterations on the new sets by finding data points that are closest to each other; the initial cluster centres are generated by reducing the mean square error of the final cluster. The proposed algorithm only produced satisfactory results for dense data sets rather than sparse data sets. Moreover, the proposed algorithm requires an iterative process to distribute image pixels into befitting clusters; this procedure however may lead to high computational complexity (Dhanachandra, Manglem and Chanu 2015).

Dhanachandra, Manglem and Chanu (2015) proposed another variant of the K-Means clustering algorithm, based on the subtractive clustering algorithm, to generate the initial cluster centres. The authors applied the partial stretching enhancement to improve the quality of the input image. The proposed subtractive cluster is used to generate the initial cluster centres and performed segmentation using the K-means clustering algorithm. Finally, a median filter is applied to the segmented image to remove unwanted regions from the segmented image. However, the algorithm is highly dependent on the input image size as its computational complexity grows exponentially.

Olugbara *et al.*, (2015) developed a fusion of both thresholding and clustering based image segmentation algorithms named the pixel intensity clustering algorithm (PICA). The proposed algorithm uniquely performs a non-iterative cluster centroid initialization, based on a linear partitioning scheme. This approach is known as Forgy strategy, a step away from the randomization strategy common to several improved variants of the K-means clustering algorithm.. In their method, they adopted the Otsu's between cluster variance criterion to distribute pixel intensities into clusters and perform clustering to obtain the final segmentation output. For performance evaluation, the proposed image segmentation algorithm was quantitatively and qualitatively compare and outperform four state of the art image segmentation algorithms used in their study. The authors reported that the proposed algorithm offers intrinsic advantages such as simplicity, reproducibility, survivability and repeatability that have engendered better greyscale image segmentation than similar algorithms in the literature. However, the selected initial cluster centroids may not be optimal, because the proposed initialization strategy does not consider the effects of all pixel intensity values in the image. This is likely to affect the quality of the segmentation results.

The foregoing review of several improved variants of the conventional K-means algorithm to address the problem of determining initial cluster centroids shows that there is no general solution to solve image clustering problem.

2.4.2 Improved Variants of the Fuzzy C-means Algorithm

To address the aforementioned problems identified by the FCM algorithm, researchers have developed several improved variants published in the literature. The researchers incorporated local spatial information into the original FCM algorithm to improve the segmentation performance, such as the possibilistic C-means (PCM) (Krishnapuram and Keller 1993) and

robust fuzzy C-means (RFCM) (Pham 2001). In 2002, Ahmed *et al.* (2002) modified the objective function of the conventional FCM algorithm. They introduced a neighbourhood averaging term in the objective function of FCM (FCM_S) which allows the labelling of image pixels to be influenced by the labels in its neighbourhood, into the objective function and also a parameter to control the effect of the neighbour term. The approach proposed to compensate for the intensity inhomogeneity in order to increase the robustness of FCM in such a way that image pixels are assigned to the clusters in homogeneous regions. Although the proposed modified FCM algorithm improved the results of the conventional FCM algorithm on noisy images, the proposed algorithm lacks adequate robustness to noise and outliers. In addition, FCM_S requires heavy computation time to compute the neighbourhood term in each iteration step (Chen and Zhang 2004).

Liew and Yan (2003) proposed an adaptive spatial constrained FCM algorithm. In their method, spatial pixel connectivity was implemented by a dissimilarity index that considers the local influence of neighbouring pixel values in an adaptive form, in place of the usual distance metric to enforce the connectivity constraint, only in the homogeneous areas. Kang, Kim and Li (2005) went further to propose a spatial homogeneity-based FCM (SHFCM) algorithm. The algorithm utilizes the statistical information about every pixel value in a local neighbourhood. Wang *et al.* (2008) incorporated both the local spatial context and non-local information into the dissimilarity measure into the standard FCM algorithm called LNLFCM. Although, these proposed modifications of the FCM algorithm can largely reduce the impact of image noise, they all have high computational complexity, due to the repeated calculation of the neighbourhood term in every iteration process (Ji *et al.*, 2011).

Subsequently, in order to reduce the computational complexity of FCM_S, Szilagyi *et al.* (2003) proposed an enhanced FCM (EnFCM) algorithm based on the grey-level histogram. First, a linear-weighted sum image is formed from both the original image and its local neighbourhood average grey image, by weightily averaging each image pixel and its neighbourhoods. Thereafter, a clustering process is performed on the summed image, based on the grey level histogram instead of pixel intensity values in the image. Moreover, the quality of the segmented image is comparable to that of FCM_S. Hence, the computational time required for the segmentation process of the EnFCM algorithm is reduced. However, the weighted coefficient values, which may affect the segmentation results, are provided by the users.

Chen and Zhang (2004) proposed two improvements of FCM_S proposed by Ahmed *et al.* (2002) to reduce computational time, FCM_S1, based on mean-filtered image. However, FCM-S1 was observed to be unsuitable for images corrupted by impulse noises. To address this, the same authors proposed another improved variant of FCM_S1, named FCM_S2. The newly proposed variant utilized the median-filtered images in place of the proposed mean filtered image to enhance the robustness of FCM_S1 to noises. The two proposed algorithms, the extra mean-filtered image and median-filtered are computed in advance before cluster processing in replacement of the neighbourhood term of FCM_S. Thus, the computational times are considerably reduced. Chuang *et al.* (2006) proposed averaging the fuzzy membership function values, reassigning the values according to a tradeoff between the original and average membership values. The proposed algorithm produced accurate clustering results as long as the tradeoff is well-adjusted. However, the algorithm is enormously time consuming (Szilágyi, Szilágyi and Benyó 2007).

Cai, Chen and Zhang (2007) proposed another variant of FCM named the fast generalized FCM algorithm (FGFCM). The algorithm introduces a new local similarity measure, which combines both the spatial information and the local grey-level information to form a non-linearly weighted sum image. The algorithm utilizes the SUSAN filter (Smith and Brady (1997), for noise reduction and image reconstruction of the main geometrical configurations, but not at the preservation of the fine structure. The clustering process was carried out based on the grey level histogram of the summed image. Thus, the computation time required for the segmentation process was reduced, similar to the EnFCM algorithm. However, EnFCM and FGFCM algorithms cannot be directly applied to original images as they both lack enough robustness to noise and intensity inhomogeneity.

Wang *et al.*, 2008, in their study, incorporated both the local spatial context and non-local information into the dissimilarity measure, and proposed the LNLFCM algorithm. The proposed algorithm largely reduces the impact of noises. However, the computational time required is very high due to the repeated calculation of the neighbourhood term during the iteration process (Ji *et al.* 2012). To address this drawback, Ji *et al.* (2012), proposed the weighted image patch-based FCM (WIPFCM) algorithm. The proposed algorithm utilized image pixels in place of the image patch to be clustered. The authors proposed a weighting scheme to adaptively determine the anisotropic weight of each image pixel in the patch. The authors reported that the WIPFCM algorithm produced good segmentation results and was robust to image noise. However, the initial cluster numbers must be provided before

implementation is carried out. In addition, the proposed algorithm requires a laborious process for the selection of the desired number of clusters (Tan, Isa and Lim 2013).

Tan, Lim and Isa (2013), presented an improved initialization strategy for the FCM algorithm, based on the Hierarchical Approach (HA) initialization strategy. The proposed HA module allows users to carry out initialization automatically and adaptively determine both cluster centres and numbers based on the global information in the histogram of the input images. Compared to the random initialization strategy, they reported that the proposed HA module computationally reduced the time required and produced good consistent clustering results. Quite a large number of modified FCM algorithms have been proposed. The authors incorporated spatial information, which led to generating more homogeneous clusters. However, the computational procedures resulted in high computational cost (Rajaby, Ahadi and Aghaeinia 2016). The table below presents the categories of pixel-based image segmentation methods, identifying benefits and limitations respectively.

Table 2.2 Summary of pixel based image segmentation algorithms.

Method	Proposed Algorithm	Benefit	Limitation
Image histogram	Bi-level thresholding algorithms	work well for bimodal images i.e. images with two classes, foreground and background	Histograms of real world greyscale images are usually multimodal, which limits the practical applications of bi-level image thresholding.
	Multi-level thresholding algorithms	Generalize bi-level thresholding algorithms. They have practical applications using real world greyscale images.	Computationally expensive. Time consuming due to exhaustive search and as the number of thresholds is increased.
	Nature-inspired optimization algorithms	Efficient for multilevel image segmentation algorithms. Solve complex optimization problems.	They are often trapped in local optimum points. They are random and stochastic, output are not always consistent, which affects its efficiency. Computational complexity makes it difficult to apply in real-life situations.

Image clustering	Soft Clustering - Fuzzy C-means (FCM) algorithm	Retains more information from the original image works well in clustering noise-free images	<p>Sensitive to initialization of cluster centres which could lead to generating poor final cluster centroids.</p> <p>Suffers lower convergence speed to local minima.</p> <p>It suffers lack of spatial information that makes it highly sensitive to image noise and generates disconnected regions.</p> <p>Random initialization of cluster centroids often leads to the dead centre syndrome, a situation that one or more clusters has no members.</p> <p>Computation time of FCM algorithm is dependent on the image size.</p>
	Hard Clustering- K-Means (KM) algorithm	<p>Simplicity, scalability in handling big data sets.</p> <p>Easy implementation</p>	<p>Strongly depend on random selection of initial cluster centres.</p> <p>Initialization of cluster centroids by randomization strategy makes the algorithm not repeatable as it yields results for multiple runs.</p> <p>K-means' dependency on selection of initial cluster centres before implementation is usually time consuming.</p>

			<p>Random initialization of cluster centroids causes convergence to the nearest or trapped into local minima.</p> <p>Random initialization of cluster centroids often leads to the dead centre syndrome, a situation that one or more clusters have no members.</p>
--	--	--	---

2.5 Colour Image Segmentation Methods

Not until recently has colour image segmentation attracted more and more attention mainly due to reasons mentioned in the chapter one of this dissertation. There has been a remarkable growth in the number of image segmentation algorithms for segmentation of colour images in the last decade. Mostly, colour segmentation methods are as a result of dimensional extensions of existing image segmentation algorithms originally proposed for greyscale images. Colour image segmentation is performed by partitioning the image pixels of an image into separate regions grouped as connected pixels sharing homogeneous colour properties (Losson, Botte-Lecocq and Macaire 2008). Pixel based image segmentation algorithms are naturally suited for segmenting colour images because of their generalization potential, such as the ability to process complex multidimensional image data. They take real advantage of the characteristics of image pixels in trichromatic red, green and blue colour channels.

The application of pixel based image segmentation algorithms to colour image segmentation is based on the fundamental assumption that homogeneous regions give rise to unique clusters when projected onto a colour model and each cluster in an image defines a class of pixels that share similar colour properties (Khattab *et al.*, 2014). Diverse pixel based image segmentation algorithms have been extensively used for colour image segmentation in different colour models, but they differ primarily on the basis of the colour histogram dimensions such as 3-D, 2-D and 1-D (Lezoray and Charrier 2009). The entire colour channels are processed concurrently for clustering algorithms that analyse a 3-D histogram of a colour image. These algorithms belong to the vectorial approach (Shih and Liu 2016). The

watershed clustering of colour images in the RGB colour model falls into this approach (Géraud et al., 2001). However, clustering a 3-D histogram is computationally expensive and memory demanding because of the huge volume of data to be processed (Xue *et al.*, 2003). The projection of the 3-D histogram onto a lower dimensional space, using the bi-marginal and marginal histogram approaches, is a holistic strategy to overcome computational complexity and memory requirement. The bi-marginal histogram approach, such as the morphological clustering, involves the analysis of a 2-D histogram that combines two Colour channels such as RG, RB and GB (Lezoray and Charrier 2009).

The use of the bi-marginal histogram approach for colour image segmentation has been reported in the literature (Rajaby et al., 2016; Lezoray and Charrier 2009) and the volume of data encountered is partially surmounted and computational complexity is to an extent reduced. However, a further reduction in data volume and lower computational complexity can be achieved using the marginal histogram approach that analyses a 1-D histogram. For this reason most approaches consider 1D histograms computed for one or more colour channels in a colour model. Therefore, marginal histogram algorithms are often used for colour image segmentation to process each colour channel separately that is the marginal correlation between colour channels is ignored and each colour component is considered as a greyscale image. Several colour image segmentation algorithms based on the marginal histogram have reported good segmentation results (Sural *et al.*, 2002; Makrogiannis *et al.*, 2005, Christ *et al.*, 2011; Jumb *et al.*, 2014; Randhawa and Mahajan 2014). However, processing each of the colour channels separately results in the loss of relevant chromatic information offered by chrominance channels of a colour model (Veganzones *et al.* 2015).

2.5.2 Colour Based Saliency Segmentation Methods

Asides the dimensional extensions of several existing image segmentation algorithms originally proposed for greyscale images to colour images. Research has revealed that humans have an inimitable ability to locate important objects in an image, identify it, comprehend the context, match the identified image with another one. The human vision system is an intelligent processing system that is capable of detecting and separating the most visually distinctive parts of an image while ignoring others. This perceptual quality that renders of an object in an image to pop out from its surroundings and immediately attract human attention in terms of their shape, symmetry, colour, brightness.

Saliency segmentation method is a task of locating the most informative region in an image, based on the human vision system whereby the salient and non-salient part of the image become foreground and background regions respectively. The task receives an image as an input, transform it into a 2-D intensity map called a saliency map. A saliency map is an image with high intensity indicating the high saliency regions that attract human attention most. The process of detecting salient objects is a challenging task because the notion that saliency is purely subjective, which is a rapidly growing research area in image processing that has received a great deal of attention in cognitive science, computer vision and related fields. Consequently, computational models for generating saliency maps from images is thus a great interest to the computer vision community because it facilitates image segmentation and feature segmentation tasks including the segmentation of foreign fibre in cotton (Yang *et al.*, 2013), content based image retrieval (Pirnog *et al.*, 2009), segmentation of skin lesion (Ahn *et al.*, 2015), among many others. Motivated by the various applications of salient object segmentation, several saliency segmentation computational models have been proposed.

Generally speaking, saliency segmentation methods can be classified into two categories which includes top-down and bottom-up (Gao *et al.*, 2014; Zhang *et al.*, 2015). The top-down method is a slow, high level task-specific search that requires prior information concerning the input image to detect the position of the salient object (Riche *et al.*, 2013; Banerjee *et al.* 2016). They require pre-specified information to analyse and process saliency information. However, these methods are memory based and hence require more memory capacity to carry out computations. Most studies on top-down saliency segmentation are still at descriptive and qualitative levels that is few completely implemented computational models are available. Therefore, it is still a difficult and deeply researched problem yet to be solved (Hou and Zhang 2007; Gu *et al.* 2015).

Contrarily, bottom-up saliency methods are purely data driven, unsupervised and task independent that predict the human visual system given a prior knowledge of the visual content, based on intrinsic low level features, such as colour contrast, intensity and texture information to identify the salient objects. The method is reportedly task independent, fast and requires a simple pre-attentive process. Consequently, several existing saliency segmentation methods are based on the bottom up approach to compute the salient object in an image. When proposing a saliency segmentation method, features such as colour, intensity, texture are the basic elements to detect a salient object in an image. Afterwards, a

computational model can be applied to compute the degree of saliency in each of the pixels. A normalization process is performed to ensure the saliency value falls between the range of 0 and 255 (Wang *et al.*, 2013).

It has been alluded by previous authors that a good saliency segmentation model must satisfy three important criteria of good segmentation, high resolution and computational efficiency (Borji *et al.*, 2014). Good segmentation means that the probability of missing real salient objects and falsely marking background regions as salient objects should be low. High resolution means that the saliency map should possess a high resolution to accurately locate salient objects and retain original image information. Computational efficiency means that saliency segmentation methods rapidly detect salient objects. In this study, we focus on relevant literature targeting the bottom up saliency segmentation methods which is directly relevant to the work reported in this study. When we look at an image, some objects attract the observer's attention due to the fact that their colours are distinct to their surrounding areas.

Since human vision is very sensitive to colour, colour plays an important role in detecting saliency. As a result of this, several existing saliency segmentation methods that have been proposed in the literature are based on image colour features. According to the spatial scope of saliency computation, bottom-up methods can further be divided into two groups: global contrast-based models and local contrast-based models (Cheng *et al.*, 2015; Kim *et al.*, 2016). The global contrast bottom-up methods detect salient object by computing the colour contrast of the region of interest over the entire image. On the other hand, local contrast bottom-up methods measure saliency by computing the colour contrast of the region of interest in a centre-surround local region (Fan and Qi 2016; Qu *et al.*, 2017).

One of the first biological inspiring models for simulating visual attention was proposed by Itti, Koch and Niebur (1998) based on Koch and Ullman's biological plausible architecture (Koch and Ullman 1987). Their study of the theory of visual receptive fields, which states that typical visual neurons are most sensitive in centre-surround regions. They proposed the first bottom up saliency segmentation method which use a difference-of-Gaussian (DoG) approach to compute local colour contrast based on low level visual features like colour, intensity and texture. The model takes in an input image, which is decomposed into three channels based on the low level visual features to yield a set of feature maps through calculating the multi-scale centre-surround differences for each of the features. The

feature maps for each of the channels are then normalized and linearly combined to create the final saliency map.

The proposed Itti and Koch's saliency model is considered as a milestone in saliency segmentation and has served as a classical benchmark model for evaluation purposes. However, the method has been criticized as being computationally expensive. It also generates saliency maps that have low resolution or poorly defined borders and it has many parameters that require to be hand-selected (Zhang *et al.*, 2008). Since Itti et al., (1998) introduced the first computational model of visual saliency, scientists in the image processing and computer vision research field have devoted considerable time and effort to develop improved computational models of visual attention which at least exhibits the characteristics of a human vision and improve the performance of Itti, Koch and Niebur (1998) in the literature. Harel *et al.*, 2003 follow Itti's modeling concept, but instead suggest a graph-based visual saliency (GBVS) saliency segmentation model.

The proposed model examines the dissimilarity of centre-surround feature histograms, formed saliency maps based on Itti's feature maps and performed normalization using graph-based statistics in a way which highlights conspicuity and admit combination with other maps. The authors reported that the proposed approach greatly improved over that of Itti's. However, while the resolution of an image is high, the computation speed of the proposed method becomes slow. Ma and Zhang (2003) proposed a local colour-contrast saliency segmentation method independent of the biological model. The proposed method computes image saliency value with a local contrast operator by considering the CIE L^*u^*v colour features using the different salient unit to describe the salient object by using fuzzy growing to extract salient objects from the saliency map. The proposed approach emphasizes regions whose local contrast is high, so the salient object edge area is often excessively highlighted, while the inner region region of the object is not highlighted consistently. Moreover, the proposed approach is relatively time consuming (Chen *et al.*, 2016).

Zhai and Shah (2006) defined pixel-level saliency by contrast to all other pixels and proposed a method to detect salient objects by comparing each pixel to all others in the image based on luminance information only, thereby ignoring distinctive information in the chrominance channels believed to convey important information in colour images. Although the proposed method is simple and computationally fast. However, the proposed method suffers difficulty in detecting image borders in sample images used for experimentation.

Shortly, Hou and Zhang (2007) extract the salient object of an image based on the assumption that salient object segmentation models assume that the central part of an image is more likely to contain the foreground information while the borders of an image are more likely to contain the background information. They proposed a method whose principle is based on the spectral domain and information theory named spectral residual approach.

The approach is based on the inverse discrete Fourier Transform (DFT) of the difference between the raw and smoothed amplitude components in the spectral domain to calculate the visual saliency of an image. The colour channels in the input image are processed independently, the image is Fourier transformed and the magnitude components are attenuated. Then, the inverse Fourier transform is calculated using the manipulated magnitude components in combination with the original phase angles. With Inverse Fourier Transform, the spectral residual is converted to spatial domain, where it is used to construct a saliency map. Although the method was computationally efficient in the frequency domain of an image and can only indicate the probable position of the salient object, but cannot find the exact position and contour of the salient object.

Guo, Ma and Zhang (2008) argued that the spectral residual of the amplitude spectrum is not essential to obtain the saliency map as proposed earlier by Hou and Zhang (2007). They applied the quaternion DFT to realize the spectral residual for quaternion images, which reduced the required number of focus of attention shifts to find manually specified objects in test images. Therefore, they proposed the use of quaternions as a holistic colour image representation for spectral saliency calculation. As an alternative to treating colour channels separately, they were able to Fourier transform the image as a whole, and consider the contrast for images from the global perspective. The authors reported that the resulting saliency maps better preserve the high level structure of an image than the ones reported in Hou and Zhang (2007) and Itti, Koch and Niebur (1998). However, these approaches suffer some shortcomings in saliency segmentation. One of them is that these proposed models cannot detect smooth-texture salient objects in the complex-textured background since the complex-texture areas are less homogeneous. Moreover, they have to resize the images into a smaller size to allow the salient object to be less homogeneous, as a result of this, these methods generate blurred saliency maps and tend to detect object boundaries rather than its entire area (Achanta *et al.*, 2009; Perazzi, *et al.*, 2012).

The importance of selecting an appropriate colour model for saliency segmentation has been emphasized in the literature. It has been reported in the literature that the choice of a colour model can significantly affect the final result of a saliency segmentation algorithm (Guo, Ma and Zhang, 2008; Hou, Harel and Koch, 2012; Schauerte and Stiefelhagen, 2012). Achanta *et al.*, 2009 suggested that the method proposed by Zhai and Shah (2006) did not perform optimally because they failed to exploit all the spatial frequency content present in the original image. They introduced a global contrast based frequency-tuned saliency segmentation algorithm that exploits low and high frequency contents using colour and intensity features.

Multiple DoGs of several narrow passbands are combined to obtain a filter and thereby computed saliency of a pixel as the difference between the averaged image and the filtered image. The experimental result shows that the proposed method produces saliency maps with uniformly highlighted and well-defined boundary saliency maps and tolerant to noise. However, the method only considers first order average colour, which can be insufficient to analyse complex variations common in natural images and does not account for any spatial relationship present in the image. Moreover, in the presence of large salient objects or complex backgrounds, the method may fail to correctly highlight the salient objects and retention of high frequencies may cause poor results as noise which makes it not flexible enough to solve complex variation of colours in natural images (Anchanta and Süsstrunk 2010).

Anchanta and Süsstrunk (2010) addressed this limitation by varying the bandwidth of the centre surround filtering. They computed the mean value as background, where such averaging operation is implemented in whole image or local region. However, such single value based background map is not robust because in natural scenes, background regions are usually complex. Therefore, background regions will be falsely marked as the salient object. Goferman *et al.*, (2012) proposed a context-aware saliency segmentation method which can highlight salient objects along with their context to generate the saliency map based on low-level clues, global considerations, visual organization rules and high-level features to build saliency segmentation model. Moreover, a context aware ability is achieved by calculating the geometric distances between every pixel to focus point. However, the method usually produces higher saliency values nears edges and cannot uniformly highlight the whole salient objects and suffered high computational complexity (Chen *et al.*, 2014).

Perazzi *et al.*, (2012) proposed a contrast-based saliency estimation method combining global contrast and spatial relations to detect salient objects. The proposed approach decomposed an input image into compact and perceptually homogeneous elements, and then considered the uniqueness and spatial distribution of these elements in the CIE L^*a^*b colour model to detect the salient objects in an image. Although the method yields satisfactory result in most of the test images used during the experiment. However, in some cases, the method cannot differentiate the salient object or region with sufficiently complete contours and detailed local texture from a complex background that is they falsely mark background as salient objects in some cases. Moreover, substantially more parameters are needed to produce satisfactory results as the method sometimes falsely identifies the background as the salient object.

Following similar trend, Yang *et al.* (2013) proposed a saliency based colour image segmentation in foreign fibre segmentation based on brightness and colour features fusion. The authors computed the mean value of the colour feature was computed over the entire image to generate the saliency map for each of the RGB colour features. The resultant saliency map was fused from three saliency maps derived from the red, green and blue channels of the RGB colour model. Chen *et al.*, 2014 proposed a multiple background map based saliency segmentation approach. Their method first generates multiple background maps through local averaging operation. Once the background maps are generated, the salient objects are estimated by measuring the differences between the original images and their corresponding background maps based on the Euclidean distance metric in CIE L^*a^*b colour model to compute candidate saliency maps. To further improve the performance of the proposed approach, they incorporated spatial distribution as a high-level factor to suppress background information and simultaneously highlight salient objects. The authors reported that experimental results reveal that the proposed approach performs well in general. However, it fails when background estimations are not valid.

Cheng *et al.*, (2015) proposed a global contrast Gaussian mixture model based abstract representation method to measure saliency. They introduced two colour histogram based saliency segmentation methods. They proposed global contrast based approaches that include a histogram-based (HC) contrast and region-based (RC) methods, by using a quantized and smoothed colour histogram to improve the salient object segmentation accuracy that simultaneously evaluates the global contrast differences and spatial coherence to capture perceptually homogeneous elements. They incorporated colour information and the

spatial information in the HC method to generate the full resolution saliency map. The HC saliency maps assign pixel-wise saliency values based on colour separation from all other image pixels to produce full resolution saliency maps. Although the proposed HC method accelerates the speed of computing global saliency. However, the method does not perform well in textured scenes. On the other hand, the RC method computes the saliency value of a region using a global contrast score, measured by the region's contrast and spatial distances to other regions in the image. Although the RC method produced saliency maps better than the HC maps by incorporating spatial relations. However, it is neither full resolution nor efficient because it considers only the colour feature at local level, thus resulting in a fuzzy salient map with incomplete contours of the object and local texture information. The authors added the proposed approach might produce sub-optimal results for with multiple objects, especially if the objects occlude each other.

Summarily, local contrast based methods perform well and produce higher saliency around the edges and textured areas that exhibit high contrast, where humans tend to focus on in an image. However, these methods produce an unsatisfactory outcome in highlighting the whole salient object or object in an image. On the other hand, global contrast methods can detect the complete object as they mainly consider a few specific colours that distinguish the foreground and the background of an image without considering the spatial relationships. However, global methods have a performance bottleneck in distinguishing similar colour features in the foreground and background regions in an image and local high contrast can be ignored. Moreover, they suffer from the involved combinatorial complexity. Hence, they are applicable only to low resolution images or colour models of reduced dimensionality (Peng *et al.*, 2013; Qi *et al.*, 2017). The human vision system follows a centre-surround approach in the early visual cortex and highly sensitive to the local high contrast. Thus, proposing the use of either global or local colour contrast measures might not be very reasonable. Hence, there is a need to develop a saliency segmentation method to generate saliency maps with full resolution in linear computation time.

2.5.3 Image Segmentation Based on Different Colour Models

The number of colour models developed for colour image segmentation task is far wider than one could imagine at a first glance. Several dozens of colour models literally exist, usually in a straight relation to their specific use. Thus, there are colour models that give optimal

performance in fabric industry, paper industry, television, computers, agriculture, biometric, medical, product images and even for foods. As earlier stated in chapter one of this dissertation that the selection of the best colour model is also one of the difficulties faced in the colour image segmentation research field. In this section, a review of existing studies has shown that selecting the optimal choice of colour model in colour image segmentation remains a challenging problem in image processing and computer vision. To date, there is no colour model that is better than the others and more suitable for all classes of images (Busin, Vandenbroucke and Macaire 2008; Jurio *et al.* 2010; Khattab *et al.* 2014).

Over the years, researchers have attempted to identify the best colour model for a specific task in diverse application areas. Kwok, Ha and Fang (2009) in an attempt to study the effect of different colour models on the performance of colour image segmentation presented a study to determine a suitable choice of colour model for aerial images, based on the YIQ, YUV, $I_1I_2I_3$, HSI and HSV colour models. They proposed a segmentation procedure based on maximizing the information contents. The information content that is measured from a colour model is obtained from the entropy calculated from the probability distribution. To verify the performance of the proposed image segmentation method, two copies of the aerial image over planted fields are used in the experiment. The authors reported that experimental results revealed that the highest information contents were obtained from the 'R' and 'Y' colour channels in the RGB and YIQ colour model respectively. Research work was about crop segmentation to achieve real-time processing in real farm fields. Ruiz-Ruiz, Gómez-Gil and Navas-Gracia (2009) presented a comparative study between RGB and HSV colour models to achieve real-time processing in real farm fields. The authors analysed the environmentally adaptive segmentation algorithm (EASA) for crop recognition. They applied a modified EASA to work on different colour models and further proposed plant segmentation algorithms to distinguish between crops and weeds. The authors reported that the best accuracy was derived using the HSV colour model.

Skin colour segmentation is one of the popularly used techniques in face detectors to detect faces in images or videos. However, there is not a common opinion about which colour model is the best option to perform this task, Chaves-González *et al.* (2010) presented a study to realize which colour model is the best option to build an efficient face detector which can be embedded in a functional face recognition system based on ten different colour models. The authors developed a K-means classifier with some improvements to carry out the experiment with images used in face recognition systems from the AR database and their corresponding ground truth image as a basis of comparison. The classification results given by

each of the colour models are compared with the ground truth images and they reported that the HSV colour produced the highest segmentation rate for human skin recognition. They added that the RGB colour model did not perform well because it is not robust to changes in illumination. However, the chrominance channel X of the XYZ colour model performed better when compared to the RGB colour model. But, it is generally unsatisfactory for colour oriented applications in the case of skin colour segmentation. Yang, Liu and Zhang (2010) proposed colour space normalization techniques (CSN) to determine the suitable colour model for enhancing the discriminating power of colour spaces for face recognition, based on six colour models. The performance of different colour models was assessed using a large scale face recognition grand challenge database. The authors reported that the assessment results reveal that colour models like $I_1I_2I_3$, YUV, YIQ and LSLM colour models produced optimal results for face recognition. However, the RGB and XYZ colour models are relatively weak for face recognition.

Biometric identification verifies user identity by comparing an encoded value with a stored value of the concerned biometric characteristics. Thepade and Bhondave (2015) investigated the effectiveness of colour models on iris and palm print images. The authors considered six colour models in their study, which are RGB, Kekre's LUV, YCbCr, YUV, YIQ and YCgCb and proposed a technique by combining finger geometry and palm print modalities to enhance identification accuracy. The proposed system based on multimodal identification, was carried out using feature extraction and query execution on selected sample images. The authors noted that amongst the six colour models used in the study, the YCgCb colour model produced the best recognition result. Still on identifying unique features based on biometric, Rungruangbaiyok, Duangoithong and Chetpattananondh (2015) proposed an Ensemble Threshold Segmentation (ETS) technique to segment hand images for hand segmentation based systems. The proposed method was designed to analyse the threshold value to segment hand image based on skin colour and compare ensemble threshold segmentation (ETS) with RGB, HSV, YCbCr, YIQ, YUV colour models. The experiment was carried in two basic steps, finding the threshold step to find the optimized threshold range and the segmentation step based on the optimized threshold range from the first step to segment the hand image. The authors reported that experimental results show that the proposed technique obtained best accuracy, using the HSV colour model.

In the medical field, researchers have also made attempts to test effectiveness of colour models using medical images. Harrabi and Ben Braiek (2014) performed colour image segmentation of breast cancer cell images to separate cells from the background using a

modified Fuzzy C-Means technique. The clustering algorithm was applied on each of the channels of the four colour models used to carry out the experiment. The proposed clustering algorithm was applied to the twelve (12) channels of RGB, HIS, YIQ and XYZ. The selection of the optimal colour model was based on the segmentation sensitivity criterion, the best components were found in the R, H, Y, X channels of the RGB, HSI, YIQ and XYZ colour models respectively using a large variety of medicinal and synthetic colour images.

The experimental results showed that R channel in the RGB colour model and H channel in the HSI produced satisfactory results. However, due to the high correlation among the components of the RGB colour model, there were missing features in some of the breast cancer cell images. Khan *et al.* (2015), carried out colour image segmentation of acne lesion using Fuzzy C-means clustering algorithm based on RGB, normalized RGB, YIQ and $I_1I_2I_3$ colour models. In the proposed approach, fifty colour images of acne patients were transformed into the various samples of colour models used, the images are then decomposed into the specified number of homogeneous regions based on the similarity of colour using fuzzy C-means cluster algorithm. The best results were obtained from the Q channel of the YIQ colour model and the I_3 channel of the $I_1I_2I_3$ colour model as they show robustness against non-uniform illumination. It was observed that the normalized RGB colour model produced a better result compared to the RGB colour model which gave a poor performance in segmentation.

Luszczkiewicz-Piatek (2014), conducted a study on the proper choice of colour model for colour image retrieval based on eight different colour models using Gaussian Mixture Model (GMM) as a colour distribution descriptor. Test colour images were selected from a corpus which consists of 1000 colour images categorized into 10 thematically consistent categories. The CIE L^*a^*b and $I_1I_2I_3$ colour model were found to be the best for image retrieval, which is as a result of the decorrelation of the RGB components. Khattab *et al.* (2014) presented a comparative study in different colour models using the automatic Grabcut technique. The authors proposed the method that utilized the (Orchard and Bouman 1991), a Colour quantization clustering technique to eliminate user interaction for initialization during segmentation process, an improvement of the original grabcut, a semiautomatic image segmentation technique. The proposed automatic Grabcut technique was experimentally tested using a corpus of different images. They reported that the RGB colour model gave the best results for most of the selected images. In addition, the YUV and XYZ colour models also gave better results. John *et al.* (2016) carried out a comparative study to test the effectiveness of ten different colour models on single image scale-up problem. The authors

conducted the experiment by transforming the scale-down image using the super resolution algorithm. The super resolution algorithm was applied to the sampled images based on the ten different colour models. The authors reported that the comparison of different colour models was carried out by visual perception and PSNR metrics. The experiment results show that the YCbCr and CMYK colour models gave better results for single image scale-up applications. A review of several colour image segmentation based on different colour models in diverse application domains has clearly shown that there is no colour model that is better than the others and more suitable for all classes of images. The table below presents the summarized review of the colour image segmentation study.

Table 2.3 Summary of Colour Image Segmentation Methods Based on Different Colour Models.

Authors	Test Image type	Colour model	Segmentation Algorithm	Evaluation Metrics	Results
Kwok, Ha and Fang (2009)	Aerial images	YIQ, YUV, I ₁ I ₂ I ₃ , HSI, HSV	Entropy based segmentation algorithm	Highest entropy found in R and Y channels of the RGB and YIQ colour models	The HSV colour model gave the best result.
Ruiz-Ruiz, Gómez-Gil and Navas-Gracia (2009)	Farmland crop images (sunflower)	RGB, HSV	K-Means clustering algorithm Bayesian classifier	False positive rate False negative rate	The HSV colour model gave the best result.
Chaves-González <i>et al.</i> (2010)	Face images	RGB, CMY, YUV, YIQ, YPbPr, YCbCr, YCgCr, YDbDr, HSV, CIE-XYZ	K-Means classifier	Right segmentation rate False positive rate False	HSV, YCgCr and YDbDr colour models gave the best results.

				negative rate	
Yang, Liu and Zhang (2010)	Face images	RGB, XYZ, HSV, L*a*b, I ₁ I ₂ I ₃ , YUV, YIQ, LSLM	Feature extraction method	Verification rate Recognition rate	I ₁ I ₂ I ₃ , YUV, YIQ, LSLM colour models gave the best results.
Jurio <i>et al.</i> (2010)	Natural images	RGB, CMY, HSV, YUV	Ignorance-based clustering algorithm Entropy-based fuzzy clustering algorithm	Similarity (SIM) metric	The CMY colour model gave the best result for both clustering algorithms
Reddy and Reddy (2014)	Natural images	RGB, YUV, XYZ, L*a*b, HSV, YCC, CMYK	Dynamic Histogram based Rough Fuzzy C-means (DHRFCM)	Davis-Bouldin index Rand index Silhouette index Jaccard index	HSV and CMYK colour models gave the best results.
Harrabi and Ben Braiek (2014)	Breast cell images	RGB, HSI, YIQ, XYZ	Modified Fuzzy C-Means algorithm	Sensitivity rate	“R” channel of RGB and H channel of HSI colour model gave satisfactory results
Luszczkiewicz-Piatek (2014)	Product images	RGB, I ₁ I ₂ I ₃ , YUV, CIE XYZ, CIE L*a*b, HSx,	Gaussian Mixture Model (GMM)	Kull back-leiber based similarity measure	I ₁ I ₂ I ₃ and CIE-L*a*b gave the best results.

		LSLM, TSL	Expectation- Maximization (EM) algorithm	Earth movers distance similarity measure Precision and recall	
Khattab <i>et al.</i> (2014)	Natural images	RGB, HSV, CMY, XYZ, YUV	Automatic Grabcut	Error rate Overlap rate	RGB, YUV, XYZ colour models obtained the best segmentation results
Khan <i>et al.</i> (2015)	Acne lesion skin images	RGB, normalized RGB, YIQ, I ₁ I ₂ I ₃	Fuzzy C- means clustering algorithm	Sensitivity Specificity Accuracy	Q channel of YIQ colour model and I ₃ channel of I ₁ I ₂ I ₃ colour models obtained the best results
Thepade and Bhondave (2015)	Iris and palm print images	RGB, L*u*v, YCbCr, YUV, YIQ, YCgCb	Feature extraction method Block Truncation Coding (BTC)	Mean Square Error (MSE) Genuine acceptance rate (GAR)	The YCgCr colour model gave the best performance result compared to the other ones
Rungruangbaiyok, Duangsoithong and Chetpattananondh (2015)	Hand images for hand segmentation	RGB, HSV, YCbCr, YIQ, YUV	Ensemble threshold segmentation	Accuracy rate	HSV and RGB colour models gave the best results for hand

					segmentation
John <i>et al.</i> (2016)	Natural images	YCbCr, YCoCg, HSV, YUV, XYZ, YCC, CMYK, YIQ, L*a*b, YPbPr	Scale-operation based on training and reconstruction	PSNR	YCbCr and CMYK colour models gave almost equal and effective results.

2.6 Image Segmentation Performance Evaluation

One of the inevitable challenges in the development of image segmentation methods is a comprehensive measure of their accuracies (Vojodi, Fakhari and Moghadam 2013). The evaluation of the quality of image segmentation algorithms is an indispensable subject in image processing and computer vision (Feng *et al.* 2016). The performance assessment of image segmentation methods in image processing depends on several factors, which includes the nature of images used for performance assessment, the algorithm parameters used during the evaluation and the evaluation method.

2.6 1 Benchmark Data sets

Benchmark data sets are valuable resources, as image segmentation algorithm developers often rely on benchmark data sets for quantitative and qualitative evaluation of performance of a newly proposed method (Khan *et al.*, 2015; Setti *et al.*, 2017). Therefore, numerous benchmark data sets have been developed for benchmarking and validation of image segmentation algorithms in the literature for diverse application domains. Examples include the Berkeley benchmark segmentation dataset (Martin *et al.*, 2001), cell image analysis (Ruusuvaori *et al.*, 2008), semantic automation, image annotations using complex scenes (Escalante *et al.*, 2010), event recognition in surveillance videos (Oh *et al.*, 2011), traffic signs benchmark dataset (Stallkamp *et al.*, 2011), motion segmentation (Mahmood *et al.*, 2017) and skin lesion analysis toward melanoma segmentation (Gutman *et al.*, 2016). The performance assessments of image segmentation algorithms do not only rely on the quality of the proposed image segmentation algorithm for validation, but also on its robustness to cope

with unknown distortions to test the robustness of the proposed algorithm. Hence, the availability of ground truth images to compare with the segmented output aside, benchmark data sets are required to contain images with distortions, varying illumination conditions, noise and other artefacts, which in some cases will include the presence of artefacts to occlude the problem region, thereby distorting the required information to be extracted from an image, usually common with medical images.

Medical image processing evaluation benchmark data sets are one of the fastest growing benchmark dataset as they are fast becoming evaluation standards for newly proposed image segmentation algorithms (Maier *et al.*, 2017). They are significant to support researchers in the development of algorithms to assist in clinical diagnosis, treatments and even in some case surgery (Gutman *et al.*, 2016; Wang *et al.*, 2016). In the medical image processing research field, the number of challenging data sets has continued to increase over the past years with diverse proposed challenges, including segmentation of tumours in MRI brain data (Menze *et al.*, 2015), lung vessel segmentation in computed tomography scans (Rudyanto *et al.*, 2014), prostate segmentation of MRI (Litjens *et al.*, 2014) and melanoma skin lesion segmentation (Gutman *et al.*, 2016). They consist of sample test images, associated ground truth created by experts following a clearly defined set of rules and evaluation metrics. Most importantly, they are usually open access for interested contestants and for benchmarking newly proposed image segmentation algorithms.

2.6.2 Image segmentation Evaluation Methods

Several algorithms for evaluating image segmentation algorithms have been reported in the literature which can be classified into qualitative (subjective) and quantitative (objective) methods (Seghir and Hachouf 2011; Feng *et al.* 2016). Qualitative evaluation is one of the most commonly used methods for assessing the quality of image segmentation algorithms (Zhang, Fritts and Goldman 2008). In this method, the human observer visually compares the image segmentation results to estimate the image quality. Subjective evaluation methods are useful for validating segmentation results, however, these methods are highly subjective because interpretations of evaluation results can vary significantly from one judge to another (Sun *et al.* 2016). Moreover, subjective evaluation of image quality is time consuming, difficult to exploit and it does not provide the capability to generalize results due to the vision discrepancy of humans. This is because it inherently limits the depth of evaluation to a

relatively small number of segmentation comparisons over a predetermined set of images (Zhang, Fritts and Goldman 2008; Johnson and Xie 2011; Liu *et al.* 2016). This has led to the development of quantitative image quality assessment metrics to compute and measure image segmentation quality (Zhang *et al.* 2011).

Quantitative evaluation methods refer to the objective assessment of image quality using well-known analytic approaches to compute visible errors between distorted images as it would be perceived by an average human (Johnson and Xie 2011). Quantitative evaluation methods can be classified into system-level and direct evaluation methods. System-level evaluation methods are popularly used in systems/application domains to examine the impact of several image segmentation methods on the overall system to determine whether or not a specific image segmentation algorithm is better than the other for a specific application domain. Meanwhile, the direct level evaluation methods are further classified into analytical and empirical methods. The analytical evaluation methods focus on analysing the properties of a proposed image segmentation algorithm, such as its processing strategy, complexity, and efficiency (Polak, Zhang and Pi 2009). Finally, the empirical methods are divided into supervised and unsupervised methods, based on whether or not prior information is available (Vojodi, Fakhari and Moghadam 2013).

Supervised evaluation methods, also called relative evaluation or empirical discrepancy methods, require prior knowledge, such as an original image or a ground truth image, to measure the error in the segmentation results (Johnson and Xie 2011). Thus, image segmentation algorithm performance is measured according to dissimilarities between the segmentation output and the ground truth image. Based on the availability of reference images, supervised objective image segmentation methods can further be classified into full-reference (FR), reduced-reference (RR) and no-reference approaches (NR) (Wang *et al.*, 2016a; Zhang *et al.*, 2016). Full-reference approaches require a complete input reference image with which the distorted/segmented image can be compared (Wu, Lin and Shi 2014; Lin *et al.* 2015). However, the disadvantage of full-reference approaches is that the reference images are not usually accessible in most practical applications (Yu *et al.* 2016). As a solution, no-reference approaches were proposed to predict the quality of distorted or the segmented images without any prior knowledge of original reference images (Wang *et al.* 2016a), however, several existing no-reference approaches may only be effective for specific types of images or specific types of distortions (Yu *et al.* 2016). As an alternative to the above mentioned approaches, reduced-reference approaches were proposed. The approaches

require partial information concerning the reference or the original image (Soundararajan and Bovik 2013).

The unsupervised evaluation methods, also called the stand alone algorithm or empirical goodness methods, quantitatively compute image segmentation quality based on some parameters relevant to the visual properties extracted from the original and the segmented image, without any prior knowledge to compute the errors in segmentation results (Vojodi, Fakhari and Moghadam 2013). In this method, no human intervention or a manually segmented image or pre-processed reference images are needed, however, experimental results have shown that the proposed unsupervised evaluation methods are far from being perfect (Zhang, Fritts and Goldman 2008).

The hierarchy of image segmentation evaluation methods is presented in the figure below.

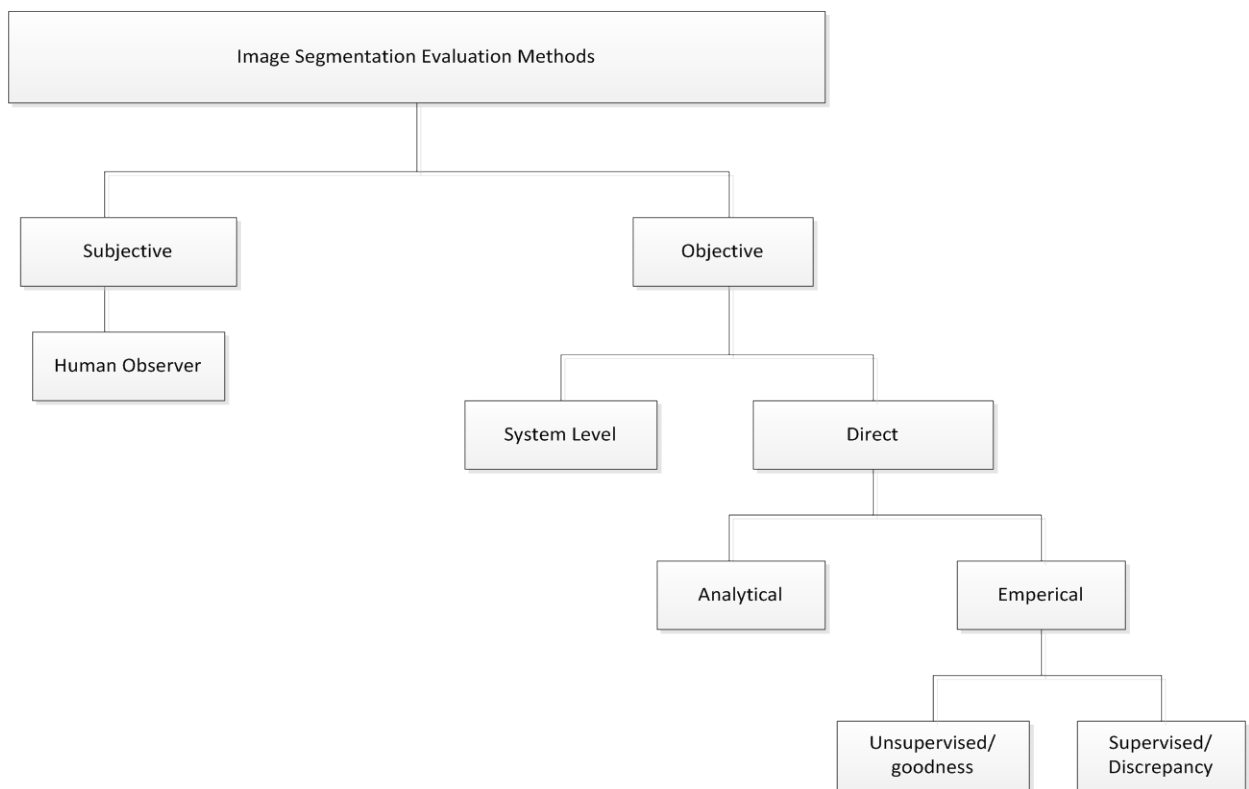


Figure 2.1: Image segmentation evaluation methods (Zhang, Fritts and Goldman 2008; Zuva et al. 2011)

2.7 Chapter summary

As a conclusion of this chapter, the chapter comprehensively review relevant publications based on an image segmentation algorithm. This serves as a foundation for the current study reported in this dissertation. This chapter, which contains six sections where each of the sections reported gives detailed description of relevant topics directly related to the current study, making special emphasis on different strategies and methods proposed in the literature by identifying their strengths and pitfalls. As described in the introductory part of this chapter that image segmentation remains a significant, but complex problem that has led to the development of countless image segmentation algorithms to address the problem. From the review, it can be observed that there is no single solution to the problem of image segmentation despite the persistent efforts of researchers in this field. This serves as a motivation for the current study to develop an image segmentation algorithm to improve the performance of colour image segmentation. The next chapter explains the methodology that was followed to reach the set research aim and objectives of this study.

CHAPTER THREE

METHODOLOGY OF THE STUDY

This chapter presents the methodological steps followed in this study in order to accomplish the research aim and objective 2 of this study as outlined in Chapter 1. Firstly, the image data set acquisition process is discussed. This is followed by the basic steps taken towards the development of the proposed image segmentation algorithm which is based on four sequential steps: colour image transformation, luminance image enhancement, salient pixel computation and image artefact filtering. The subsequent sections will then elaborate on each stage of the proposed segmentation algorithm.

3.1 Image Datasets Acquisition

The researcher mentioned in the previous chapter two of this study that the development of a unified image segmentation algorithm that can be applied to all classes of images is still a challenging task and remains an open problem in image processing research field. Since there exist several image data sets that offer diverse classes of experimental images. It becomes interesting that different image segmentation algorithms are likely to perform differently across diverse image data sets. Essentially, a good method should be able to perform optimally over diverse data sets so as to draw both qualitative and quantitative conclusions. Therefore, in this study, the researcher chooses to explore four publicly available segmentation benchmark data sets; two melanoma skin lesion image data sets and two real life natural image data sets. Moreover, the selection of diverse image data sets will inject diversity so as to avoid the tendency of the segmentation results being biased. Four image data sets explored in this study include the International Symposium on Biomedical Imaging (ISBI) 2016 challenge dataset, Pedro Hispano Hospital (PH2) data set, Microsoft Research Asia dataset (MSRA) and the Extended Complex Scene Saliency Dataset (ECSSD). These image data sets are selected based on the following accompanying attributes:

1. They are public and easily accessible,
2. They provide diverse image types and quality levels, but challenging images for various computer vision applications,
3. They contain a substantial number of images,

4. They are prospective benchmark image data sets

Moreover, most of the images available in these image data sets fit into the class of binary image segmentation for foreground and background separation. The four different types of image data sets explored in this study are discussed in detail below.

3.1.2 ISBI 2016 Challenge Dataset

The first dataset explored in this study is ISBI 2016 challenge dataset. The dataset is a subset of the large international skin imaging collaboration archive for the 2016 International Symposium on Biomedical Imaging (ISBI) challenge titled “Skin lesion analysis toward melanoma detection” (Gutman *et al.*, 2016). It contains melanoma images acquired from a variety of different devices at numerous leading international clinical centres. The dataset contains 900 melanoma skin lesion images. The skin image sizes vary from 1022 by 767 to 2848 by 4288 and ground truth images provided by expert dermatologists are made available in the dataset. The ISBI dataset, particularly inspired the researcher because it contains numerous challenging melanoma skin lesion images. A melanoma skin lesion image is considered to be “challenging” if one or more of the undesirable factors are met such as low contrast between the lesion and the healthy skin, presence of thick and thin hairs, air bubbles. For the purpose of experimentation performed in this study, ten images are randomly selected from each of the seven categories of low contrast, thin air, thick air, irregular border, fuzzy border, air bubble and variegated colouring (<https://isic-archive.com/-90>). Figure 3.1 presents the melanoma skin lesion images selected in each of the categories listed above for experimentation.

Bubbles	Fuzzy border	Irregular border	Low contrast	Thick hair	Thin hair	Variegated Colouring



Figure 3.1 Melanoma skin lesion images selected from the ISBI 2016 challenge dataset

3.1.3 Pedro Hispano Hospital Dataset

The second dataset explored in this study is the Pedro Hispano Hospital dataset popularly referred to as PH2 dataset. The data set was jointly collected by the Universidade do Porto, Técnico Lisboa and the dermatology service of Hospital Pedro Hispano in Matosinhos, Portugal (Mendonça *et al.*, 2013). The dataset is composed of 200 melanoma skin lesion images in 8-bit RGB colour with 768 by 560 pixel resolution using a magnification of 20 \times under unchanged conditions. In addition, manually annotated lesions from expert dermatologists were also provided in the dataset to serve as ground truth for performance evaluation of different computer aided diagnosis systems. For the purpose of experimentation, a total number of fifty melanoma skin lesion images were randomly selected from the PH2 dataset. Figure 3.2 presents the melanoma skin lesion images selected for experimentation

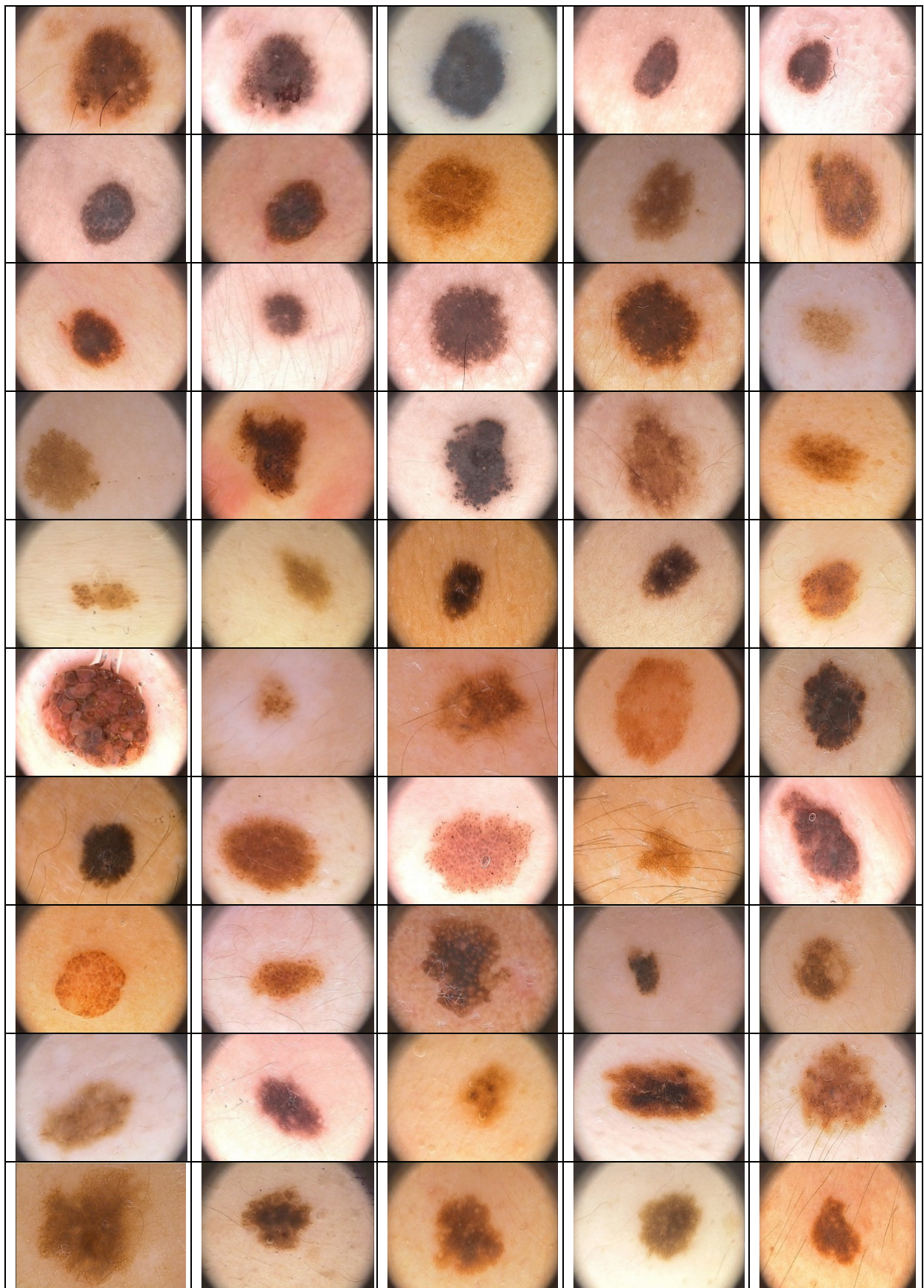
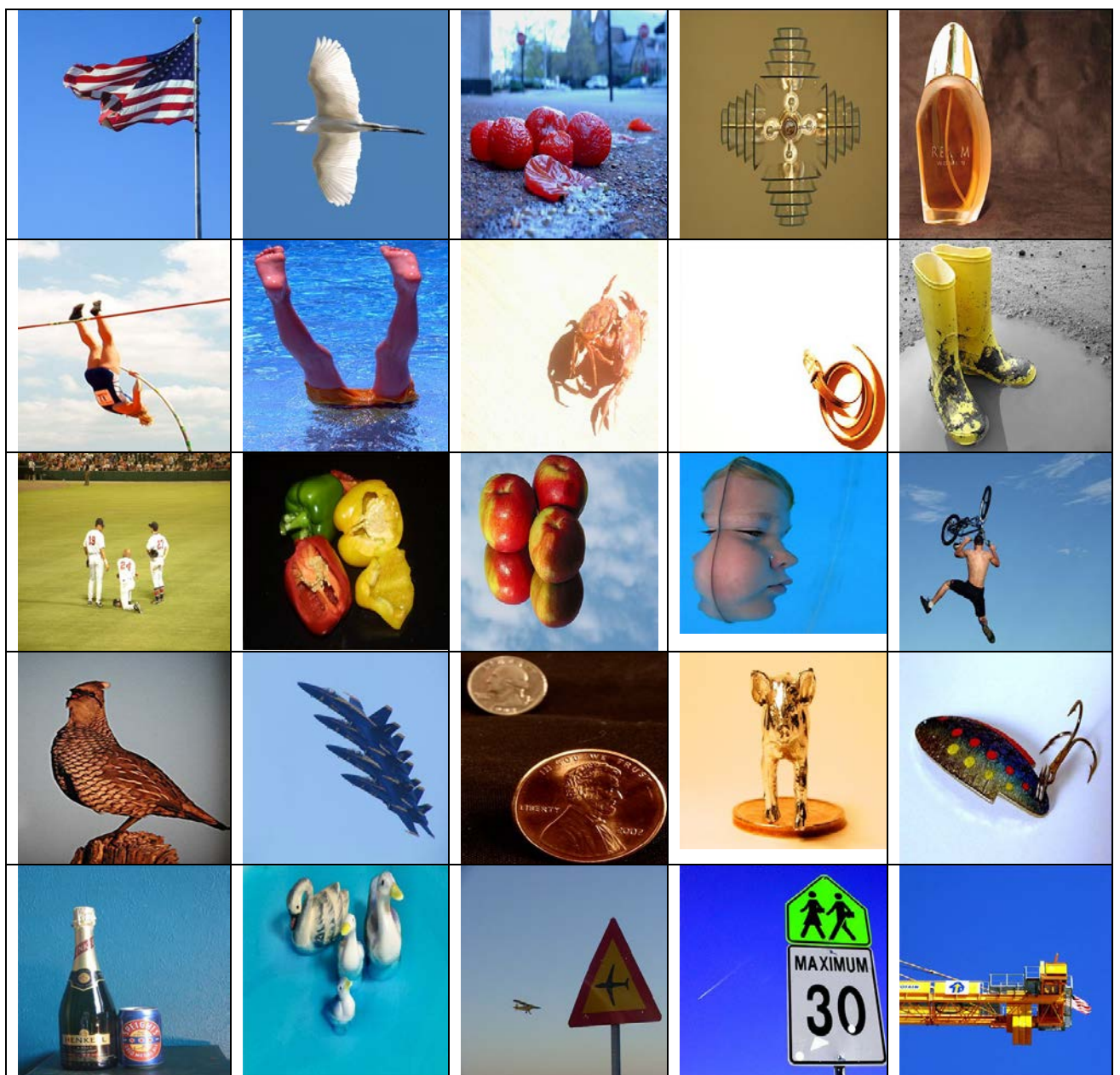


Figure 3.2 Melanoma skin lesion images selected from the PH2 dataset

3.1.4 Microsoft Research Asia Dataset

The third dataset explored in this study is the Microsoft Research Asia (MSRA) dataset. The MSRA salient object dataset is one of the most widely used publicly available benchmark salient object segmentation dataset. The data set features a large variation in natural images of about 10,000. The images provided in this data set are diverse with one or multiple salient objects in an image in different colour and shapes. The human labelled ground truth images for an accurate evaluation are also provided in the dataset. In this study, a total number of forty natural images were selected for validation purpose. Figure 3.3 presents the natural images selected from the MSRA dataset for experimentation.



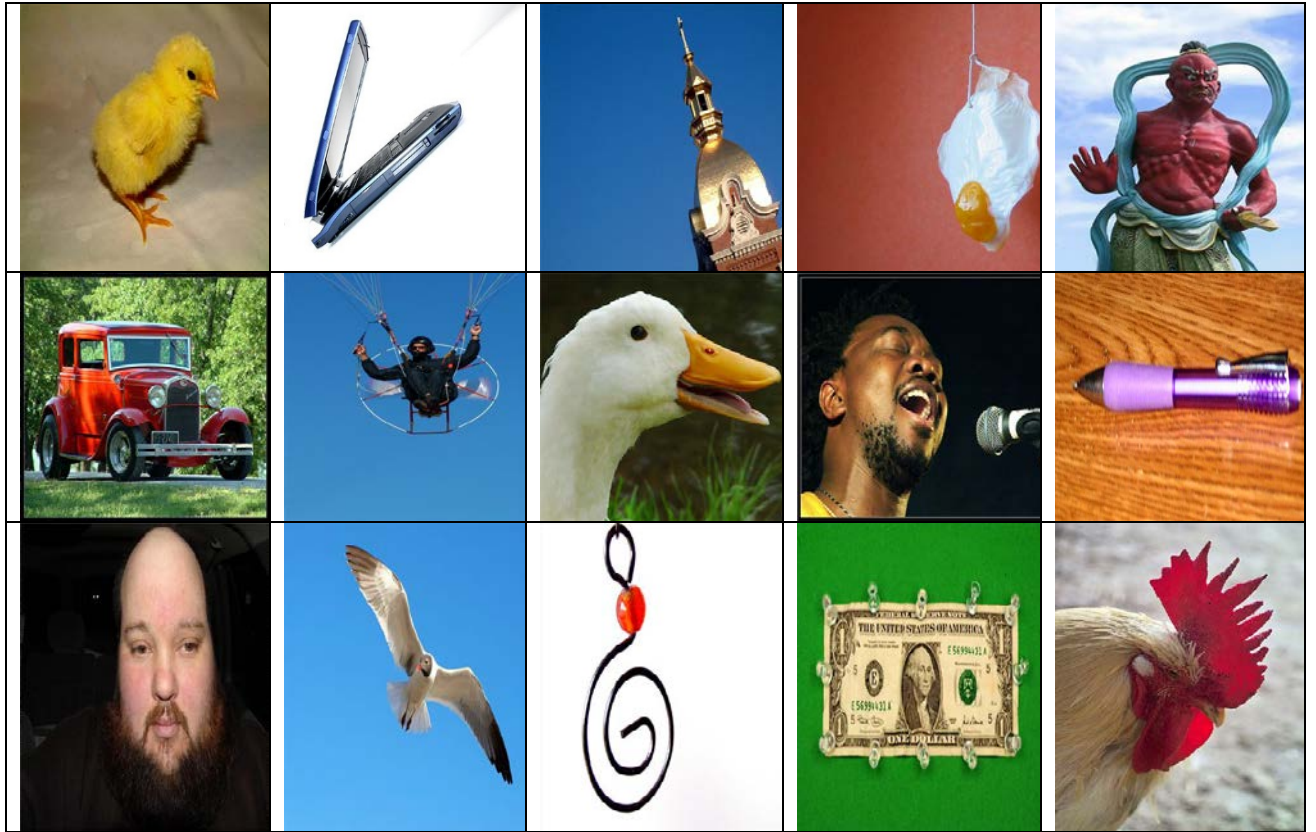


Fig 3.3 Natural images selected from the MSRA dataset.

3.1.5 Extended Complex Scene Saliency Dataset

The Extended Complex Scene Saliency Dataset (ECSSD) consists of a collection of natural images from one of the most widely used benchmark image segmentation dataset, the Berkeley segmentation benchmark data set for both greyscale and colour image segmentation (Arbelaez et al., 2007). The dataset contains of diversified patterned natural images of diverse scene categories with complex foreground and background patterns that are semantically meaningful. This attribute makes the data set one of the top choices of dataset suitable to evaluate the robustness of different salient and non-salient object detection algorithms. The images in this data set cover a wide range of natural scene categories such as animals, portraits, landscapes even human. In this study, thirty sample images were randomly selected in varying categories are shown in Figure 3.4 below.

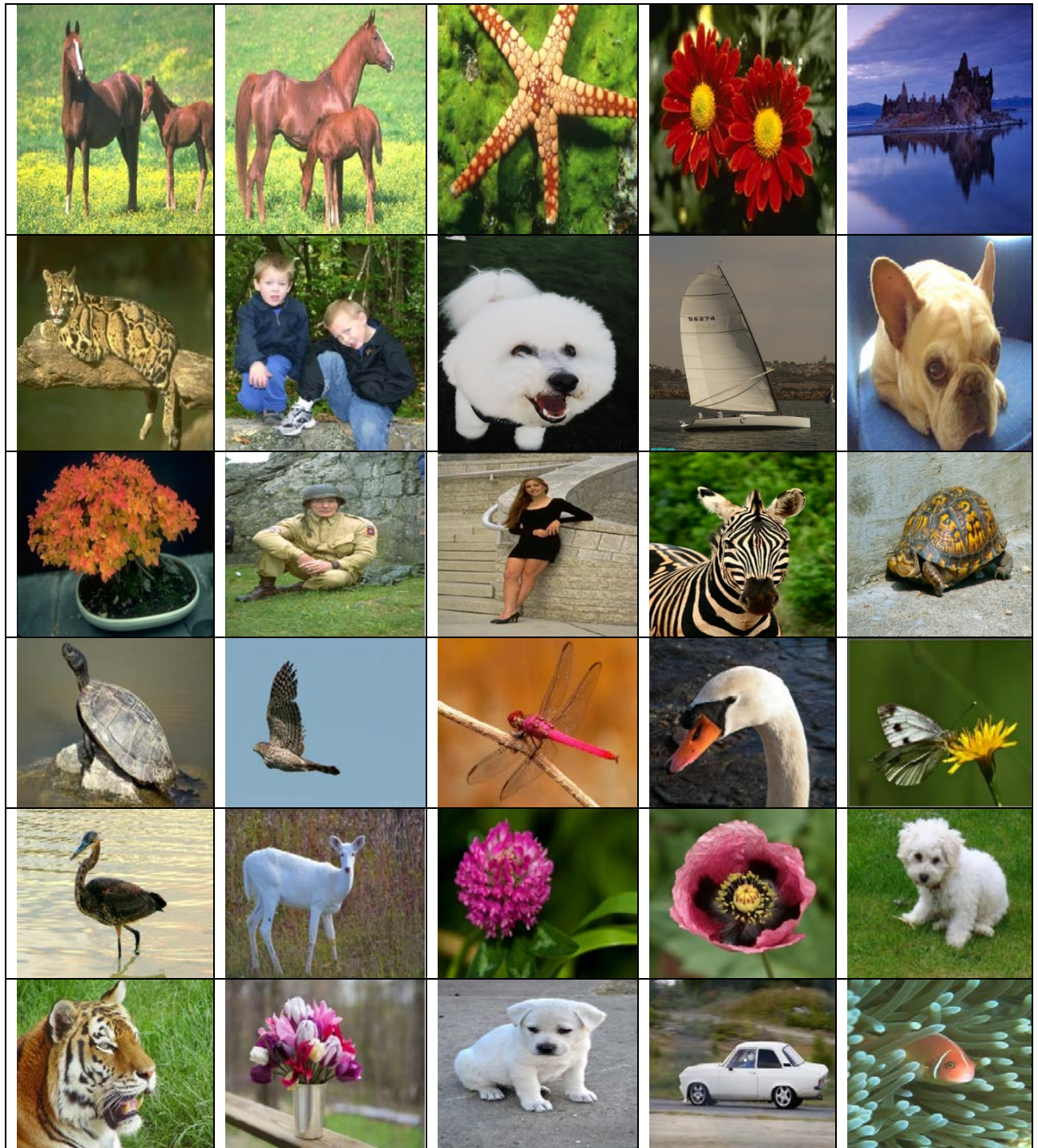


Fig 3.4 Natural images selected from ECSSD.

3.2.1 Colour Image Transformation

The input to the perceptual colour difference saliency (PCDS) segmentation algorithm is RGB colour image of $M \times N \times 3$ dimensions, where M and N are the number of rows and columns respectively. The red (R), green (G) and blue (B) channels of the input image have values in the range $[0, 1]$ and the image is transformed into the CIE $L^*a^*b^*$ colour image in

order to achieve perceptual saliency. The process of transforming an Adobe RGB colour image to the CIE L*a*b colour image is usually performed in two steps (Dowlati *et al.*, 2013, Hosseinpour *et al.*, 2013). The first step converts the Adobe RGB image to the CIE XYZ image according to the following equation (Dowlati *et al.*, 2013, Hosseinpour *et al.*, 2013):

$$\begin{bmatrix} X \\ Y \\ Z \end{bmatrix} = \begin{bmatrix} 0.5767 & 0.2973 & 0.0270 \\ 0.1855 & 0.6273 & 0.0706 \\ 0.1882 & 0.0752 & 0.9912 \end{bmatrix} \begin{bmatrix} r \\ g \\ b \end{bmatrix} \quad (3.1)$$

Where r , g and b are defined in terms of the constant gamma value which in this study is $\gamma_c = 2.4$ for non-hair occluded and natural images and $\gamma_c = 1/2.4$ for hair occluded skin lesion images. This can reduce the effects of hair or hair stubble on the segmentation results by reducing its lightness as most hairs contain the similar luminance value as the skin lesion region. The parameters $\alpha_1 = 0.055$ and $\alpha_2 = 1.055$ in equation (3.2) are added to correct the RGB values obtained from the digital cameras in order to obtain the best possible calibration of the transformation model (Valous *et al.*, 2009; Dowlati *et al.*, 2013, Hosseinpour *et al.*, 2013):

$$\left. \begin{aligned} r &= \left(\frac{R + \alpha_1}{\alpha_2} \right)^{\gamma_c} \\ g &= \left(\frac{G + \alpha_1}{\alpha_2} \right)^{\gamma_c} \\ b &= \left(\frac{B + \alpha_1}{\alpha_2} \right)^{\gamma_c} \end{aligned} \right\} \quad (3.2)$$

The second transformation step converts the CIE XYZ image to the CIE L*a*b image following the ITU-R BT.709 recommendation (equation 3.3). The illuminant D65 is used in this study, where $X_n = 0.95047$, $Y_n = 1.00000$ and $Z_n = 1.08255$ are the CIE XYZ tristimulus values of standard light source (Dowlati *et al.*, 2013; Filko *et al.*, 2016). The transformed image serves as input to the image enhancement processing stage.

$$\left. \begin{aligned} L^* &= 116 * \left[f\left(\frac{Y}{Y_n}\right) - \frac{16}{116} \right] \\ a^* &= 500 * \left[f\left(\frac{X}{X_n}\right) - f\left(\frac{Y}{Y_n}\right) \right] \\ b^* &= 200 * \left[f\left(\frac{Y}{Y_n}\right) - f\left(\frac{Z}{Z_n}\right) \right] \end{aligned} \right\} \quad (3.3)$$

Where the auxiliary function $f(s)$ is defined as follows:

$$f(s) = \begin{cases} s^{1/3}, & \text{if } s > \left(\frac{6}{29}\right)^3 \\ \left(\frac{841}{108}\right) * s + \frac{4}{29}, & \text{if } s \leq \left(\frac{6}{29}\right)^3 \end{cases} \quad (3.4)$$

3.2.2 Luminance Image enhancement

The transformation of colour image alone does not alleviate the adverse effect of illumination, low contrast or enhance the image quality significantly. The reason is that an absolute separation between the luminance and chrominance channels is not achievable for the RGB colour model because of the high correlation between its channels (Shi 2010; Rahman et al., 2016). It is therefore desirable to enhance the luminance channel of the image which does not change the original colour of a pixel (Rahman et al., 2016). The adaptive gamma correction function has been recommended for this purpose because a fixed gamma correction function is not always desirable for all image types (Rahman et al., 2016). The following adaptive gamma correction function is applied in this study to enhance the luminance channel of the input image:

$$L_{out} = \frac{L_{in}^{\gamma_a}}{1 + H(0.5 - \mu)(\mu^{\gamma_a} - 1)(1 - L_{in}^{\gamma_a})} \quad (3.5)$$

The images L_{in} and L_{out} are input luminance and output luminance respectively. The parameter γ_a is the adaptive gamma correction value that controls the slope of the transformation function. The Heaviside function $H(x)$ returns a value of 1 if its argument is greater than 0, otherwise it returns a value of 0. Rahman et al. (2016) gave logarithm and exponential adaptive gamma correction functions to enhance low contrast image and high contrast image respectively. The functions gave impressive segmentation results for a number

of images, but for some high contrast images, for instance an image with a mean value of 0.7097, standard deviation of 0.1513 and gamma value of 1.0720, the image enhancement needs further improvement as shown in Figure 3.5c. The segmentation result has improved as shown in Figure 3.5d with an increased in the gamma value from 1.0720 to 2.9212 using the following product of logarithm and exponential functions as the gamma correction function:

$$\gamma_a = -\log_2(\sigma) \exp((1 - \mu - \sigma) / 2) \quad (3.6)$$

where σ and μ are the global standard deviation and global mean of the luminance image respectively. The enhanced image serves as input to the saliency computation processing stage.



Figure 3.5: Enhancement of luminance channel using the adaptive gamma correction. (a) Original image, (b) ground truth, (c) enhanced saliency segmentation using exponential gamma function, (d) enhanced saliency segmentation using the product of logarithmic and exponential gamma functions.

3.2.3 Salient Pixel Computation

The saliency of a pixel in an input image can be computed in terms of the difference of the image colour feature with the mean value of this colour feature. The mean value of colour feature was computed globally over the entire image (Yang *et al.*, 2013). However, this method has difficulty in distinguishing similar colour features in the foreground region of the object region in an image (Qi *et al.*, 2017). To correct this problem, we compute the mean value of the background colour features and the mean value of object colour features to compute the saliency map. The mean value of the background colour feature is estimated by the mean of the pixel values on an ellipsoidal patch drawn close to the image borders and mean value of the object colour features is estimated by the mean of the pixel values within a rectangular patch drawn over the image centre. This design principle follows the assumption that images are acquired in such a way that the object is approximately positioned in the central portion of the images (Cavalcanti and Scharcanski 2013; Flores and Scharcanski

2016; Zortea *et al.*, 2017) and that background pixels are located at the image borders (Yang *et al.*, 2013; Pennisi *et al.*, 2016).

The mean value (m_{bl}, m_{ba}, m_{bb}) and the standard deviation value $(\sigma_{bl}, \sigma_{ba}, \sigma_{bb})$ of the background colour feature are computed from the values of image pixels on an ellipsoidal patch traced by an efficient midpoint ellipse algorithm (Van 1984; Agatho *et al.*, 1998). Moreover, the mean value (m_{ol}, m_{oa}, m_{ob}) of the object colour feature is computed from the values of image pixels within a rectangular patch whenever the inequality $p(x, y) < m_{bi} - \eta\sigma_{bi}$ or $p(x, y) > m_{bi} + \eta\sigma_{bi}$ is satisfied. Where $i = l, a, b$ are the image channels, $p(x, y)$ is image colour features at a given image pixel, $x = 1, 2, \dots, M$, $y = 1, 2, \dots, N$, $M \times N$ is the image dimension and $\eta = 1.00$ standard deviation is used in this study. Figure 3.5 shows the diagrammatic illustration of patches that are used for the computation of mean values of image colour features.

The ellipse in yellow font represents the set of pixels that are used for the computation of the mean value of background colour feature and the solid rectangle in red font represents the set of pixels that are used for the computation of the mean value of the object colour feature. The difference can be noticed between Figures 3.5b and 3.5d from the rectangular shapes as the segmentation algorithm computes mean value of object colour features for those pixels within the rectangular patch that differ from the background pixels. This decision follows the assumption that both object and background, possess different colour distributions (Zortea *et al.*, 2011). In Figure 2b not all pixels in the rectangular patch are object pixels, but in Figure 2d all pixels in the rectangular patch are object pixels, hence the principal reason for the observed difference in the rectangular shapes.

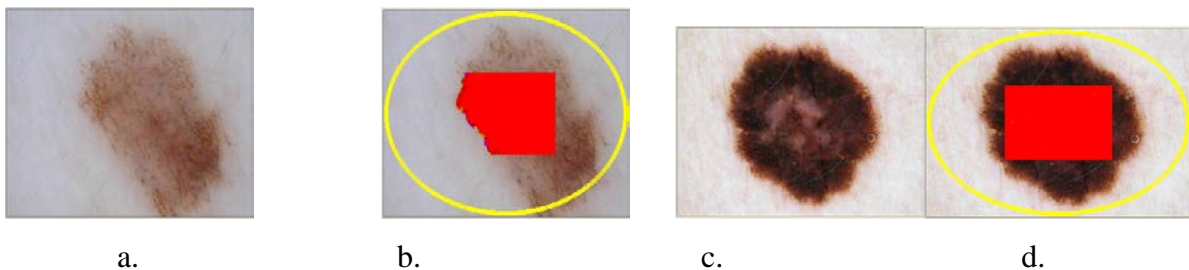


Fig. 3.5 Selection of background and object pixels. (a) input image, (b) ellipsoidal patch in yellow font contains background pixels and portion of object pixels in red font are covered by the rectangular patch, (c) input image, (d) ellipsoidal patch in yellow font contains background pixels and portion of object pixels in red font are fully covered by the rectangular patch.

The difference of background colour (ΔB_p) feature with the mean value of this colour feature and difference of object colour (ΔO_p) feature with the mean value of this colour feature is computed for each pixel to preserve spatial information. These two measures are aggregated to create a greyscale saliency map $S = \{s(x, y)\}$ whose entry $s(x, y)$ is determined as follows:

$$s(x, y) = \frac{255 * \Delta B_p(x, y)}{\Delta B_p(x, y) + \Delta O_p(x, y)} \quad (3.7)$$

To realize a saliency map that provides high resolution and good detection, according to the requirements of a good saliency detection (Borji *et al.*, 2014), the greyscale saliency map is converted to a binary saliency map $B = \{b(x, y)\}$ such that $b(x, y)$ tends to the maximum greyscale value of 255 for a salient pixel and minimum greyscale value of 0 for a background pixel according to the following simple decision.

$$b(x, y) = \begin{cases} 255, & \text{if } \Delta O_p(x, y) < \Delta B_p(x, y) \\ 0, & \text{if } \Delta O_p(x, y) \geq \Delta B_p(x, y) \end{cases} \quad (3.8)$$

The parameters $\Delta B_p(x, y)$ and $\Delta O_p(x, y)$ are computed using the accurate CIEDE2000 colour difference formula. Given two colour values $p_1(L_1, a_1, b_1)$ (mean of colour feature) and $p_2(L_2, a_2, b_2)$ (colour feature of a pixel) in the CIE L*a*b* colour model and for a given set of parametric weighting factors K_L, K_C, K_H , the CIEDE2000 Colour difference, $\Delta E_{2000}(p_1, p_2)$ between these colour values is defined as (Pant and Farup 2010; Sharma *et al.*, 2005)

$$\Delta E_{2000}(p_1, p_2) = \sqrt{\left(\frac{\Delta L_p}{K_L S_L}\right)^2 + \left(\frac{\Delta C_p}{K_C S_C}\right)^2 + \left(\frac{\Delta H_p}{K_H S_H}\right)^2 + R_T \left(\frac{\Delta C_p}{K_C S_C}\right) \left(\frac{\Delta H_p}{K_H S_H}\right)} \quad (3.9)$$

Where the differential colour vector components of the standard colour difference formula are given as follows:

$$\left. \begin{aligned} \Delta L_p &= L_2 - L_1 \\ \Delta C_p &= C_{2P} - C_{1P} \\ \Delta H_p &= 2\sqrt{C_{1P} * C_{2P}} * \sin\left[\frac{\Delta h_p}{2}\right]^0 \end{aligned} \right\} \quad (3.10)$$

where

$$\Delta h_p = \begin{cases} h_{2p} - h_{1p} - 360, & \text{if } h_{2p} - h_{1p} > 180 \\ h_{2p} - h_{1p} + 360, & \text{if } h_{2p} - h_{1p} < -180 \\ h_{2p} - h_{1p}, & \text{else} \end{cases} \quad (3.11)$$

The rotation function R_r appearing in the standard colour difference formula is mathematically expressed as follows:

$$R_r = -2 \sin \left[60 \exp \left\{ - \left(\frac{h_{pa} - 275}{25} \right)^2 \right\} \right]^r * \sqrt{\frac{C_{pa}^7}{C_{pa}^7 + 25^7}} \quad (3.12)$$

The parametric weighting functions appearing in the standard colour difference formula are expressed as follows:

$$\left. \begin{aligned} S_L &= 1 + \frac{0.015(L_{pa} - 50)^2}{\sqrt{20 + (L_{pa} - 50)^2}} \\ S_C &= 1 + 0.045 * C_{pa} \\ S_H &= 1 + 0.015 * C_{pa} * \left(\begin{aligned} &1 - 0.17 * \cos[h_{pa} - 30]^r + 0.24 * \cos[2 * h_{pa}]^r + \\ &0.32 * \cos[3 * h_{pa} + 6]^r - 0.20 * \cos[4 * h_{pa} - 63]^r \end{aligned} \right) \end{aligned} \right\} \quad (3.13)$$

The symbols used in the rotation function and parametric weighting functions are defined in terms of the hue angle for a pair of colour samples as follows:

$$\left. \begin{aligned} L_{pa} &= \frac{L_1 + L_2}{2} \\ C_{pa} &= \frac{C_{1P} + C_{2P}}{2} \end{aligned} \right\} \quad (3.14)$$

$$h_{pa} = \left\{ \begin{array}{l} h_{1p} + h_{2p}, \text{ if } C_{1p} * C_{2p} = 0 \\ \frac{h_{1p} + h_{2p}}{2}, \text{ if } |h_{2p} - h_{1p}| \leq 180 \\ \frac{h_{1p} + h_{2p} + 360}{2}, \text{ if } h_{2p} + h_{1p} < 360 \\ \frac{h_{1p} + h_{2p} - 360}{2}, \text{ else} \end{array} \right\} \quad (3.15)$$

where

$$h_{1p} = \left\{ \begin{array}{l} 0, \text{ if } a_{1p} = b_1 = 0 \\ \tan^{-1} \left[\frac{b_1}{a_{1p}} \right]^0 + 360^0, \text{ else} \end{array} \right\} \quad (3.16)$$

$$h_{2p} = \left\{ \begin{array}{l} 0, \text{ if } a_{2p} = b_2 = 0 \\ \tan^{-1} \left[\frac{b_2}{a_{2p}} \right]^0 + 360^0, \text{ else} \end{array} \right\}$$

Given that $[x]^o$ in equations (3.10) and (3.16) means that expression 'x' in radian is to be converted to degree and $[x]^r$ in equations (3.12) and (3.13) indicates that 'x' in degree is to be converted to radian. The other symbols of the colour difference formulae are defined as follows.

$$\left. \begin{array}{l} C_{1p} = \sqrt{a_{1p}^2 + b_1^2} \\ C_{2p} = \sqrt{a_{2p}^2 + b_2^2} \end{array} \right\} \quad (3.17)$$

$$\left. \begin{array}{l} a_{1p} = (1 + G)a_1 \\ a_{2p} = (1 + G)a_2 \end{array} \right\} \quad (3.18)$$

$$G = 0.5 \left(1 - \sqrt{\frac{C_{pa}^7}{C_{pa}^7 + 25^7}} \right) \quad (3.19)$$

$$\left. \begin{array}{l} C_1 = \sqrt{a_1^2 + b_1^2} \\ C_2 = \sqrt{a_2^2 + b_2^2} \\ C_{pa} = \frac{C_1 + C_2}{2} \end{array} \right\} \quad (3.20)$$

3.2.4 Image Artefact Filtering

The input to the artefact filtering routine is the binary output image of the saliency computation function. The prime objective of the artefact filtering stage is to fill holes, remove any extra element that might be remaining of hair or other artefacts and select a single connected region that is more likely to be the actual object. There are two possible stages in which artefacts can be removed, which are pre-processing (before segmentation) or post-processing (after segmentation). This study uses the post-processing stage to filter artefacts that are not catered for during the segmentation process. This achieves computation efficiency by not processing all the three image channels following the requirements of good saliency detection (Borji *et al.*, 2014).

The artefacts filtering process applies the morphological operations on the binary input image to remove undesired elements. Morphological operations are important in the digital image processing, because they can rigorously quantify many aspects of the geometrical structure of the image in a way that agrees with the human intuition and perception (Wang *et al.*, 2011; Premaladha and Ravichandran 2016). The relationship between each part of the image can be identified when processing images with morphological theory (Wang *et al.*, 2011; Zortea *et al.*, 2017). Accordingly, the structural character of the image in the morphological approach is analysed in terms of some predetermined geometric shape known as q structuring element (Zortea *et al.*, 2017). The morphological transformation aims at removing the outlier pixels that can be introduced in the image acquisition phase while maintaining the properties of the lesion region.

The median filter algorithm with structuring element of size 11 x11 is first executed on the binary image to eliminate hairs and smooths the image against noise. The filter of size of 11 x11 was used because of its ability to reduce bubble intensity and prevent fuzzy edges (Kasmi *et al.*, 2016; Premaladha *et al.*, 2016). The filter considers each pixel in the image in turn and looks at its nearby neighbours to decide whether or not it is a representative of its surroundings. It is widely used in digital image processing because under certain conditions, it preserves edge information while removing over segmentation. The median is evaluated by first sorting all the pixel values from the surrounding neighbourhood in numerical order and then replacing the pixel being considered with the middle pixel value (Li *et al.*, 2009). Then the disk structure element is created to preserve the circular nature of the lesion when performing the morphological opening operations. The radius of the structuring element is specified as 11 pixels, so that the large gaps can be filled. The opening operation is

morphological erosion followed by morphological dilation. The opening operation smooths object contours, breaks thin connections, removes thin protrusions and eliminates those objects that are smaller than the structuring element. The resulting binary image is then closed using the morphological closing operation which is dilation followed by erosion. The same disk structure element that was created in the previous step is used for both operations. The closing operation smooths object contours, joins narrow breaks, fills long thin gulfs and holes that are smaller than the structuring element. The “clear border” operation is finally used to remove vignette and disconnected objects touching the image border.

3.3 Algorithmic Implementation of the PCDS Algorithm

The algorithmic implementation of the proposed PCDS segmentation algorithm is succinctly outlined based on the mathematical descriptions (equations 3.1-3.20). The asymptotic time complexity of the PCDS algorithm is $O(M \times N \times 3)$ for an input colour image of dimensions $M \times N \times 3$. The PCDS algorithm is succinctly described as follows.

Input: $M \times N \times 3$ RGB colour image.

Output: $M \times N$ greyscale saliency map, $M \times N$ silhouette saliency map.

It is assumed that the standard colour difference formula described by equations (3.9) to (3.20) has been implemented to be invoked in the computation of a saliency map in step 12 of this algorithm.

- (1) **for all** $x=0, 1, \dots, M-1$ **do**
- (2) **for all** $y=0, 1, \dots, N-1$ **do**
- (3) transform the Adobe RGB image to the CIE XYZ image using equations (3.1) and (3.2).
- (4) transform the CIE XYZ image to the CIE Lab image using equations (3.3) and (3.4).
- (5) **end for**
- (6) **end for**
- (7) enhance the luminance channel of the CIE Lab image using equations (3.5) and (3.6).
- (8) compute mean of representative background pixels on an ellipsoidal patch.
- (9) compute mean of representative object pixels within a rectangular patch.
- (10) **for all** $x=0, 1, \dots, M-1$ **do**

- (11) **for all** $y=0, 1, \dots, N-1$ **do**
- (12) compute the greyscale saliency map using equation (3.7).
- (13) compute the binary saliency map using equation (3.8).
- (14) **end for**
- (15) **end for**
- (16) perform morphological analysis on the binary saliency map to filter artefacts.
- (17) **stop**

3.4 Chapter Summary

This chapter has presented the methodological steps taken to achieve the second objective of this research study. The chapter discusses in detail the implementation processes of the proposed perceptual colour difference saliency segmentation algorithm. At the first stage, the chapter provided vivid information about the image data set acquisition process. As a reminder, four publicly available image data sets have been selected to validate the effectiveness of the proposed PCDS segmentation algorithm. The first two data sets explored in this study contain melanoma skin lesion images in varying conditions while the other image data sets consist of natural images. This was followed by the four procedural steps towards achieving the main contribution of this study. The next chapter provides the evaluation experiments, results and interpretations.

CHAPTER FOUR

EVALUATION EXPERIMENTS, RESULTS AND INTERPRETATIONS

This chapter presents the evaluation experiments, the results of the experiments and their corresponding interpretations to accomplish the third objective of this study. The chapter begins with an analysis of performance evaluation. This is followed by the qualitative analysis of saliency and non-saliency results of the four image data sets explored in this study. The next section presents the quantitative analysis of the binary segmentation results. In the quantitative analysis section, the four statistical evaluation metrics used in this study and their mathematical representations are presented. Next to this is the quantitative results obtained from each of the evaluation metrics and their respective interpretations.

4.1 Analysis of Performance Evaluation

The universal problem in the development of an image segmentation algorithm, which is approachable through experimentations, is a comprehensive measure of its accuracy to validate that one algorithm is better than the other. Moreover, if the image segmentation algorithm is better than its counterparts, will it be consistent under varying image conditions and other factors? These questions are thereby answerable using the following procedures.

1. Two or more image data sets that offer different image conditions should be used to observe the behaviour of a segmentation algorithm to ensure its consistency across the image data sets.
2. Both qualitative and quantitative evaluation techniques should be adopted to cater for the deficiency by using one evaluation technique.
3. Qualitative evaluation should be carried out to judge the quality of the segmentation results quality based on the capability of segmentation to accurately segment the salient object in an image.
4. During the quantitative evaluation, a minimum number of three evaluation metrics should be used to ensure that the overall performance of a segmentation algorithm is significant to an extent.

4.1.1 Comparison with State-of-the-art Saliency and Non-Saliency Segmentation Algorithms

In this section, to validate the effectiveness of the proposed PCDS segmentation algorithm, the researcher compares the performance of PCDS segmentation algorithm qualitatively and quantitatively with four benchmark saliency segmentation algorithms which are Spatially Weighted Dissimilarity (SWD) [Duan *et al.*, 2011], Principal Component Analysis (PCA) [Margolin *et al.*, 2013], Markovian Chain (MC) [Jiang *et al.*, 2013] and Saliency-based Skin Lesion Segmentation (SSLS) [Ahn *et al.*, 2015] as well as four state-of-the-art non-saliency image segmentation algorithms which are the Otsu thresholding method [Otsu 1979], K-means [Lloyd 1982], FCM [Dunn 1973] and modified JSEG [Celebi *et al.*, 2007]. The SSLS source code for the comparative saliency segmentation algorithms with default parameter settings was provided by the author of the method. The source codes for SWD, PCA and MC methods are available at the web link <https://github.com/MingMingCheng/SalBenchmark/tree/master/Code/matlab>.

4.2 Qualitative Analysis of Experimental Results

The goal of this section is to test the effectiveness of the experimental results computed by the PCDS segmentation algorithm by visual inspection of the selected experimental test images across the four data sets explored in this study. For qualitative comparison, some samples of the generated saliency map results of the PCDS segmentation algorithm and the other four benchmark saliency segmentation algorithms are presented. In a similar vein, binary segmentation results of the proposed PCDS default thresholding technique are compared with the four non-saliency state-of-the-art image segmentation algorithms in the absence of image artefact filtering.

4.2.1 Qualitative Analysis of Saliency Results with Images from ISBI 2016 Challenge Dataset



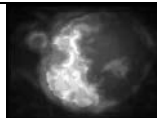
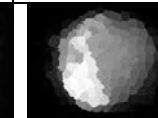
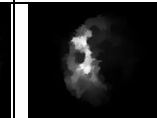
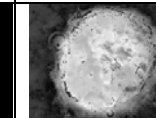



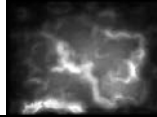
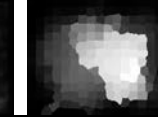
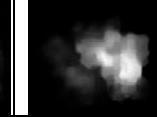
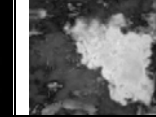



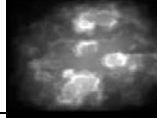
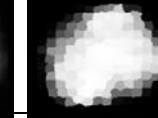
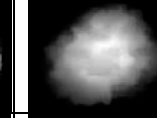
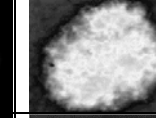



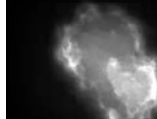


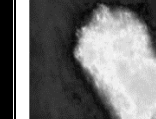

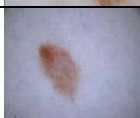


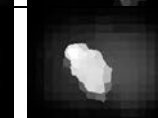
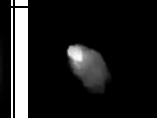
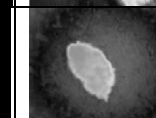

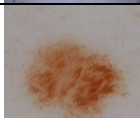

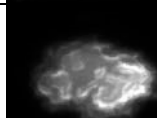
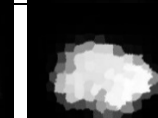
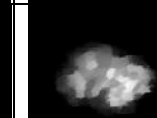
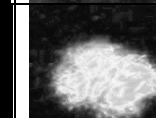

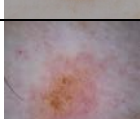

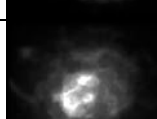
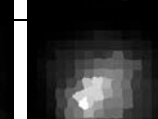

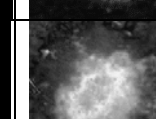

In this section, the researcher qualitatively evaluates and verifies the robustness of the proposed PCDS segmentation algorithm in direct comparison with the four benchmark saliency segmentation algorithms using some samples of melanoma skin lesion images selected from the ISBI 2016 challenge dataset. A few examples of the challenging melanoma skin lesion images in varying image conditions such as the presence air bubbles (Im1 and

Im2), low contrast between lesion and healthy skin (Im3 to Im8), presence of thin hair (Im9), presence of thick hair (Im10).

The results of Figure 4.1 show that most of the salient lesion objects were correctly segmented by the proposed PCDS segmentation algorithm and largely consistent across the entire melanoma skin lesion images displayed in the figure 4.1. It can be observed from Im1 when melanoma skin lesion image possesses air bubbles and illumination variation, this is a situation whereby the lesion object colour distribution appears to be uneven. It can be seen that compared to the other four benchmark saliency segmentation algorithms, the proposed PCDS segmentation algorithm highlights the complete salient lesion object more effectively thereby producing a better saliency map representation. This apparent improvement can be linked to the proposed luminance image enhancement using the adaptive gamma correction implemented in this study to improve the quality of saliency segmentation. Similarly, it can be observed in Im2 that in the presence of air bubbles and at the same time little contrast between the lesion and healthy skin. The CPDS segmentation algorithm generates an improved saliency map with more defined image borders compared to other four benchmark saliency segmentation algorithms.

It is worth mentioning from observation that for virtually all the melanoma skin lesion images displayed in Figure 4.1, the SWD segmentation algorithm has the poorest performance as the algorithm generates saliency maps with low resolution, blurry and poorly defined borders. From Im3 to Im8 when there is low contrast between the lesion and healthy skin, the qualitative results show that the PCA and SSLS segmentation algorithms do not uniformly highlight the salient lesion objects. As it can be seen that the PCA and SSLS saliency segmentation algorithms only highlighted certain parts of the lesion while some parts share a similar colour intensity with the background colour. Though the MC segmentation algorithm produced better saliency maps compared to the PCA and SSLS saliency segmentation algorithms, yet one can observe that the saliency maps generated by the MC algorithm possess the heterogeneous lesion object, salient object borders are imprecise and fuzzy across the entire melanoma skin lesion images presented in Figure 4.1. Furthermore, the SSLS segmentation algorithm produced saliency maps that are quite smaller in size as compared to the ground truth images in virtually all the melanoma skin lesion images presented in Figure 4.1.

The proposed PCDS segmentation algorithm, on the other hand, shows improved saliency maps across the melanoma skin lesion images than the other algorithms. The PCDS segmentation algorithm completely and uniformly highlighted the lesion objects with no varying lesion colour. This is an indication that the PCDS segmentation algorithm assigned pixels within the salient lesion objects with uniform saliency values. Im9 is an indication that all the saliency segmentation algorithms are able to achieve satisfactory results for melanoma skin lesion image has high contrast between lesion and healthy skin. Another important observation from Figure 4.1 below can be seen in Im10, when melanoma skin lesion image possesses thin hair. Although it can be observed that the other benchmark saliency segmentation algorithms highlighted only the visible part the lesion object which as a result of this could lead to diagnostic error. By contrast, it can be observed that the proposed PCDS segmentation algorithm highlighted the almost invisible tail end of the lesion as seen in the human reference standard not highlighted by the other saliency segmentation algorithms. This improvement in the performance of the PCDS segmentation algorithm can be attributed to object and background colour contrast difference measurement based on the CIEDE2000 colour difference formula implemented in this study.

S/N	Original image	SWD	PCA	MC	SSLs	PCDS	Ground Truth
Im1							
Im2							
Im3							
Im4							
Im5							
Im6							
Im7							

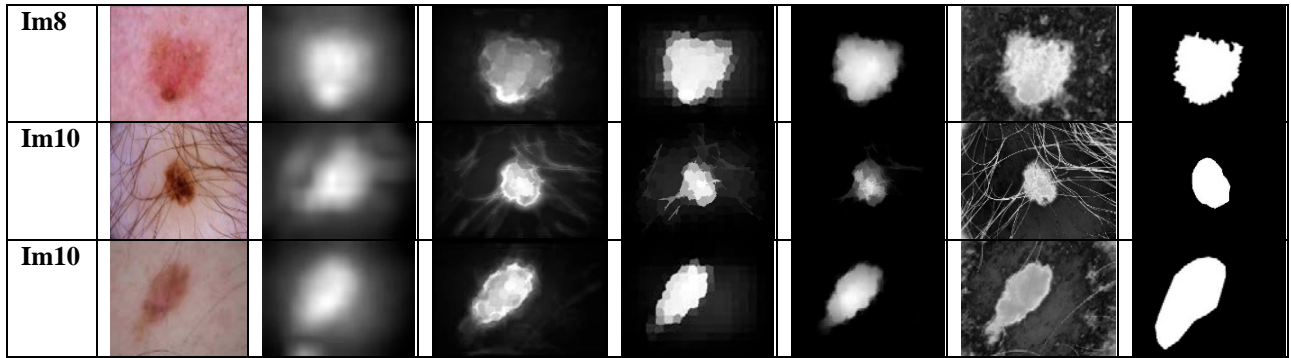


Fig 4.1: Qualitative illustration of saliency segmentation results obtained using four benchmark saliency segmentation algorithms and PCDS segmentation algorithm on the melanoma skin lesion images from ISBI 2016 challenge dataset.

4.2.2 Comparison of Non-Saliency Results with Images from ISBI 2016 Challenge dataset without Image Artefact Filtering

In this section, the researcher presents the binary segmentation results of the proposed PCDS segmentation algorithm using the default thresholding technique executed on the saliency maps to obtain a binary image of the lesion boundary using melanoma skin lesion images from the ISBI 2016 challenge corpus. The result of Fig.4.2 shows some of the examples of the binary segmentation results produced by the proposed PCDS segmentation algorithm and the four non-saliency image segmentation algorithms. The melanoma skin lesion images presented in this section for qualitative comparison are the same as the melanoma skin lesion images from the ISBI 2016 challenge dataset presented in Fig.4.1 in the absence of artefact filtering. It is worth mentioning that the modified JSEG algorithm source code provided by the author of the method is inherently embedded with both preprocessing and postprocessing techniques, as it can be observed that the resulting images by the modified JSEG algorithm do not contain image artefacts.

The results of Figure 4.2 show that despite the absence of image artefact filtering, an observer can easily note that the binary segmentation results produced by the proposed PCDS segmentation algorithm show an improvement in its overall performance. For example, the binary segmented image of the proposed PCDS segmentation algorithm shows a better segmentation performance for Im1. It is observed that the Otsu thresholding, K-means and FCM image segmentation algorithms produced incomplete binary segmented images that are smaller in size compared to the one in the ground truth image. Furthermore, it can be seen that there is also a considerable amount of border irregularities in the segmented lesion border of the binary segmented image produced by the modified JSEG algorithm. This is a demerit

as border irregularities caused by inaccurate segmentation can mislead the automatic diagnosis process. Moreover, the binary segmentation results produced by the three non-saliency image segmentation algorithms can be attributed to the illumination variation in the original skin lesion image which was corrected at the luminance image enhancement stage proposed in the methodology chapter of this study.

The second image that is Im2 also reveals that the first three non-saliency image segmentation algorithms exhibit poor performance when the image has little contrast between the lesion and healthy skin. It is also noticeable that apart from the presence of image artefacts in the binary segmented images produced by the Otsu thresholding, K-means and Fuzzy C-means, some part of the healthy skin in the binary segmented results produced by these algorithms have similar colour intensity as the lesion. This is an indication that Im2 contains heterogeneous regions with different visual properties. Most especially when the healthy skin colour intensity is similar to the lesion, as it can be seen that the healthy skin in the segmented binary images produced by the first three algorithms share a similar colour intensity as the lesion region as seen also in Im5. Still on Im2, there is an indication that the modified JSEG algorithm failed to produce a binary segmented image. This is because the algorithm was unsuccessful at segmenting Im2. It was observed by the researcher that the modified JSEG algorithm at the initial stage performed preprocessing of all the input melanoma skin lesion images in the absence or presence of image artefacts.

As a result of the modified JSEG algorithm to suppress the presence of oil bubbles in Im2, the contrast between the lesion and healthy skin becomes weakened, which in turn causes the algorithm to be unsuccessful at segmenting the lesion where there is a weak contrast between the lesion and healthy skin, which can be seen in the case of Im4. The unsuccessful cases recorded by the modified JSEG algorithm as reported in this study is not first of its kind. The original authors of the algorithm reported similar unsuccessful cases produced by the algorithm during experimentation (Celebi *et al.*, 2007). Norton *et al.*, (2012) also reported unsuccessful case of the modified JSEG where it failed for fourteen images during experimentation in the most challenging situations. On the other hand, the proposed PCDS segmentation algorithm successfully segmented the lesion in Im2. Moreover, it can be seen that in the absence of image artefact filtering, the binary segmented image produced by the PCDS segmentation algorithm does not contain oil bubbles as in seen in the original image. It is evident that the binary segmented results produced by the PCDS segmentation algorithm much more than better than the segmented images produced by the other

algorithms. The results of Im2 and Im5 indeed show the improved separability of the lesion and healthy skin of the proposed PCDS segmentation algorithm over the four state of the art image segmentation algorithms.

In Im3, it can be seen that the binary segmented image produced by the proposed PCDS segmentation algorithm is almost comparable to the result of the modified JSEG algorithm even in the absence of image artefact filtering. This is because the appearance of binary segmentation results of the proposed PCDS segmentation algorithm in Im3 and Im6 produced well connected and precise lesion boundary than the Otsu thresholding, K-means and Fuzzy C-means image segmentation algorithms. Im7 is also an apparent evidence of when melanoma skin lesion possesses low contrast between the lesion and healthy skin, it can be observed that the performance of the Otsu thresholding, K-means and FCM image segmentation algorithms are similar to Im2 except for the absence of image artefact in Im7. One can easily note that the first three non-saliency image segmentation algorithms faced difficulty in segmenting the lesion object from the healthy skin. This is because there is low contrast between the lesion and healthy skin. In addition, it can be observed that the modified JSEG tried to segment the lesion region. However, the algorithm produced binary segmentation results with smaller lesion object compared to the ground truth image.

The proposed PCDS segmentation algorithm, on the other hand, irrespective of the low contrast between the lesion and healthy skin produced a significantly improved segmentation result for this image. The PCDS algorithm segmented the lesion area of healthy skin in spite of the presence of the low contrast between the lesion region and the healthy skin. This is one of the numerous proofs that the proposed PCDS segmentation can improve the performance of colour image segmentation, especially in a situation whereby the contrast between the object and background is extremely low. Besides the presence of thick hair in Im9, it can be observed that virtually all the four non-saliency image segmentation algorithm produced binary segmented images close to the ground truth. This happens when there is a good contrast between the lesion and healthy skin, thus the lesion boundaries are well defined. However, it can be observed that the modified JSEG algorithm segmented hair trace to be part of the lesion which as earlier stated can result in automatic diagnosis error.

Furthermore, Im10 has shown that the proposed PCDS segmentation algorithm produced a full representation of the lesion compared to other four non-saliency image segmentation algorithms. It can be observed that the tailed end of the segmentation results as

seen in the first four segmentation algorithms has been distorted. In conclusion, the results presented in Figure 4.2 that when melanoma skin lesion images selected from the ISBI 2016 challenge dataset with image artefact filtering, the PCDS segmentation algorithm has consistently produced segmented binary images with an improved performance than the four image segmentation algorithms with no report of unsuccessful cases.



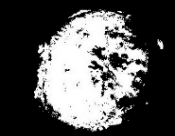

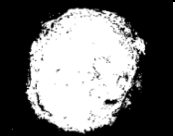
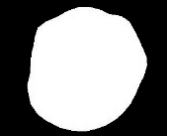
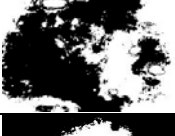



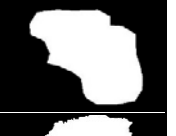























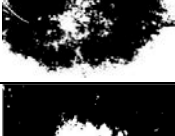
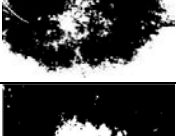
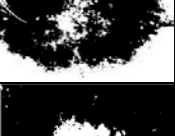



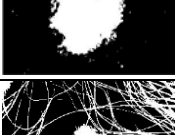
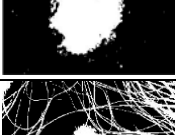
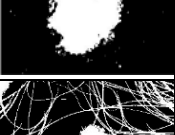

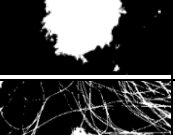
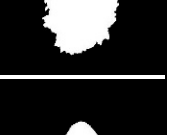
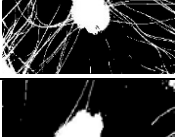
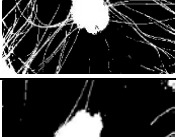
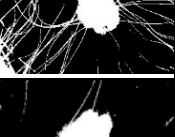

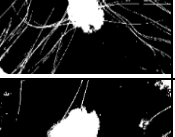







S/N	Otsu	K-means	Fuzzy C-means	Modified JSEG	PCDS	GT
Im1						
Im2				FAILED		
Im3						
Im4				FAILED		
Im5						
Im6						
Im7						
Im8						
Im9						
Im10						

Fig 4.2: Qualitative illustration of binary segmentation results obtained using four state-of-the-art non-saliency image segmentation algorithms and the PCDS segmentation algorithm on melanoma skin lesion images from the ISBI challenge dataset.

4.2.3 Comparison of Saliency Results with Images from PH2 Dataset

In this section, the qualitative comparison of saliency results with images from PH2 dataset to validate the performance of the proposed PCDS segmentation algorithm in direct comparison with the four saliency segmentation algorithms is presented. Some examples of the generated saliency maps produced by the CPDS segmentation algorithm and the four benchmark saliency segmentation algorithms are presented in Figure 4.3. From observation, it can be seen that the proposed PCDS segmentation algorithm achieves good performance against the other four benchmark saliency segmentation algorithms. This is because the PCDS segmentation algorithm has an advantage of uniformly highlighting the whole salient object with high resolution compared to the other benchmark non-saliency segmentation algorithm that a good saliency segmentation algorithm must possess as seen across the entire melanoma skin lesion images presented in Figure 4.3.

The SWD segmentation algorithm as is seen in the figure has the least performance on the PH2 dataset. It can be observed that the output saliency maps generated by the SWD segmentation algorithm are blurry and do not convey too much useful information with respect to segmenting the lesion object in the image. Although the PCA segmentation algorithm can correctly locate the lesion in the images, but usually the algorithm highlights some parts of the salient lesion boundaries as seen in Im6 and Im7 which can lead to error during diagnosis. Moreover, it can be observed that the PCA segmentation algorithm failed at precisely locating the salient lesion object. For instance, the Im1 produced by the PCA segmentation algorithm segmented the salient lesion region in such a way that it touches the image border.

The MC segmentation algorithm highlights the object boundaries and detects the salient lesion region. However, it can be seen that the output saliency map boundaries are imprecise and fuzzy across the test images. Besides, imprecise and fuzzy object boundaries produced by the MC segmentation algorithm can easily result in the segmentation of background region as a lesion region for fuzzy based similarity image segmentation algorithms. Furthermore, it can be observed that the SSLS segmentation algorithm can highlight the salient lesion boundaries, but still cannot assign uniform salient pixel values in

the inner part of the salient object as in Im3, Im4 and Im6. Moreover, it is also observed that the saliency map produced by the SSLS segmentation algorithm in Im7 is smaller than the actual lesion region as seen in the ground truth image. By contrast, it can be seen that the PCDS segmentation algorithm developed in this study uniformly highlighted the complete salient object, predicted the precise location of the salient lesion region, produced well defined salient lesion borders with high resolution across the images displayed in the figure. This is an indication that the PCDS segmentation algorithm shows a good performance and desirable saliency segmentation.

S/N	Original Image	SWD	PCA	MC	SSLS	PCDS
Im1						
Im2						
Im3						
Im4						
Im5						
Im6						
Im7						
Im8						
Im9						
Im10						

Fig 4.3: Qualitative illustration of saliency segmentation results obtained using four benchmark salient segmentation algorithms and PCDS segmentation algorithm on PH2 dataset

4.2.4 Comparison of Non-Saliency Segmentation Results with Images from PH2 dataset without Image Artefact Filtering

In this section, the researcher reports some samples of binary segmentation results of the PCDS segmentation algorithm with the four state-of-the-art non-saliency image segmentation algorithms with melanoma skin lesion images selected from PH2 dataset. The binary segmentation results presented in Figure 4.4 below shows that for some of the melanoma skin lesion images, there are no apparent differences in the binary segmentation results produced by the PCDS segmentation algorithm and the four non-saliency image segmentation algorithms. This is because melanoma skin lesion images from the PH2 dataset are not varying image conditions and challenging compared to the melanoma skin images provided in the ISBI 2016 challenge dataset.

It is important to note that the white borders seen in the image borders on the segmented images in Figure 4.4 are as a result of the vignette effect. As seen in the original images, the darkened image corners are as a result of the round circular lens designed for a smaller sensor used during image capturing. The image vignette has been seen in most cases has approximately similar intensity as the lesion and can be easily removed by morphological analysis as seen in the modified JSEG algorithm. Furthermore, it is evident that from the original melanoma skin lesion images presented in Figure 4.3, quite a large number of the melanoma skin lesion images possess good contrast between the lesion and healthy skin except for Im5 and Im8. For Im5 and Im8, it can be observed that the PCDS segmentation results show an improvement in performance compared to the binary segmentation results produced by the Otsu, K-means and Fuzzy C-means segmentation algorithms when there is low contrast between the lesion and healthy skin.

Moreover, border irregularities can be observed in Im3, Im6, Im7 and Im10 of binary segmentation results produced by the modified JSEG algorithm when compared to the ground truth image. The Im8, 9 and 10 images are clear cases of when there is little contrast between the lesion and healthy skin, thus lesion pixels can easily be mistaken for healthy skin. This can be seen in the binary segmentation results produced by the Otsu thresholding, K-means,

Fuzzy C-means algorithms. These algorithms have failed at segmenting the lesion for Im8, Im9 and Im10.










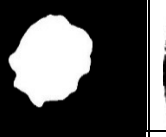





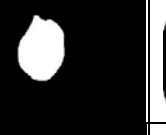






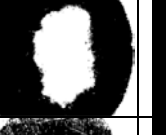

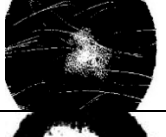
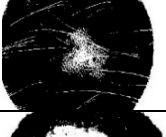
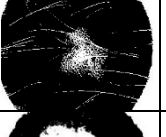



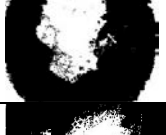
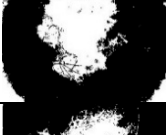


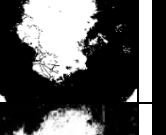










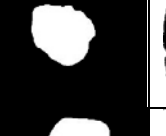














S/N	Otsu	K-means	Fuzzy C-means	Modified JSEG	PCDS	Ground Truth
Im1						
Im2						
Im3						
Im4						
Im5						
Im6						
Im7						
Im8						
Im9						
Im10						

Fig 4.4: Qualitative illustration of binary segmentation results obtained using four state-of-the-art non-saliency image segmentation algorithms and the PCDS segmentation algorithm on PH2 dataset.

In summary, these sections have presented both qualitative results of the saliency and non-saliency segmentation algorithms for melanoma skin lesion images selected from the ISBI 2016 challenge and PH2 datasets. The experimental results presented in the first four figures in this chapter have shown that the proposed PCDS segmentation algorithm produced good segmentation results. The figures have also shown that the results produced by the PCDS segmentation algorithm compared to the eight saliency and non-saliency image segmentation is more robust even in challenging imaging conditions, especially where there is low contrast between the lesion and healthy skin for melanoma skin lesion images selected from the medical image datasets explored in this study.

4.2.5 Qualitative Analysis of Saliency Results on MSRA Dataset




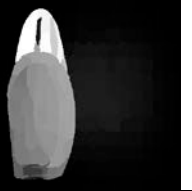
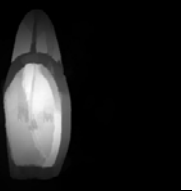
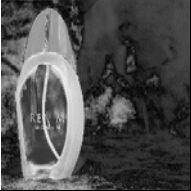








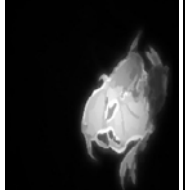

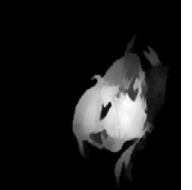





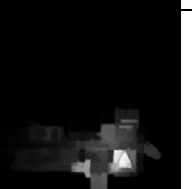



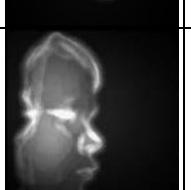

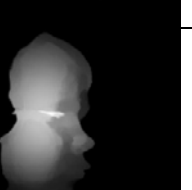
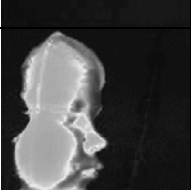


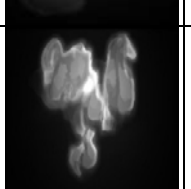
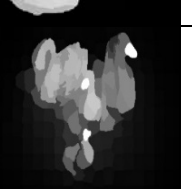

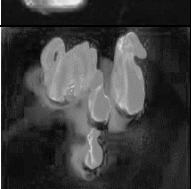
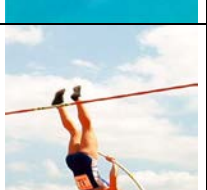




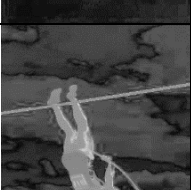


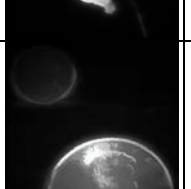


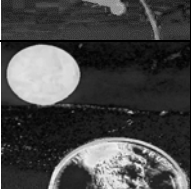



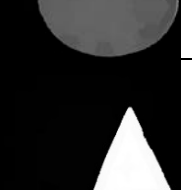

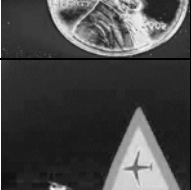
This section presents the qualitative analysis of saliency results with natural images selected from the MSRA dataset. The results presented in Figure 4.5 illustrate some examples of the saliency maps generated by the PCDS segmentation algorithm with the other four benchmark saliency segmentation algorithms. The first column shows the original image. Meanwhile, the second, third, fourth, fifth and sixth columns are the resultant saliency maps obtained when the SWD, MC, PCA, SSLS segmentation algorithms and the proposed PCDS segmentation algorithm were processed. To show the qualitative comparison results clearly, the selected images for qualitative analysis include difficult scenes, such as low background and foreground contrast, salient object not situated in the centre, multiple salient objects in an image and salient object that touches the image boundary.

The results in figure 4.5 below shows that the saliency maps produced by the proposed PCDS segmentation algorithm are distinct from the other four benchmark saliency segmentation algorithms. One can see vividly that the PCDS saliency maps convey much more useful information, especially in difficult scenes, such as low background and foreground contrast, salient objects that are close or touches the image borders. Similar to previous saliency results presented in the previous Figures, it can be observed that the saliency maps generated by the SWD segmentation algorithm show the least performance because it produced saliency maps with low resolution across the selected experimental

images from the MSRA dataset. From the results in Figure 4.5 below, at least three key observations can be derived from the saliency maps displayed.

To begin with, it can be observed that for natural images with simple object and smooth background, for example Im1, Im5 and Im6, the PCA, MC, SSLS and the proposed PCDS segmentation algorithms produced pretty good saliency maps with high resolution. However, for complicated images with low foreground and background contrast and structurally complex background, the benchmark saliency segmentation algorithms exhibited weak performances, such as im7 where the gymnast held a stick, it can be observed that both sticks were completely erased by the SSLS segmentation algorithm and almost invisible for the MC segmentation algorithm and slightly visible for the PCA segmentation algorithm. In actual fact, it is clear that the four benchmark saliency segmentation algorithms only highlighted the salient object with high contrast, but fail to pop out the whole salient objects uniformly. Oppositely, the proposed PCDS segmentation algorithm uniformly highlighted the salient objects more effectively than the other benchmark saliency segmentation algorithms.

Secondly, the proposed PCDS segmentation algorithm is capable of segmenting multiple salient objects such as the two coins in Im8. Here, it can be observed that besides from the MC segmentation algorithm, the SSLS and PCA saliency segmentation algorithms failed at segmenting both salient objects simultaneously. It can be seen that for the PCA segmentation algorithm, the smallest coin that touches the upper border is rarely visible. On a related note, for the SSLS segmentation algorithm, some parts of the bigger coin that touches the image border is invisible. Likewise, the sign post and aircraft image in Im9, a close observation shows that the MC segmentation algorithm clearly erased the aircraft in the scene leaving just the signpost. Moreover, the SSLS and PCA algorithms faintly reveal the aircraft with a closer look at the image even though it appears almost invisible looking at the saliency map generated by the SSLS segmentation algorithm. Contradictory to this, the proposed PCDS segmentation algorithm reveals the two salient objects in the image.

S/N	Original Image	SWD	PCA	MC	SSLS	PCDS
Im1						
Im2						
Im3						
Im4						
Im5						
Im6						
Im7						
Im8						
Im9						

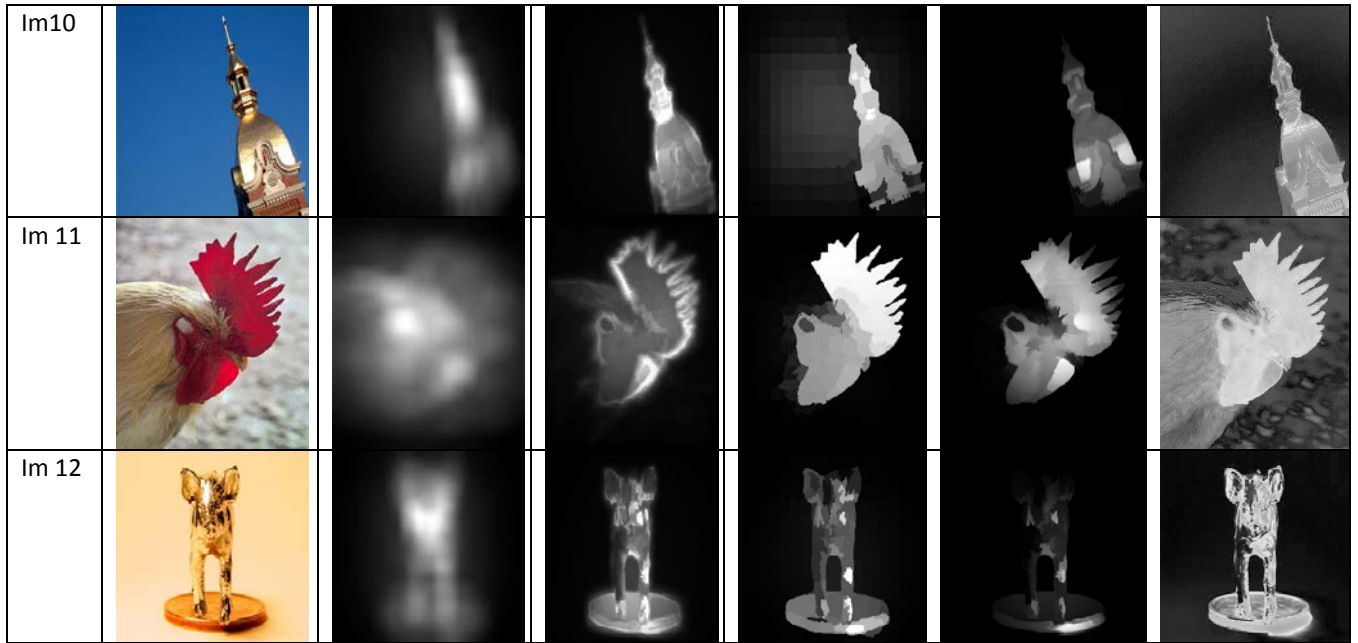


Fig 4.5: Qualitative illustration of saliency segmentation results obtained using four saliency segmentation algorithms and PCDS segmentation algorithm on MSRA dataset.

Another interesting phenomenon in Figure 4.5 is when the salient object does not fall in the centre of the image. For example, Im3 and Im10 are really good examples. It can be observed that in this case, the proposed PCDS segmentation algorithm segmented the whole salient objects clearly. To be specific, one can see that the uppermost part of Im3 close to the image border is assigned similar intensity as the background colour as seen in the PCA, MC and the SSLS segmentation algorithms. In Im10, an observer can see that the MC and SSLS segmentation algorithms suppressed the information in the lower part of the image. Different from this, the proposed PCDS segmentation algorithm uniformly highlighted the salient object, even as the bottom part touches the image border.

Thirdly, the images in Im4 and Im12 are clear indications that it is risky to simply assume that image pixels along the image boundaries contain only background information. Im4 and Im12 have clearly revealed that the assumption can be easily broken and is bound to fail when some parts of the salient object touch the image boundaries. It can be observed that the MC and SSLS segmentation algorithms failed at segmenting the part of a long-range homogeneous salient object in Im4. In Im11, one can see that the PCA, MC and SSLS algorithms completely failed at segmenting the body of the cock that touches the image boundary. It can be seen that the benchmark saliency segmentation algorithms were only able to highlight the later part of the bridge in Im4 and just the head of the cock in Im11. It can be

seen that the situation is completely different from the proposed PCDS segmentation algorithm. It is clear that the proposed segmentation algorithm highlighted the whole salient objects in the Im4 and Im11 even as they touch the image boundaries without any loss of vital information where the other four benchmark saliency segmentation algorithms failed.

Lastly, close attention should be paid to Im12, the researcher mentioned earlier in the literature chapter that most computational saliency segmentation algorithms are built on the assumption that the salient object in an image requires high colour contrast between the background and foreground. It is interesting to show that high colour contrast in some cases is insufficient to help a salient object stand out when the colour contrast between foreground and background is low. The scenario is illustrated using the calf statue in Im12 where both foreground and background share approximately homogeneous colour properties. It is observed that although the benchmark saliency segmentation algorithms highlighted the salient object in the image. It can be seen that the saliency maps produced by the MC, PCA and SSLS segmentation algorithms are not uniformly highlighted as one can see that some parts of the image are almost similar to the background colour especially for the SSLS segmentation algorithm. Moreover, the resolution between the foreground and background saliency maps generated by the PCA, MC and SSLS algorithms are not high as the saliency map produced by the proposed PCDS segmentation algorithm.

In a nutshell, the qualitative comparison with the other benchmark saliency segmentation algorithms with images from the MSRA dataset shows evidence that the PCDS segmentation algorithm achieves an improved performance on these images in terms of the precise location of salient objects, complete segmentation of salient object and robust in different image scenarios. The PCDS segmentation algorithm has also shown superiority in some of the issues raised during the experimental results analysis, some of which are a case of part of the object touching the border. The qualitative results have shown that that proposed PCDS algorithm acted differently compared to the other benchmark saliency segmentation algorithms by not suppressing the object colour intensity in such cases. This behaviour can be attributed to the fact that the PCDS segmentation algorithm does not automatically assume that object parts that touch the image boundaries always contain background information. Moreover, in cases where the colour contrast of the object and background are approximately similar, the CIEDE2000 colour difference formula implemented in this study to measure the contrast difference showed superiority in performance when the other benchmark saliency segmentation algorithms failed.

4.2.6 Qualitative Analysis of Non-Saliency Results on MSRA Dataset without Image Artefact Filtering

This section presents the qualitative analysis of non-saliency results with images selected from the MSRA data set in the absence of image artefact filtering. The results presented in Figure 4.6 illustrates samples of segmented binary images for the proposed PCDS thresholding technique against four state-of-the-art non-saliency image segmentation algorithms used in this study based on their capability to detect the important regions in the image. The first and last columns in Figure 4.6 represent the original image and their corresponding ground truth images. The second to sixth columns are the resultant segmented binary images obtained when the Otsu thresholding, K-means, Fuzzy C-means and modified JSEG segmentation algorithms and the PCDS default thresholding technique were processed on the natural images selected from the MSRA dataset respectively.

For this qualitative analysis presented in this section, twelve out of the selected images are chosen to illustrate the performance of the PCDS default thresholding technique on MSRA dataset. Generally, the PCDS segmentation algorithm produced improved segmented binary images compared with the four state-of-the-art image segmentation algorithms. For example, Im1, it can be seen that the PCDS segmentation algorithm outperforms the Otsu thresholding, K-means and FCM and Modified JSEG algorithms by producing well clustered segmented binary image. However, one can easily observe that a considerable number of background pixels are assigned to the object pixel for the Otsu thresholding, K-means and FCM algorithms. Moreover, it can be seen that modified JSEG failed was not successful for this image. For the *bird* in Im2, it is acceptable for an observer to say the proposed PCDS segmentation algorithm performed better in segmenting the *bird* as compared to the other four state of the art non-saliency algorithms. A segmentation error can be observed around the neck/head part of the bird are segmented as background pixels for the Otsu thresholding, K-means and FCM algorithms. The modified JSEG failed producing the head and tail part of the *bird* image. The PCDS segmentation algorithm shows a better segmentation results and preserves important parts of the image.









































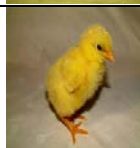






From the result of the *crab* image in Im3, it can be observed that the upper part of the crab close to the image border shares similar colour intensity with the background pixels for segmented binary images produced by the Otsu, K-means and FCM algorithms. The result is

similar to those produced by the other four benchmark saliency segmentation algorithms in Figure 4.5. The modified JSEG algorithm produced a better segmented image compared to its counterparts. However, the algorithm failed at completely segmenting the *crab* image as the legs of the *crab* were detached by the algorithm. On the other hand, the PCDS segmentation algorithm shows better segmentation result than the Otsu, K-means and FCM and modified JSEG algorithms. It is clear that the crab image was properly segmented in reference to the ground truth image. The *swimmer's legs* in Im4 shows that the PCDS segmentation algorithm produced a well clustered and more uniform homogeneous *legs* than the Otsu thresholding, K-means and FCM algorithms. Although these algorithms segmented the image, however, it can be observed that background pixels are present in the object image. In fact, the modified JSEG algorithm completely failed in segmenting the *swimmer's legs*. The same scenario is repeated for the *apple* image in Im6, it can be seen that the segmented objects produced by the four state-of-the-art image segmentation algorithms combine both background pixels in the object. The case is completely different from PCDS default thresholding technique as it produces more homogeneous *apple* image.

In Im7, an observer can notice that the final binary segmented images produced by the first three non-saliency segmentation algorithms do not convey any useful information about the image. Again, the modified JSEG was unsuccessful as the algorithm produced no segmentation result. The PCDS segmentation algorithm, on the other hand produced a segmented image that conveys vital information concerning the image. Although one can see that heads of the salient objects are missing in the binary image produced by the PCDS segmentation algorithm, which leaves room for further improvement. Furthermore, the binary segmentation result produced by the PCDS segmentation algorithm, one can deduce that there are three salient objects in the image and the algorithm also succeeded in suppressing majority of the background information compared to the results of the Otsu thresholding, K-means and Fuzzy C-means algorithms.

The Im8 also shows major segmentation errors experienced by the Otsu thresholding, K-means and Fuzzy c-means algorithms, as it can be observed that the algorithms failed at separating the background from the foreground accurately which is similar to their performances shown in Im9. Although the modified JSEG algorithm showed an improvement in its segmented binary image in Im8. However, the algorithm failed for Im9. Remarkably, the segmentation error in the resultant binary image produced by the PCDS segmentation algorithm are minimal. This similar behaviour can be observed across the Im10 to Im12,

practically all the four non-saliency image segmentation algorithms did not perform well for this set of images. Seamlessly, the resultant segmented images for Im10 to Im12 produced by the PCDS segmentation algorithm contains more homogeneous object and background regions than those produced by the four non-saliency image segmentation algorithms. It is worth mentioning that the segmented images produced by the PCDS segmentation algorithm in Im10 and Im12 are quite impressive even in the absence of image artefact filtering when compared to their corresponding ground truth images. Conclusively, the qualitative analysis of the binary segmentation results with images from the MSRA dataset without image artefact filtering has proven that the PCDS segmentation algorithm proposed in this study shows a great deal of improvement in colour image segmentation.

S/N	Original	Otsu	K-means	FCM	Modified JSEG	PCDS	Ground truth
Im1					FAILED		
Im2							
Im3							
Im5							
Im6							
Im7					FAILED		
Im8							

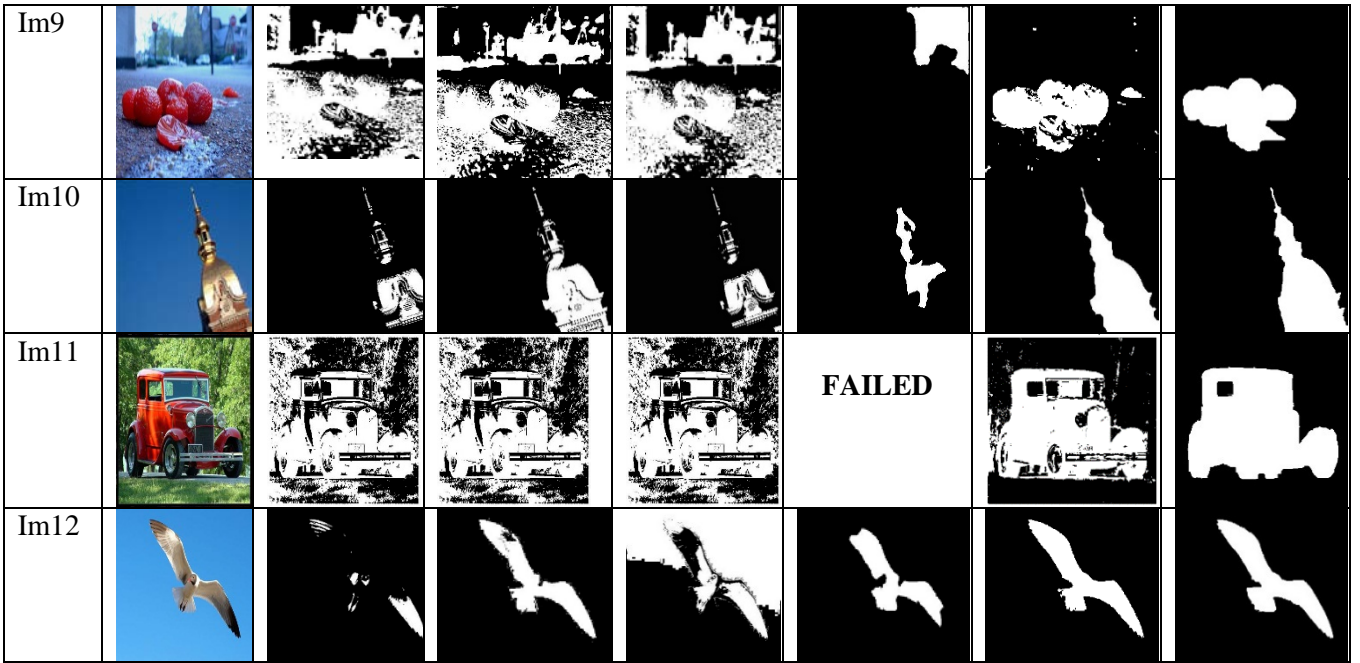



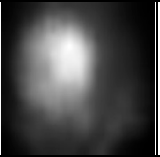
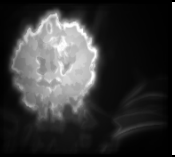
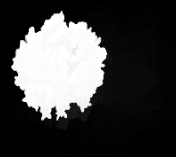
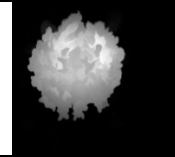
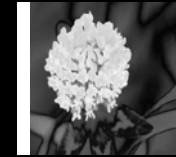


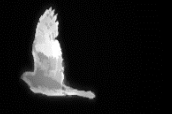




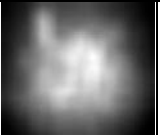





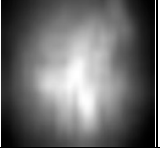



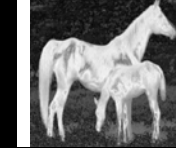


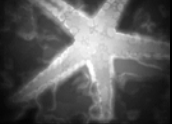









Fig 4.6: Qualitative illustration of binary segmentation results obtained using four state-of-the-art image segmentation algorithms and our default thresholding technique on MSRA dataset.

4.2.7 Qualitative Analysis of Saliency Results on ECSSD

This section presents the qualitative analysis of saliency results of the proposed PCDS segmentation algorithm on natural images selected from the ECSSD. As seen in the previous figures, some samples of saliency maps generated by the proposed PCDS segmentation algorithm as well as the four benchmark saliency segmentation algorithms are displayed in Figure 4.7 for visual comparison. From the figure below, it can be seen that saliency maps generated by the PCDS segmentation algorithm are higher resolution and maintains its good performance, despite the scrambled backgrounds and heterogeneous foregrounds the test images possess. It can be seen that in reference to the qualitative analysis of saliency results presented in the previous figures, the SWD segmentation algorithm still maintains its poor performance with saliency maps with low resolution, blurry and poorly defined borders, carrying less or no information.

The Im1 and Im2 images in Figure 4.7 are examples of when there is high contrast between the salient object and background. It is noticeable that the PCA, MC and SSLs saliency segmentation algorithms, including the PCDS segmentation algorithm produced credible saliency maps for the images in Im1 and Im2. Im3 shows that the PCDS segmentation algorithm highlighted the salient object more accurately and does not lose the

real image information, see the legs of the animals in Im2 compared to the PCA and SSLS algorithm. A similar occurrence can be observed for salient objects in Im3, the PCA and SSLS algorithms, generate saliency maps with very low resolution, closely related to the background colour and the output are not prominently salient. The MC and PCDS segmentation algorithm produced satisfactory results. However, the MC segmentation algorithm suffered information loss at the lower part of the image (see legs of animals in Im3 and Im4) while the PCDS segmentation algorithm preserves the information. This ongoing qualitative analysis takes the researcher to Im5. Virtually all the four benchmark saliency segmentation algorithms realized that there is an object in the image. However, these algorithms failed at uniformly highlighting of some parts of the salient object. It can be observed that the saliency map produced by the SSLS algorithm is low and some parts of the background is being highlighted. By sharp contrast, the PCDS segmentation algorithm successfully suppresses the image shadow and shows precise salient object segmentation with high resolution saliency maps.

S/N	Original image	SWD	PCA	MC	SSLS	PCDS
Im1						
Im2						
Im3						
Im4						
Im5						
Im6						

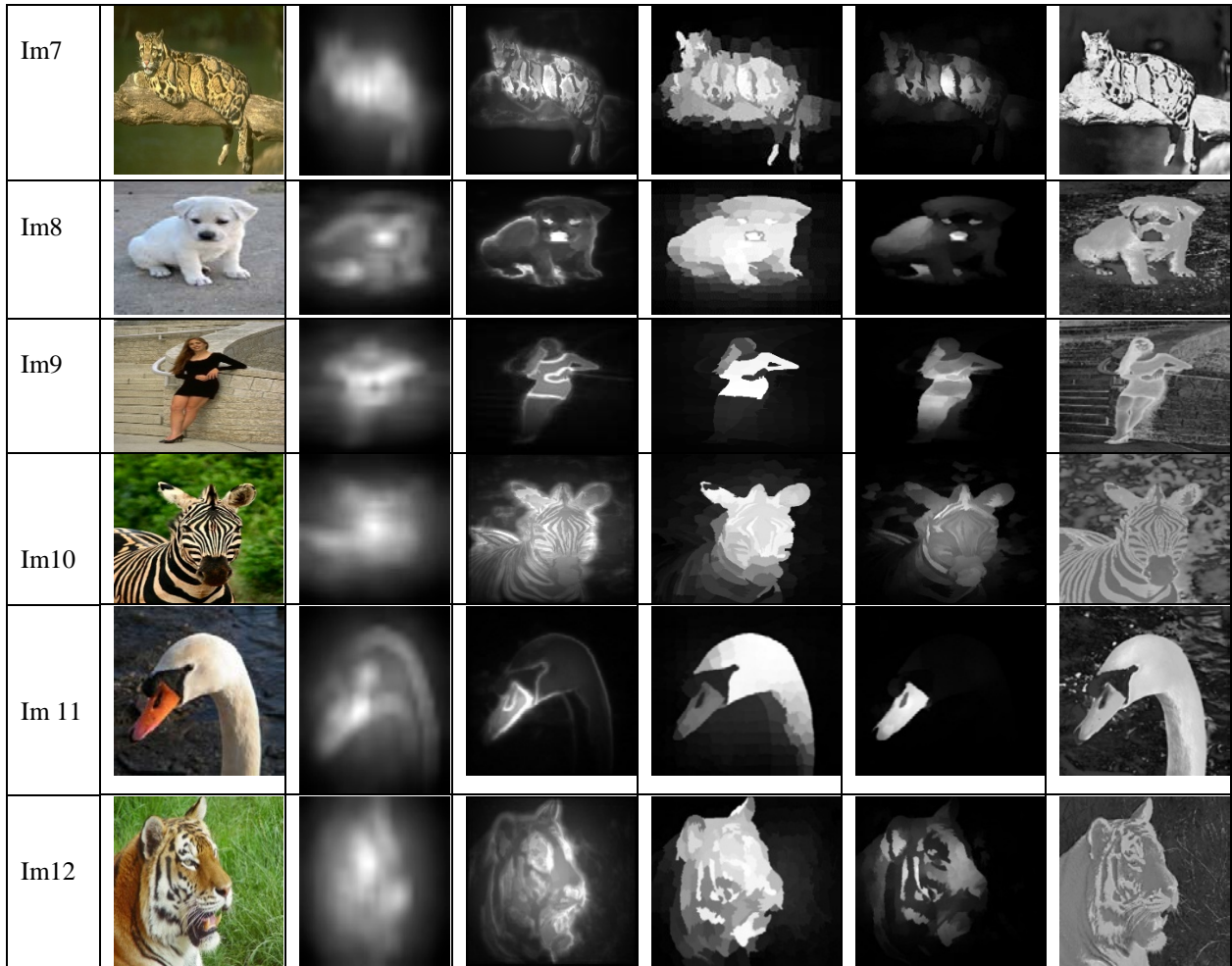


Fig 4.7: Qualitative illustration of saliency segmentation results obtained using four benchmark salient object segmentation algorithm and the proposed PCDS segmentation algorithm on ECSSD.

In continuation to the qualitative analysis of Fig 4.7, some examples of different scenarios are discussed, when the contrast between the foreground and background is low, as shown in Im6 and Im7, it can be seen that the four benchmark saliency segmentation algorithms struggled to highlight the butterfly in this scenario. In Im7, one can see that the MC segmentation algorithm produced imprecise and fuzzy image border. Moreover, it can be observed that the saliency maps produced by the PCA and SSLs algorithms have low resolution. Another observation is that the some parts of log of wood the animal rested on have been suppressed by PCA, MC and SSLs algorithms when the edges of the wood touch the image borders. Interestingly, the proposed PCDS segmentation algorithm effortlessly produced saliency maps highlighting both salient objects in Im6, high resolution saliency maps in Im6 and Im7, clearly defined image borders for Im6 and Im9. The image in Im8 has similar object and background colour. It is evident that the PCA and SSLs algorithms failed at highlighting the salient object. But, the proposed PCDS segmentation algorithm

highlighted the complete salient objects in Im8, Im9. The outputs generated by the PCDS segmentation algorithm can be attributed to the overall implementation steps taken within the proposed framework of this study.

The image in Im9 shows that all the four benchmark saliency segmentation algorithms highlighted certain part of the salient object, it can be seen that the PCA, MC and SSLS segmentation algorithm suppressed the lady's legs in the image, highlight just the body area. This qualitative result is different in the case of the proposed PCDS segmentation algorithm as it uniformly highlights the whole salient object in the image. Besides, the performance of the PCDS segmentation algorithm is also consistent when the salient objects pop into the image boundaries as seen in Im10, Im11 and Im12. It is s clear that the other four benchmark saliency segmentation algorithms failed at segmenting the image parts that touch the image boundaries. The attractiveness of the proposed PCDS segmentation algorithm is that the extracted salient objects do not lose any information whatsoever and the salient objects are evenly highlighted. The qualitative results presented in this section have also shown and validate the proposed PCDS segmentation algorithm's strong potential in handling images with complex scenes than the other four benchmark saliency segmentation algorithms.

4.2.8 Qualitative Analysis of Non-Saliency Results With Images on ECSSD without Image Artefact Filtering

This section presents the qualitative analysis of non-saliency results with images selected from the ECSSD without image artefact filtering. The results presented in Figure 4.8 illustrates the resultant segmented binary images produced by the PCDS segmentation algorithm and the four state-of-the-art saliency image segmentation algorithms based on their proficiency to separate the important regions in the image from the background region. The first and last columns in Figure 4.8 represent the original image and their corresponding ground truth images. The second to the sixth columns are the resultant segmented binary images of the Otsu thresholding, K-means, Fuzzy C-means and modified JSEG segmentation algorithm and the PCDS default thresholding technique respectively.

To carry out the qualitative analysis, twelve out of the selected images from the ECSSD data set were used to illustrate the performance of the PCDS default thresholding technique. It can be seen from Figure 4.8 that PCDS default thresholding technique produces better segmentation results compared with the four non-saliency image segmentation

algorithms. The segmented binary images presented in the figure below show that the Otsu, K-means and FCM algorithms contain several in-homogeneous object regions. Moreover, due to the complexity of the natural images from ESCCD, the modified JSEG algorithm failed for quite a large number of images used during experimentation.






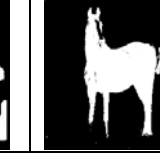
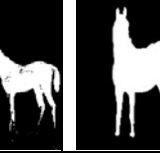
























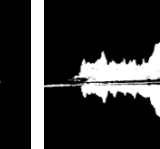
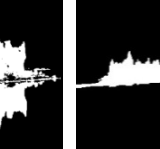
From observation, it can be seen that the four state-of-the-art non-saliency image segmentation algorithms produced poor segmentation results compared to the proposed PCDS segmentation algorithm. The resultant segmented binary image produced by the modified JSEG algorithm in Im1 does not convey any usable information about the image. Moreover, the modified JSEG algorithm failed at producing the segmentation results for Im2 and Im3. On the contrary, the proposed PCDS segmentation algorithm produced an improved, neater, segmented binary images even in the absence of image artefact filtering. The *flower* image as shown in Im4, it can be seen that the proposed PCDS segmentation algorithm shows a better segmentation result as compared with the four non-saliency image segmentation algorithms. It is noticeable that the segmented binary image produced by the proposed PCDS segmentation algorithm contains more information about the image than the Otsu thresholding, K-means Fuzzy C-means and modified JSEG algorithms.

A more significant qualitative comparison between the Otsu, K-means and FCM algorithm and the proposed PCDS segmentation algorithm can be observed in Im5. It can be seen that the object pixels in the image foreground are segmented with the background. Therefore, making the segmentation error to be quite visible in this instance. The segmented binary images produced by the PCDS segmentation are quite similar for Im5. However, one can see that the ground truth image does not contain information about the lower part of the image as seen in the original. This is one of many cases whereby the ground truth image does not necessarily correspond with the original image. With reference to Im6, it can be seen that similar to Im5, background pixels are visible in the salient object produced by the Otsu thresholding, K-means and Fuzzy C means algorithms. Moreover, the modified JSEG algorithm as seen in Im6 suffered information loss. In a different way, the PCDS segmentation algorithm produced a full segmented binary image with less noisy pixels.

The structure of the *bird* in Im7 was maintained in the segmentation results produced by the Otsu thresholding, K-means and FCM algorithms. However, it can be observed that these algorithms contain white noisy pixels at the background region. The modified JSEG segmented some parts of the image out such as the head and legs of the bird. The proposed

PCDS segmentation algorithm, on the other hand maintained the structural information of the image with no noisy pixel. The image in Im8 shows that the modified JSEG algorithm produced better segmentation results followed by the proposed PCDS segmentation algorithm. The segmented binary images produced by the Otsu, K-means and FCM algorithms contain more background pixels in the object region and object pixels in the background region.

Out of the four images that is from Im9 to Im12, the modified JSEG algorithm failed for three of the four images. The otsu thresholding, K-means and Fuzzy C-means algorithms produced similar binary segmentation results as seen in the figure below. Based on the resultant images from the Im9 to Im12, the Otsu thresholding, K-means and Fuzzy C-means algorithms did not perform well as to what is expected as seen in the corresponding ground truth columns. Contrarily, the proposed PCDS segmentation algorithm produced improved binary segmentation results, separating the salient object from the background. The overall suggestion based on the qualitative analysis presented in this section, the proposed PCDS segmentation algorithm evidently produced a better segmentation performance compared to the four state-of-the-art non-saliency image segmentation algorithms regardless of the image complexity.

S/N	ORIGINAL	OTSU	K-means	FCM	Modified JSEG	PCDS	Ground truth
Im1							
Im2					FAILED		
Im3					FAILED		
Im4							
Im5							

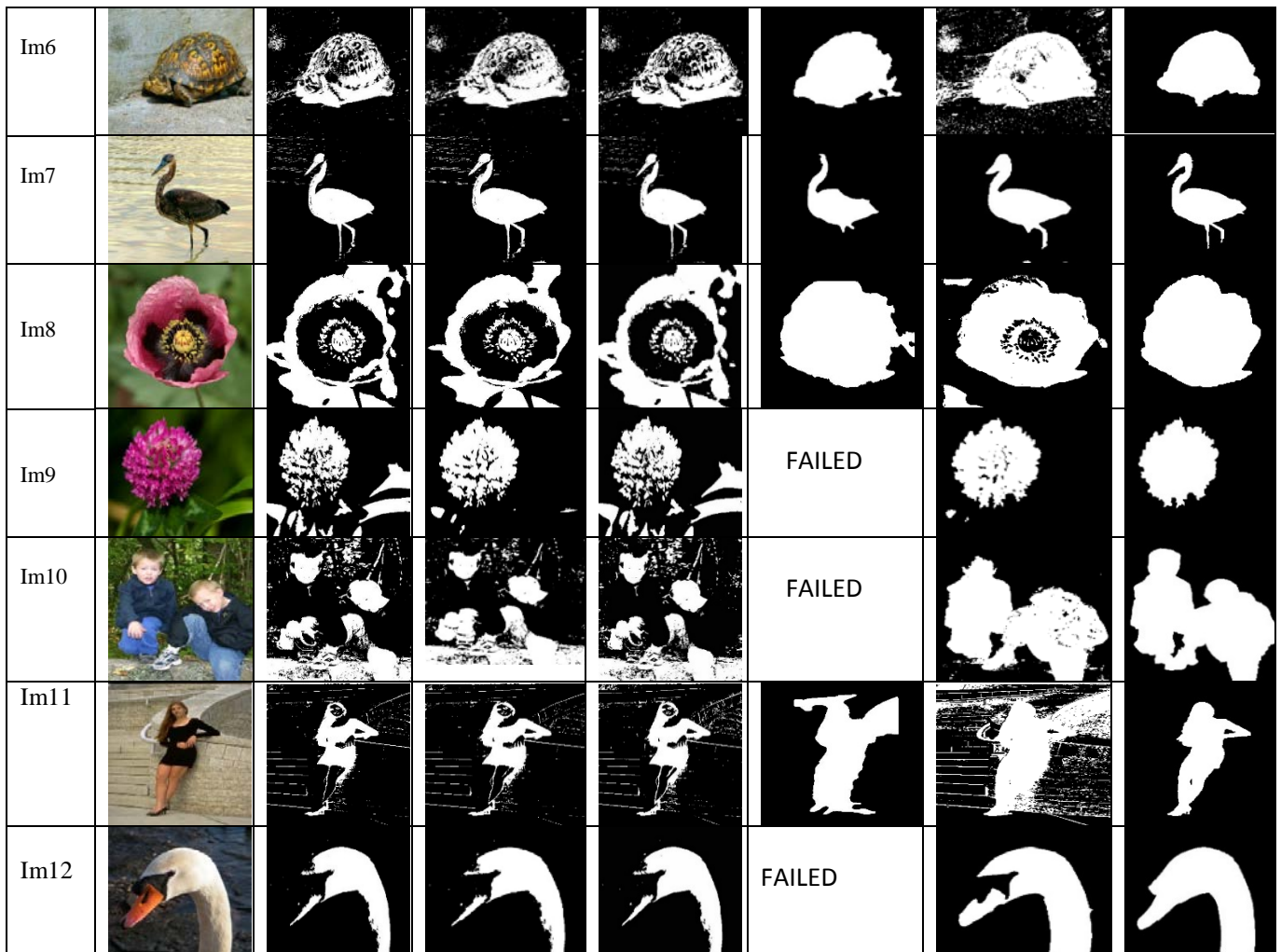


Fig 4.8: Qualitative illustration of binary segmentation results obtained using four state-of-the-art non-saliency image segmentation algorithms and PCDS segmentation algorithm on ECSSD.

4.3 Quantitative Analysis of Binary Segmentation Results

The purpose of the comparison is to quantitatively test for the effectiveness of the PCDS segmentation algorithm using the existing state of the art saliency and non-saliency segmentation methods. To perform the quantitative comparison, the supervised quantitative evaluation method was carried out in this study due to the availability of manual segmented ground truth images made available by the four corpora explored in this study using four widely used state of the art evaluation metrics. Since thresholding based algorithms are conventionally applied to generate a binary saliency map from the greyscale saliency, for the fairness of comparison of the experimental results, all saliency maps produced by the four benchmark saliency segmentation methods and our PCDS segmentation algorithm were segmented by the traditional Otsu thresholding method (Otsu 1979) to convert the greyscale saliency map to a binary image.

Moreover, we compare the performance of our simple default thresholding decision technique with the traditional Otsu algorithm to test its effectiveness. Consequently, we have realized ten variants of segmentation algorithms for quantitative comparison purpose. It is also important to note that to make a fair comparison, the image artefacts filtering procedure implemented in this study was applied on the segmented images produced by the four state-of-the-art non-saliency image segmentation algorithms except for the modified JSEG algorithm that is inherently embedded with a preprocessing and post-processing techniques so there was no need to consider further lesion enhancement.

4.3.1 Evaluation Metrics

There are several ways to quantitatively measure the agreement between the final binary segmentation result and ground truth image. The main objective of a segmentation algorithm is to capture as accurately as possible the object of interest in an image, the effectiveness of the proposed methodology needs to be proven for quality using suitable evaluation metrics. In this study, to assess the quality of the results of the proposed PCDS segmentation algorithm with the other state-of-the-art saliency and non-saliency image segmentation algorithms. A total number of four universally agreed, standard, and easy-to-understand statistical evaluation metrics in terms of *precision*, *F-measure*, *error* and *dice* to numerically score the segmentation results. They are computed based on the following parameters described below:

1. *True Positive* (TP): the number of true positive pixels, foreground pixels that are correctly identified as foreground;
2. *False Positive* (FP): the number of false positive pixels, background pixels that are incorrectly identified as foreground;
3. *True Negative* (TN): the number of true negative pixels, background pixels that are correctly identified as background region.

4.3.1.1 Precision

The precision score, also known as the positive predictive value computes the fraction of the number of ground truth pixels segmented as the salient (foreground) region to the total number of pixels segmented as the salient (foreground) region. It penalizes for classifying background pixels as foreground (Qi *et al.*, 2017; Pont-Tuset *et al.*, 2017). It is also referred to as the measure of quality. It is mathematically defined as:

$$\text{Precision} = \frac{TP}{TP + FP} \quad (4.1)$$

4.3.1.2 F-measure

The F-measure score is the weighted average between precision and recall and can be regarded as an overall performance measurement to produce a more comprehensive metric (Khelifi and Mignotte 2017; Tokmakov *et al.*, 2017). It is calculated using the equation below;

$$F_{\beta} = \frac{(1 + \beta^2) \text{Precision} \times \text{Recall}}{\beta^2 \times \text{Precision} + \text{Recall}} \quad (4.2)$$

Where β^2 represents a non-negative harmonic weight between the precision and the recall. $\beta^2=0.3$ is recommended to emphasize precision rate, which is agreed to be more important than recall to build significance in the accuracy esteem for better quantitative interpretation (Qi et al., 2017).

4.3.1.3 Error Rate

The error rate measures the ratio of pixels incorrectly identified as part of the foreground or background over all the pixels. In this case, a lower value of error indicates better segmentation (Sumithra et al., 2015; Fan et al., 2017).

$$Error = \frac{FP + FN}{TP + FP + TN + FN} \quad (4.3)$$

4.3.1.4 Dice

The Dice coefficient similarity measure computes the agreement between binary segmented image and the ground truth image. In this case, a value of 0 means the segmented result does not match the ground truth while a value close to 1 indicates good segmentation (Fan et al., 2017; Patel et al., 2017).

$$Dice = \frac{2TP}{2TP + FP + FN} \quad (4.4)$$

It is important to note that amongst the four evaluation metrics discussed above, high precision, F-measure, dice and low error values connote a good segmentation output.

4.3.2 Quantitative Analysis of Precision Scores

This section presents quantitative experimental results of the proposed PCDS segmentation algorithm with the other eight state-of-the-art saliency and non-saliency image segmentation algorithms. Table 4.1 lists the average (AVE) and standard deviation (STD) precision scores calculated for the overall resultant test images selected from the four data sets explored in this study. Comparing the statistical values in Table 4.1, the proposed PCDS segmentation algorithm consistently outperforms the other eight state-of-the-art saliency and non-saliency image segmentation algorithms. It can be observed that the precision scores of the proposed PCDS segmentation algorithm are consistently higher than the other algorithms across the four data sets.

Specifically, it can be observed that the performances of the overall average precision scores of the K-means algorithm continue to deteriorate as the dataset becomes challenging. As a matter of fact, the overall performance of the algorithm drops from ISBI 2016 challenge dataset with an overall average precision value of **0.8420** to **0.7904** on PH2 dataset, **0.7250** on the MSRA dataset and **0.6843** on ESCCD. Likewise, Fuzzy C-means algorithm experienced a fall in its overall performance from overall average precision scores of **0.8464**, **0.7480**, **0.7691**, **0.6976** for ISBI 2016 challenge, PH2 and MSRA and ECSS data sets respectively. Oppositely, it can be observed that the overall performance of the modified JSEG algorithm improved across the first two data sets with overall average precision values of **0.8681** and **0.8984** for melanoma skin lesion images from the ISBI 2016 challenge and PH2 data sets respectively.

In fact, it is worth mentioning that the algorithm scored higher values in the overall average precision on melanoma skin lesion images from the ISBI 2016 challenge dataset than the other four state-of-the-art saliency segmentation algorithms, despite the fact that the algorithm failed for four out of the seventy melanoma skin lesion images selected from the ISBI challenge dataset. However, the algorithm recorded the overall least average precision values on natural images selected from the MSRA and ECSSD data sets. The performance is a clear indication that the algorithm lacks robustness when extended to natural images as the researcher recorded fourteen and nineteen failed cases on MSRA and ECSS data sets respectively. Therefore, one can note that the drop in the performances of the four state-of-the-art non-saliency segmentation algorithms in the overall precision scores across the data sets are a pointer to the fact that it becomes harder to segment multiple salient objects in complex scenes.

The statistical values of the overall average precision scores of the four benchmark saliency segmentation algorithms explored in this study show that the performance of these algorithms improves for melanoma skin lesion images from ISBI 2016 challenge and PH2 data sets and then decreases for natural images from MSRA dataset and ECSSD. It is easy for one to observe that each of the benchmark saliency segmentation algorithms ranks differently across the data sets. Specifically, it can be observed that the PCA segmentation algorithm ranks the highest amongst its benchmark counterparts with an average precision value of **0.8593** and **0.9141** on melanoma skin lesion images selected from the ISBI 2016 challenge and PH2 data sets respectively. Meanwhile, SWD segmentation algorithm ranks the highest amongst its counterparts on selected natural images from the MSRA and ESCC data sets with

an average precision value of **0.7964** and **0.7924** respectively. Moreover, the SSLS segmentation algorithm consistently ranks the lowest amongst its counterparts across the four data sets with an average precision value of **0.6439**, **0.8318**, **0.6014** and **0.5643** for ISBI 2016 challenge, PH2, MSRA and ECSS data sets respectively.

Impressively, from the quantitative results, it can be seen that the proposed PCDS segmentation algorithm outperforms the eight state-of-the-art saliency and non-saliency image segmentation algorithms across the four image data sets explored in this study. Specifically, Otsu thresholding method for the proposed PCDS map computation achieves an overall outstanding average and standard deviation of **0.9617 (0.0497)** and **0.9308 (0.0763)** on PH2 and MSRA data sets respectively. Similarly, the default thresholding technique for the PCDS saliency computation achieves an overall outstanding average and standard deviation of **0.8911(0.01157)** and **0.9087(0.1039)** on the ISBI 2016 challenge and ECSS data sets respectively despite the complexity of images selected from the data sets.

In summary, the quantitative performance comparison of the overall average precision values in Table 4.1 demonstrates that the proposed PCDS segmentation algorithm can better segment salient objects, even in complex natural images than the eight state-of-the-art saliency and non-saliency image segmentation algorithms.

Table 4.1: Precision scores of saliency and non-saliency image segmentation algorithms on ISBI 2016, PH2, MSRA and ECSS data sets.

METHOD	ISBI		PH2		MSRA		ECSSD	
	AVE	STD	AVE	STD	AVE	STD	AVE	STD
Otsu	0.8134	0.2428	0.5557	0.3660	0.6437	0.2350	0.6524	0.2176
K-means	0.8420	0.1985	0.7904	0.2000	0.7250	0.2252	0.6843	0.1981
Fuzzy C-means	0.8464	0.1965	0.7480	0.3229	0.6976	0.1785	0.7691	0.1464
Modified JSEG	0.8681	0.2346	0.8984	0.2414	0.4128	0.3916	0.2681	0.3928
SWD + Otsu	0.8437	0.1998	0.9118	0.2364	0.7964	0.1681	0.7924	0.1454
PCA + Otsu	0.8593	0.1663	0.9141	0.1985	0.7816	0.1884	0.6957	0.2254
MC + Otsu	0.8495	0.1869	0.8969	0.1453	0.7689	0.2361	0.7727	0.2283

SSLS + Otsu	0.6439	0.2139	0.8318	0.2074	0.6014	0.2620	0.5643	0.2808
PCDS + Otsu	0.8823	0.1218	0.9617	0.0497	0.9308	0.0763	0.9005	0.1304
PCDS + Default	0.8911	0.1157	0.9499	0.0548	0.8667	0.1322	0.9087	0.1039

4.3.3 Quantitative Analysis of F-measure Scores

This section presents the overall average (AVE) and standard deviation (STD) of F-measure scores for all test images selected from the four data sets explored in this study. The least scores for the first two data sets according to the overall average and standard deviation values for the four state-of-the-art non-saliency image segmentation algorithms as presented in the Table 4.2 below can be linked to the Otsu thresholding algorithm. The algorithm recorded an overall average F-measure values of **0.8354 (0.2374)** and **0.5837 (0.3709)** for melanoma skin lesion images selected from the **ISBI 2016 challenge** and **PH2** dataset. From these values, especially from the overall standard deviation values, it is clear that the algorithm did not perform well for some melanoma skin lesion images during experimentation. Relatedly, modified JSEG algorithm recorded the least performance with overall F-measure score of **0.4170 (0.3809)** and **0.2634 (0.3772)** for natural images selected from the **MSRA dataset and ESCCD** respectively, following the number of failed cases recorded for the modified JSEG algorithm.

One can also observe from the numerical figures in the Table 4.2 that the modified JSEG algorithm scored higher than the other state-of-the-art non-saliency image segmentation algorithm with an overall average F-measure score of **0.8793** on ISBI 2016 challenge dataset, which means that for sixty-six out of the seventy melanoma skin lesion images selected from the ISBI 2016 challenge dataset, the overall average F-measure shows that the algorithm was able to segment the lesion appropriately more than the other three state of the art non-saliency image segmentation algorithms. However, it is noticeable that the overall standard deviation value is higher, the ones recorded for K-means and Fuzzy C-means algorithms even though the algorithm recorded slightly higher overall average higher values than K-means and Fuzzy C-means algorithms. The overall standard deviation value of **0.2312** reflects the failed cases recorded for this algorithm. However, when there are no failed cases recorded for the algorithm on the PH2 data set, it can be observed the overall average value recorded for the algorithm matches the standard deviation values of **0.8888** and **0.2338**.

By observing the numerical values in Table 4.2, it is evident that for melanoma skin lesion images selected from the ISBI 2016 challenge, the SSLS segmentation algorithm scored the least overall F-measure value of **0.6907** across all the eight state-of-the-art saliency and non-saliency segmentation algorithms. On a similar note, SWD segmentation algorithm produced the least overall F-measure amongst the state-of-the-art saliency segmentation algorithms on melanoma skin lesion images selected from the PH2 data sets with an overall average F-measure score of **0.8280** with a relatively high standard deviation value of **0.2150**. The least performance value recorded for each of these algorithms shows that across these two melanoma skin lesion data sets, these algorithms were only able to accurately segment some parts of the lesion. Preceding to the last two data sets, one can also observe that the consistency in the poor performance of the SSLS segmentation algorithm following the overall F-measure scores recorded for the algorithm for MSRA and PH2 data sets. For the sake of emphasis, the SSLS segmentation algorithm recorded an overall least average F-measure score of **0.6433** and **0.6000** for MSRA dataset and ECSSD respectively, which is an indication that segmentation did not perform in segmenting the salient objects.

In spite of the fact that the MC segmentation algorithm scored high average F-measure for skin lesion images selected from the PH2 dataset and natural images from the ECSSD, one can easily observe that the performance of the MC segmentation algorithm is not consistent across the four data sets, which means the overall performance of the algorithm is dependent of the image dataset used. Contradictorily, it is evident that the overall performance of the PCDS segmentation algorithm is consistent across the data sets. For the sake of emphasis, it is notable that the proposed PCDS segmentation algorithm scores an overall highest F-measure score of **0.9096** which is also supported by the least standard deviation value of **0.0966** on melanoma skin lesion images selected from the ISBI 2016 challenge dataset. The overall average and standard deviation values shows that the performance of the PCDS segmentation algorithm was quite consistent even with complicated image conditions. This impressive performance of the PCDS segmentation can be observed in the melanoma skin lesion images selected from the **PH2** dataset as Otsu thresholding on PCDS map computation shows a significant improvement with an overall average F-measure of **0.9580**. In fact, it is worthy of note that the default thresholding technique for PCDS map computation scored the least standard deviation and the second highest value F-measure value of **0.0396** and **0.9504** respectively.

Furthermore, it can be observed that the overall F-measure score of the Otsu thresholding on the proposed PCDS map computation shows a slightly higher performance on natural images selected from the MSRA dataset. It was noticed during experimentation that for natural images selected from the MSRA dataset, some of the images consist of certain details of which its corresponding ground truth image expects it to be white, the researcher took note of the fact the proposed PCDS thresholding technique produced segmented images with details unlike the Otsu thresholding method that generalizes. Finally, one can see that the PCDS segmentation algorithm outperforms all the eight state-of-the-art image segmentation algorithms for natural images selected from the ECSSD with the highest overall average and the least standard deviation F-measure values of **0.9043** and **0.1092** respectively. While Otsu thresholding on the proposed PCDS map computation scored the second best average and standard F-measure scores of **0.8888** and **0.1401** respectively.

Table 4.2: F-measure scores of saliency and non-saliency image segmentation algorithms on ISBI 2016 challenge, PH2, MSRA and ECSS data sets

METHOD	ISBI		PH2		MSRA		ECSSD	
	AVE	STD	AVE	STD	AVE	STD	AVE	STD
Otsu	0.8353	0.2374	0.5837	0.3709	0.6491	0.2214	0.6154	0.2015
K-means	0.8656	0.1897	0.8079	0.2964	0.7319	0.2241	0.6561	0.1909
Fuzzy C-means	0.8678	0.1895	0.7677	0.3224	0.6746	0.2188	0.7065	0.1436
Modified JSEG	0.8793	0.2312	0.8888	0.2338	0.4170	0.3809	0.2634	0.3772
SWD + Otsu	0.8213	0.1915	0.8280	0.2150	0.7373	0.1435	0.7567	0.1401
PCA + Otsu	0.8792	0.1634	0.8953	0.1909	0.8055	0.1676	0.7154	0.2062
MC + Otsu	0.8763	0.1496	0.9288	0.1410	0.7938	0.2159	0.7930	0.2063
SSLS + Otsu	0.6907	0.2029	0.8538	0.2015	0.6433	0.2579	0.6000	0.2684
PCDS + Otsu	0.8963	0.1055	0.9580	0.0440	0.9176	0.0751	0.8888	0.1272
PCDS + Default	0.9096	0.0966	0.9504	0.0396	0.8803	0.1144	0.9043	0.1092

4.3.4 Quantitative Analysis of Error Scores

This section describes the overall average (AVE) and standard deviation (STD) of error scores for all experimental images selected from the four data sets explored in this study.

From the numerical values presented in the Table 4.3 below, one can easily note that out of the four non-saliency image segmentation algorithms, the modified JSEG algorithm scored the highest average and standard deviation error values of **0.0810** and **0.2281** respectively for melanoma skin lesion images selected from the ISBI 2016 challenge dataset. These figures can be tied to the performance of the algorithm on ISBI 2016 challenge dataset as it was earlier mentioned by the researcher that the algorithm recorded a total number of four failed cases for melanoma skin lesion images selected from the ISBI 2016 challenge dataset. But for PH2 dataset with no failed cases recorded, one can observe that the difference in the error values compared to the ISBI 2016 challenge dataset is minimal.

The Otsu thresholding method which recorded the least average F-measure score for melanoma skin lesion images selected from the ISBI 2016 challenge and PH2 data sets maintained its position as the algorithm scored the second highest average and standard deviation scores after modified JSEG with error values of **0.0544** and **0.1196** respectively. On the PH2 dataset, the algorithm ranked the least with an overall average and standard deviation error scores of **0.0579** and **0.0631** respectively. The fuzzy c-means algorithm performed better than its counterparts with an overall average error values of **0.0423 (0.0566)** and **0.0255 (0.0388)** for melanoma skin lesion images from the ISBI 2016 challenge and PH2 data sets. Across natural images selected from the MSRA and ECSS data sets, one can see that the high number of failed cases recorded for modified JSEG algorithm also reflected in its overall error performance. It can be observed that the algorithm recorded the overall highest error values for all the eight state-of-the-art image segmentation algorithms used in this study. Next to this is the Otsu thresholding algorithm, the overall average error scores recorded shows that the algorithm did not perform well for quite a large number of experimental images from the MSRA and ESCC data sets.

Following the performance of the Otsu thresholding is the K-means algorithm with an overall average and standard deviation values of **0.0870 (0.1218)** and **0.1797 (0.1633)** respectively. Again, Fuzzy C-means algorithm performed better than its counterparts with lower average and standard deviation error values of **0.0846 (0.1015)** and **0.0711 (0.1103)**. So it is safe for one to say that the performance of Fuzzy C-means algorithm was consistent across the four image data sets in terms of the error values. A step away from the four non-saliency segmentation algorithms to the other four saliency segmentation algorithms shows that for melanoma skin lesion images selected from the ISBI 2016 challenge, SSLS segmentation algorithm recorded the highest overall average error value of **0.1132**. The

overall average error value greatly supports the algorithm's least overall F-measure score recorded in the previous table. This performance is followed by the SWD segmentation algorithm with an overall average error value of **0.1038**. It is interesting to note that although SSLs segmentation scored a higher overall average error value than SWD segmentation algorithm. It should be observed that the overall standard deviation score of the SWD segmentation algorithm is higher compared to SSLs segmentation algorithm. This indicates that the SWD segmentation algorithm performed poorly for some of the melanoma skin lesion images selected from the ISBI 2016 challenge data sets.

Moving from ISBI 2016 challenge dataset with PH2 data set, one can observe that SWD segmentation algorithm recorded the highest average and standard deviation error values of **0.0815 (0.1160)** while the MC segmentation algorithm shows an improvement compared to its counterparts on both ISBI and PH2 data sets. For natural images selected from the MSRA and ECSS data sets, SWD segmentation algorithm consistently recorded the highest error values followed by the SSLs segmentation algorithms. Again, the MC segmentation algorithm shows a better overall error value than its counterparts. From the following observations, one can depict that SWD segmentation algorithm consistently did not perform well across the four image data sets which is relative to the saliency results produced by the algorithm in the qualitative result analysis section. On the other hand, MC segmentation algorithm's performance is quite consistent across the data sets. Remarkably, PCDS segmentation algorithm demonstrated its effectiveness with an outstanding **least** average across the four data sets.

Emphatically, it can be observed that the binary segmentation of the saliency map using the simple default thresholding technique for the proposed PCDS recorded an outstanding overall minimum average and standard deviation error scores of **0.0231(0.0300)** and **0.0321(0.0498)** on ISBI 2016 challenge and ECSS data sets respectively. On a similar note, it can be observed that when Otsu thresholding was applied to the proposed PCDS saliency map computation, the researcher recorded the least average and standard deviation error values of **0.0112 (0.0112)** and **0.0335 (0.0592)** on PH2 and MSRA data sets respectively. The 0.001 difference in the standard deviation values of the Otsu thresholding method for PCDS map computation and the default thresholding technique is also commendable. This is an indication shows that the proposed PCDS default thresholding technique performed well for quite a large number of melanoma skin lesion images selected from the PH2 dataset.

Table 4.3: Error scores of saliency and non-saliency image segmentation algorithms on ISBI 2016 challenge, PH2, MSRA and ECSSD data sets

METHOD	ISBI		PH2		MSRA		ECSSD	
	AVE	STD	AVE	STD	AVE	STD	AVE	STD
Otsu	0.0544	0.1196	0.0579	0.0631	0.0980	0.0837	0.1872	0.1486
K-means	0.0428	0.0576	0.0265	0.0543	0.0870	0.1218	0.1797	0.1633
Fuzzy C-means	0.0423	0.0566	0.0255	0.0388	0.0846	0.1015	0.0711	0.1103
Modified JSEG	0.0810	0.2281	0.0271	0.0428	0.4242	0.4378	0.6936	0.4346
SWD + Otsu	0.1038	0.1181	0.0815	0.1160	0.1232	0.0735	0.1415	0.0658
PCA + Otsu	0.0502	0.0707	0.0322	0.0349	0.0564	0.0623	0.1111	0.0901
MC + Otsu	0.0429	0.0727	0.0139	0.0169	0.0547	0.0746	0.0757	0.0824
SSLS + Otsu	0.1132	0.1079	0.0263	0.0378	0.0838	0.0762	0.1284	0.0965
PCDS + Otsu	0.0378	0.0507	0.0112	0.0112	0.0335	0.0592	0.0563	0.0658
PCDS + Default	0.0231	0.0300	0.0153	0.0113	0.0358	0.0321	0.0498	0.0645

4.3.5 Quantitative Analysis of Dice Scores

This section presents the overall average (AVE) and standard deviation (STD) of Dice scores that measures the overall structural agreement between binary segmentation result and ground truth image. Table 4.4 is a reflection of the segmentation performance of the eight state-of-the-art image segmentation algorithms and the proposed PCDS segmentation algorithm. From observation, it can be observed that out the four non-saliency image segmentation algorithm, Fuzzy C-means algorithm produced slightly higher average Dice values of **0.8977** for melanoma skin lesion image selected from the ISBI 2016 challenge dataset followed by the K-means algorithm with an overall dice value of **0.8949**. However, Fuzzy C-means algorithm produced a higher standard deviation value compared to the K-means algorithm, which means that the K-means algorithm must have maintained the structural information for certain melanoma images than the Fuzzy c-means algorithms. Oppositely, Otsu thresholding method produced the least overall average and standard deviation in dice values of **0.8665** and **0.2296** on ISBI 2016 challenge dataset.

Further observation of the overall Dice performance of non-saliency image segmentation algorithms shows that the modified JSEG algorithm produced a higher overall average and standard deviation Dice value of **0.8812 (0.2306)** for melanoma skin lesion images selected from **PH2** database compared to the other non-saliency image segmentation algorithms. On this same data set, K-means algorithm followed suit as it ranks the second after modified JSEG algorithm with an overall average and standard deviation Dice values of **0.8336 (0.2899)**, followed by the Fuzzy C-means algorithm. Across the melanoma skin lesion image data sets, Otsu thresholding algorithm recorded the least overall average and standard deviation Dice values. Across MSRA and ECSSD data sets, the overall average and standard deviation of modified JSEG is a result of the recorded failed cases. Otsu thresholding has also demonstrated its inability to maintain structural information following the overall average Dice values the algorithm attained across MSRA and ECSS data sets. The overall average Dice value of the K-means algorithm shows that the algorithm was able to preserve the structural information than its counterparts on the experimental images selected from the MSRA dataset. The Fuzzy C-means algorithms, on the other hand performed better than the others for selected experimental images from ECSSD. On a general note, the four state-of-the-art non-saliency image segmentation algorithms have demonstrated their inconsistencies across varying image data sets.

As revealed in Table 4.4, none amongst the four benchmark saliency segmentation algorithms score higher overall dice values across the four image data sets. But, one can see that the MC segmentation algorithm came close enough by performing better than its counterparts on three out of four image data sets which are ISBI, PH2 and ECSS data sets. Meanwhile, PCA segmentation algorithm performed better than its counterparts on experimental images selected from the MSRA dataset. By sharp contrast, the proposed PCDS segmentation algorithm shows substantial improvements with an outstanding overall average Dice values of **0.9342**, **0.9522** and **0.9024** for ISBI 2016 challenge PH2 and ECSS data sets respectively. Moreover, the Otsu thresholding on the proposed PCDS map computation produced the highest overall Dice values of **0.9129**. This indicates that a higher percentage of the images selected across the four data sets can be well segmented by the proposed PCDS segmentation algorithm as the improvement demonstrated by the PCDS segmentation algorithm is statistically significant and highly consistent.

Table 4.4: Dice scores of saliency and non-saliency image segmentation algorithms on ISBI 2016 challenge, PH2, MSRA and ECSSD data sets.

METHOD	ISBI		PH2		MSRA		ECSSD	
	AVE	STD	AVE	STD	AVE	STD	AVE	STD
Otsu	0.8665	0.2296	0.6262	0.3777	0.6786	0.2203	0.6118	0.2233
K-means	0.8949	0.1757	0.8336	0.2899	0.7539	0.2308	0.6577	0.2136
Fuzzy C-means	0.8977	0.1806	0.7962	0.3204	0.6886	0.2515	0.6778	0.1907
Modified JSEG	0.8941	0.2284	0.8812	0.2306	0.4347	0.3833	0.2662	0.3772
SWD + Otsu	0.8061	0.1806	0.7542	0.2079	0.7044	0.1545	0.7340	0.1401
PCA + Otsu	0.9067	0.1235	0.8762	0.1867	0.8416	0.1398	0.7480	0.1811
MC + Otsu	0.9120	0.1253	0.9291	0.1395	0.8087	0.2250	0.7931	0.2324
SSLS + Otsu	0.7601	0.1807	0.8631	0.2293	0.7067	0.2447	0.6591	0.2475
PCDS + Otsu	0.9166	0.0811	0.9360	0.1424	0.9129	0.1001	0.8820	0.1343
PCDS + Default	0.9342	0.0704	0.9522	0.0284	0.9008	0.0941	0.9024	0.1109

4.4 Chapter conclusion

This chapter has dealt with the empirical validation of the proposed PCDS segmentation algorithm segment by comparing its performance with eight state-of-the-art saliency and non-saliency image segmentation algorithms with the ground truth images made available in the data sets. Therefore, the validation method quantitatively evaluates the similarity between the ground truth images with the computed segmented binary images. The experiments conducted using four benchmark segmentation data sets have pointed to a high correlation between the ground truth image and the binary segmentation results produced by PCDS segmentation algorithm. The computed scores across the four evaluation metrics scored relatively high overall average values across the data sets.

CHAPTER 5

SUMMARY AND CONCLUSIONS

This chapter is the concluding part of this dissertation. The chapter presents possible research recommendations for further improvements based on the proposed approach.

5.1 Summary

In this study, a new perceptual colour difference saliency segmentation algorithm was investigated. The overarching goal of this study was to investigate the effectiveness of perceptual colour difference saliency method to improve the performance of colour image segmentation. The research objectives have been met in order to achieve the goal of this study. They are thereby summarized for the sake of clarities as follows:

1. To comprehensively review relevant publications based on image segmentation algorithms.

The first objective which was to comprehensively review relevant publications based on image segmentation was presented in the chapter 2 of this study. Chapter 2 presented a comprehensive survey of image segmentation algorithms and several developments of new algorithms that address the research gaps in the literature. The chapter begins with the three fundamental classifications of image segmentation algorithms and their limitations. This led to the survey of diverse improvements, the extension of conventional image segmentation to colour image segmentation and the diverse challenges faced. The chapter also includes the introduction of colour object salient segmentation that has been proposed to facilitate the performance of colour image segmentation. Subsequently, the researcher reviews how different colour models have been investigated for colour image segmentation and performance evaluation methods.

2. To develop an image segmentation algorithm based on perceptual colour difference Saliency Segmentation.

The development of a new image segmentation algorithm based on perceptual colour difference saliency segmentation was presented in the chapter three of this study. The proposed PCDS segmentation algorithm integrated both background and foreground information which complement each other in the accurate salient object segmentation.

The methodology of the proposed PCDS segmentation algorithm was implemented based on four major stages: colour image transformation, luminance image enhancement, salient pixel computation and image artefact filtering. First, the transformation of colour image is performed to convert Adobe RGB colour image to the CIE L*a*b colour image to achieve perceptual saliency. This is followed by the adaptive gamma correction that was performed on the image luminance channel to enhance the luminance channel of the image. To compute the salient pixel, the mean value of the background object colour was estimated by the mean of image pixel values on an ellipsoidal patch drawn close to the image boundaries. Afterwards, the mean value of object colour was estimated by the mean of image pixels within a rectangular patch drawn over the image centre. Thereafter, the computed object and background mean values are aggregated to create a greyscale saliency map followed by a simple thresholding technique to realize a binarized image. The CIEDE2000 colour difference formula implemented in this study was used to compute the difference of background colour and difference of object colour. Finally, morphological analysis was performed on the resultant segmented binary image to filter artefacts. All of these steps have contributed to the overall performance of the proposed PCDS segmentation algorithm.

3. To experimentally compare the performance of the developed segmentation algorithm with existing state of the art image segmentation algorithms using well known statistical evaluation metrics. The third objective was intrinsically met by experimentally validating the performance of the proposed PCDS algorithm with existing state-of-the-art saliency and non-saliency image segmentation algorithms using well known statistical evaluation metrics. For the purpose of the performance evaluation of the investigated perceptual colour difference saliency segmentation algorithms, the proposed saliency segmentation algorithm was tested on a hundred and ninety challenging diversified medical and non-medical images acquired from four diverse benchmark corpora. Both qualitative and quantitative evaluation methods were explored for performance evaluation. For qualitative measures, the evaluation was carried with comparison with state of the art saliency segmentation algorithms to test the effectiveness of the saliency maps produced by the newly developed colour difference perception saliency segmentation algorithm. The performance of the

default thresholding binary segmentation results was also compared state of the art image segmentation algorithms.

For the quantitative performance evaluation, eight state-of-the-art saliency and non-saliency image segmentation algorithms were used to test the effectiveness of the newly developed colour difference saliency segmentation algorithm with default thresholding technique with five well known statistical evaluation metrics, namely, *precision*, *F-measure*, Error and Dice. The experimental results reported in this study confirm that the proposed colour difference saliency segmentation algorithm significantly outperforms eight state-of-the-art segmentation algorithms. More importantly, the research reported in this study has proven the effectiveness of the newly proposed perceptual colour difference saliency segmentation to improve colour image segmentation performance.

5.2 Future Work

Despite significant research progress in colour image segmentation research field, there is always room for improvement in the image processing field. The researcher presents possible applications and extensions by highlighting a few of the many exciting future works using the preliminary version of the proposed segmentation algorithm in this study. In the view of the researcher, the following studies are worth continuing;

1. As a scope of further research, the proposed PCDS segmentation algorithm can be extended to extract distinctive features for the skin lesion classification of melanoma skin lesion images.
2. The proposed PCDS segmentation method can be extended to other well-known existing colour models and colour difference formulae for comparative purposes.
3. It will be prudent to look at more challenging practical application areas.
4. Besides colour information, the combination of other visual features such as shape, texture, motion is an approach that merits further study.

5.3 Conclusion

This dissertation investigated the problem of colour image segmentation, as an image segmentation and salient object segmentation task. A comprehensive review of research work was presented. It is unfortunate that despite vast research efforts, image segmentation remains an important problem that is yet unsolved. The work reported in this study has investigated a new PCDS segmentation algorithm towards improved colour image segmentation. The proposed PCDS segmentation algorithm was tested on four benchmark image data sets to measure its accuracy, effectiveness and validate its performance. The proposed PCDS segmentation has proven to be comparable to and even outperform other existing state-of-the-art saliency and non-saliency image segmentation algorithms. Moreover, the application of the proposed PCDS segmentation algorithm to melanoma skin lesion segmentation has indeed shown that the algorithm is feasible and successful for such an application.

References

- Abe, B., Olugbara, O. and Marwala, T. 2014. Experimental comparison of support vector machines with random forests for hyperspectral image land cover classification. *Journal of Earth System Science*, 123(4): 779-790.
- Abo-Eleneen, Z. 2011. Thresholding based on fisher linear discriminant. *Journal of Pattern Recognition Research*, 6(2): 326-334.
- Achanta, R., Hemami, S., Estrada, F. and Susstrunk, S., 2009. Frequency-tuned salient object detection. *Computer Vision and Pattern Recognition*, 1597-1604.
- Adetiba, E. and Olugbara, O. O. 2015a. Improved classification of lung cancer using radial basis function neural network with affine transforms of voss representation. *PloS one*, 10(12): e0143542.
- Adetiba, E. and Olugbara, O.O., 2015b. Lung cancer prediction using neural network ensemble with histogram of oriented gradient genomic features. *The Scientific World Journal*, 1-17.
- Agathos, A., Theoharis, T. and Boehm, A., 1998. Efficient integer algorithms for the generation of conic sections. *Computers & Graphics*, 22(5): 621-628.
- Ahirwal, B., Khadtare, M. and Mehta, R. 2007. FPGA based system for color space transformation RGB to YIQ and YcbCr. *Intelligent and Advanced System*, 1345-1349.
- Ahmed, M. N., Yamany, S. M., Mohamed, N., Farag, A. A. and Moriarty, T. 2002. A modified fuzzy c-means algorithm for bias field estimation and segmentation of MRI data. *IEEE Transactions on Medical Imaging*, 21(3): 193-199.
- Ahn, E., Bi, L., Jung, Y. H., Kim, J., Li, C., Fulham, M. and Feng, D.D., 2015. Automated saliency-based lesion segmentation in dermoscopic images. *Medicine and Biology Society*, 3009-3012.
- Ahn, E., Kim, J., Bi, L., Kumar, A., Li, C., Fulham, M. and Feng, D., 2017. Saliency-based lesion segmentation via background detection in Dermoscopic Images. *Journal of Biomedical and Health Informatics*, PP(99).
- Akay, B. 2013. A study on particle swarm optimization and artificial bee colony algorithms for multilevel thresholding. *Applied Soft Computing*, 13(6): 3066-3091.

Alam, S., Dobbie, G. and Rehman, S. U. 2015. Analysis of particle swarm optimization based hierarchical data clustering approaches. *Swarm and Evolutionary Computation*, 25, 36-51.

Alihodzic, A. and Tuba, M. 2014. Improved bat algorithm applied to multilevel image thresholding. *The Scientific World Journal*, 1-16.

Al-Kharusi, H. and Al-Bahadly, I., 2014. Intelligent parking management system based on image processing. *World Journal of Engineering and Technology*, 2(02): 55.

Anand, A., Tripathy, S. S. and Kumar, R. S. 2015. An improved edge detection using morphological Laplacian of Gaussian operator. *Signal Processing and Integrated Networks*, 532-536.

Anderberg, M.R., 1973. Cluster analysis for applications. Monographs and textbooks on probability and mathematical statistics.

Apró, M., Novaković, D., Pál, S., Dedijer, S. and Milić, N. 2013. Colour space selection for entropy-based image segmentation of folded substrate images. *Acta Polytechnica Hungarica*, 10(1): 43-62.

Arbelaez, P., Fowlkes, C. and Martin, D. 2007. The berkeley segmentation dataset and benchmark. see <http://www.eecs.berkeley.edu/Research/Projects/CS/vision/bsds>.

Arora, S., Acharya, J., Verma, A. and Panigrahi, P. K. 2008. Multilevel thresholding for image segmentation through a fast statistical recursive algorithm. *Pattern Recognition Letters*, 29(2): 119-125.

Arthur, D. and Vassilvitskii, S. 2007. k-means++: The advantages of careful seeding. *ACM-SIAM Symposium on Discrete algorithms. Society for Industrial and Applied Mathematics*, 1027-1035.

Asmare, M. H., Asirvadam, V. S. and Iznita, L. 2009. Colour space selection for colour image enhancement applications. *Signal Acquisition and Processing*, 208-212.

Bai, L., Liang, J., Dang, C. and Cao, F. 2012. A cluster centers initialization method for clustering categorical data. *Expert Systems with Applications*, 39 (9): 8022-8029.

Ball, G. H. and Hall, D. J. 1965. *A novel method of data analysis and pattern classification*. Isodata, DTIC Document.

- Banerjee, S., Mitra, S. and Shankar, B. U. 2016. Single seed delineation of brain tumor using multi-thresholding. *Information Sciences*, 330, 88-103.
- Basaeed, E., Bhaskar, H. and Al-Mualla, M. 2016. Supervised remote sensing image segmentation using boosted convolutional neural networks. *Knowledge-Based Systems*, 99: 19-27.
- Basavaprasad, B. and Ravi, M. 2014. A comparative study on classification of image segmentation methods with a focus on graph based techniques. *International Journal of Research in Engineering and Technology*, 3(3): 310-314.
- Bayindir, F., Kuo, S., Johnston, W.M. and Wee, A.G., 2007. Coverage error of three conceptually different shade guide systems to vital unrestored dentition. *The Journal of prosthetic dentistry*, 98(3): 175-185.
- Ben Chaabane, S., Sayadi, M., Fnaiech, F. and Brassart, E. 2008. Color image segmentation based on Dempster-Shafer evidence theory. *Electrotechnical*, 862-866.
- Bhandari, A. K., Singh, V. K., Kumar, A. and Singh, G. K. 2014. Cuckoo search algorithm and wind driven optimization based study of satellite image segmentation for multilevel thresholding using Kapur's entropy. *Expert Systems with Applications*, 41 (7): 3538-3560.
- Bhattacharjee, R. and Saini, L. M. 2015. Detection of Acute Lymphoblastic Leukemia using watershed transformation technique. *Signal Processing, Computing and Control*, 383-386.
- Bindu, C. H. and Prasad, K. S. 2012. An efficient medical image segmentation using conventional OTSU method. *International Journal of Advanced Science and Technology*, 38, 67-74.
- Blum, C. and Roli, A. 2001. Metaheuristics in Combinatorial Optimization: Overview and Conceptual Comparison. *ACM Computing Surveys*, 35(3): 268-308.
- Bodhe, T. S. and Mukherji, P. 2013. Selection of color space for image segmentation in pest detection. *Advances in Technology and Engineering*, 1-7.
- Bonde, D.J., Shende, R.S., Kedari, A.S., Gaikwad, K.S. and Bhokre, A.U., 2014 . Automated car parking system commanded by Android application. *Computer Communication and Informatics*, 1-4.

- Bora, D. J. and Gupta, A. K. 2014. Clustering Approach Towards Image Segmentation: An Analytical Study. *arXiv preprint arXiv:1407.8121*,
- Borji, A., Cheng, M. M., Jiang, H. and Li, J. 2014. Salient object detection: A survey. *arXiv preprint arXiv:1411.5878*.
- Bouaziz, A., Draa, A. and Chikhi, S. 2015. Artificial bees for multilevel thresholding of iris images. *Swarm and Evolutionary Computation*, 21: 32-40.
- Bozorgtabar, B., Abedini, M. and Garnavi, R. 2016. Sparse Coding Based Skin Lesion Segmentation Using Dynamic Rule-Based Refinement. *Machine Learning in Medical Imaging*, 254-261.
- Busin, L., Vandenbroucke, N. and Macaire, L. 2008. Color spaces and image segmentation. *Advances in imaging and electron physics*, 151(1): 1.
- Busin, L., Vandenbroucke, N. and Macaire, L. 2009. Color spaces and image segmentation. *Advances in imaging and electron physics*, 151, 65-168.
- Busin, L., Vandenbroucke, N., Macaire, L. and Postaire, J. G. 2004. Colour space selection for unsupervised colour image segmentation by histogram multithresholding. *ICIP*, 203-206.
- Cai, H., Yang, Z., Cao, X., Xia, W. and Xu, X. 2014. A new iterative triclass thresholding technique in image segmentation. *IEEE Transactions on Image Processing*, 23(3): 1038-1046.
- Cai, W., Chen, S. and Zhang, D. 2007. Fast and robust fuzzy c-means clustering algorithms incorporating local information for image segmentation. *Pattern recognition*, 40(3): 825-838.
- Campos, I., Neale, C. M., Calera, A., Balbontín, C. and González-Piqueras, J. 2010. Assessing satellite-based basal crop coefficients for irrigated grapes (*Vitis vinifera* L.). *Agricultural Water Management*, 98(1): 45-54.
- Cano, J. R., Cordon, O., Herrera, F. and Sánchez, L. 2002. A greedy randomized adaptive search procedure applied to the clustering problem as an initialization process using K-Means as a local search procedure. *Journal of Intelligent & Fuzzy Systems*, 12 (3, 4): 235-242.
- Cao, J., Zhang, X., Wang, Y. and Zhao, Q. 2016. Subsurface geobody imaging using CMY color blending with seismic attributes. *Journal of Electrical and Computer Engineering*, 1-16.

Castillo, O., Neyoy, H., Soria, J., Melin, P. and Valdez, F. 2015. A new approach for dynamic fuzzy logic parameter tuning in Ant Colony Optimization and its application in fuzzy control of a mobile robot. *Applied Soft Computing*, 28, 150-159.

Cavalcanti, P. G. and Scharcanski, J., 2013. Macroscopic pigmented skin lesion segmentation and its influence on lesion classification and diagnosis. *Color Medical Image Analysis*, 15-39.

Celik, T. and Demirel, H. 2009. Fire detection in video sequences using a generic color model. *Fire Safety Journal*, 44(2): 147-158.

Celik, T., Demirel, H., Ozkaramanli, H. and Uyguroglu, M. 2007. Fire detection using statistical color model in video sequences. *Journal of Visual Communication and Image Representation*, 18(2): 176-185.

Chaabane, S. B., Sayadi, M., Fnaiech, F. and Brassart, E. 2009. Dempster-Shafer evidence theory for image segmentation: application in cells images. *International Journal of Signal Processing*, 5(1).

Chaabane, S. B., Sayadi, M., Fnaiech, F. and Brassart, E. 2010. Colour image segmentation using homogeneity method and data fusion techniques. *Eurasip Journal on Advances in Signal Processing*, 1.

Chamorro-Martinez, J., Sanchez, D. and Prados-Suarez, B. 2003. A fuzzy color image segmentation applied to robot vision. *Advances in Soft Computing*. 129-138.

Chandler, D. M. 2013. Seven challenges in image quality assessment: past, present, and future research. *ISRN Signal Processing*, 1-53.

Chaves-González, J. M., Vega-Rodríguez, M. A., Gómez-Pulido, J. A. and Sánchez-Pérez, J. M. 2010. Detecting skin in face recognition systems: A colour spaces study. *Digital Signal Processing*, 20(3): 806-823.

Chebbout, S. and Merouani, H. F. 2012. Comparative study of clustering based colour image segmentation techniques. *Signal Image Technology and Internet Based Systems*, 839-844.

Chen, K., Zhou, Y., Zhang, Z., Dai, M., Chao, Y. and Shi, J. 2016. Multilevel image segmentation based on an improved firefly algorithm. *Mathematical Problems in Engineering*, 1-12.

- Chen, S. and Zhang, D. 2004. Robust image segmentation using FCM with spatial constraints based on new kernel-induced distance measure. *IEEE Transactions on Systems, Man, and Cybernetics, Part B: Cybernetics*, 34 (4): 1907-1916.
- Chen, S., Yao, L. and Chen, B. 2016. A parameterized logarithmic image processing method with Laplacian of Gaussian filtering for lung nodule enhancement in chest radiographs. *Medical & biological engineering & computing*: 1-14.
- Cheng, H. D. and Sun, Y. 2000. A hierarchical approach to color image segmentation using homogeneity. *IEEE Transactions on Image Processing*, 9(12): 2071-2082.
- Cheng, H. D., Jiang, X., Sun, Y. and Wang, J. 2001. Color image segmentation: advances and prospects. *Pattern recognition*, 34(12): 2259-2281.
- Cheng, M.M., Mitra, N.J., Huang, X., Torr, P.H. and Hu, S.M., 2015. Global contrast based salient object detection. *IEEE Transactions on Pattern Analysis and Machine Intelligence*, 37(3), 569-582.
- Chien, C. L. and Tseng, D. C. 2011. Color image enhancement with exact HSI color model. *International Journal of Innovative Computing, Information and Control*, 7(12): 6691-6710.
- Christ, M. J. and Parvathi, R. M. S., 2011. Segmentation of medical image using clustering and watershed algorithms. *American Journal of Applied Sciences*, 8(12): 1349-1352.
- Chuang, K. S., Tzeng, H. L., Chen, S., Wu, J. and Chen, T. J. 2006. Fuzzy c-means clustering with spatial information for image segmentation. *computerized medical imaging and graphics*, 30(1): 9-15.
- Cuevas, E., Sención, F., Zaldivar, D., Pérez-Cisneros, M. and Sossa, H. 2012. A multi-threshold segmentation approach based on artificial bee colony optimization. *Applied Intelligence*, 37 (3): 321-336.
- D’Orazio, T., Leo, M., Spagnolo, P., Nitti, M., Mosca, N. and Distanto, A., 2009. A visual system for real time detection of goal events during soccer matches. *Computer Vision and Image Understanding*, 113(5): 622-632.
- Dai, J., He, K. and Sun, J. 2015. Boxesup: Exploiting bounding boxes to supervise convolutional networks for semantic segmentation. *Computer Vision*. 1635-1643.

- Das, S., Abraham, A. and Konar, A. 2008. Automatic clustering using an improved differential evolution algorithm. *IEEE Transactions on Systems, Man and Cybernetics, Part A: Systems and Humans*, 38 (1): 218-237.
- de Amorim, R. C. 2012. An empirical evaluation of different initializations on the number of k-means iterations. *Artificial Intelligence*. 7629, 15-26.
- de Amorim, R. C. and Mirkin, B. 2012. Minkowski metric, feature weighting and anomalous cluster initializing in K-Means clustering. *Pattern recognition*, 45(3): 1061-1075.
- Deelers, S. and Auwatanamongkol, S. 2007. Enhancing K-means algorithm with initial cluster centers derived from data partitioning along the data axis with the highest variance. *International Journal of Computer Science*, 2(4): 247-252.
- Delon, J., Desolneux, A., Lisani, J. L. and Petro, A. B. 2007. A nonparametric approach for histogram segmentation. *IEEE Transactions on Image Processing*, 16(1): 253-261.
- Despotović, I., Goossens, B. and Philips, W. 2015. MRI segmentation of the human brain: challenges, methods, and applications. *Computational and Mathematical Methods in Medicine*, 1-23.
- Despotović, I., Goossens, B., Vansteenkiste, E. and Philips, W. 2010. An improved fuzzy clustering approach for image segmentation. *Image Processing*, 249-252.
- Dhanachandra, N., Manglem, K. and Chanu, Y. J. 2015. Image segmentation using K-means clustering algorithm and subtractive clustering algorithm. *Procedia Computer Science*, 54: 764-771.
- Dirami, A., Hammouche, K., Diaf, M. and Siarry, P. 2013. Fast multilevel thresholding for image segmentation through a multiphase level set method. *Signal Processing*, 93 (1): 139-153.
- Dong, L., Yu, G., Ogunbona, P. and Li, W. 2008. An efficient iterative algorithm for image thresholding. *Pattern Recognition Letters*, 29 (9): 1311-1316.
- Dong, X., Shen, J., Shao, L. and Van Gool, L., 2016. Sub-Markov random walk for image segmentation. *IEEE Transactions on Image Processing*, 25(2): 516-527.
- Dorigo, M. and Stützle, T. 2003. The ant colony optimization metaheuristic: Algorithms, applications, and advances. *Metaheuristics*, 57, 250-285.

- Dowlati, M., Mohtasebi, S. S., Omid, M., Razavi, S. H., Jamzad, M. and De La Guardia, M. 2013. Freshness assessment of gilthead sea bream (*Sparus aurata*) by machine vision based on gill and eye color changes. *Journal of Food Engineering*, 119(2): 277-287.
- Duan, L., Wu, C., Miao, J., Qing, L. and Fu, Y., 2011. Visual saliency detection by spatially weighted dissimilarity. *Computer Vision and Pattern Recognition*, 473-480.
- Dunn, J. C. 1973. A fuzzy relative of the ISODATA process and its use in detecting compact well-separated clusters, *Journal of Cybernetics*, 3(3): 32-57.
- Durgadevi, R., Hemalatha, B. and Kaliappan, K. V. K. 2014. Detection of mammograms using honey bees mating optimization algorithm. *Computing and Communication Technologies*, 50-53.
- Eberhart, R. C. and Kennedy, J. 1995. A new optimizer using particle swarm theory. *Micro Machine and Human Science*. 1, 39-43.
- El-Sayed, M. A. 2012. A new algorithm based entropic threshold for edge detection in images. *arXiv preprint arXiv:1211.2500*.
- Escalante, H.J., Hernández, C.A., Gonzalez, J.A., López-López, A., Montes, M., Morales, E.F., Sucar, L.E., Villaseñor, L. and Grubinger, M., 2010. The segmented and annotated IAPR TC-12 benchmark. *Computer Vision and Image Understanding*, 114(4): 419-428.
- Esme, E. and Karlik, B. 2016. Fuzzy c-means based support vector machines classifier for perfume recognition. *Applied Soft Computing*, 46, 452-458.
- Everingham, M., Eslami, S. A., Van Gool, L., Williams, C. K., Winn, J. and Zisserman, A. 2014. The Pascal visual object classes challenge: A retrospective. *International journal of computer vision*, 111(1): 98-136.
- Fahim, A., Salem, A., Torkey, F. and Ramadan, M. 2006. An efficient enhanced k-means clustering algorithm. *Journal of Zhejiang University SCIENCE A*, 7(10): 1626-1633.
- Fan, H., Xie, F., Li, Y., Jiang, Z. and Liu, J., 2017. Automatic segmentation of dermoscopy images using saliency combined with Otsu threshold. *Computers in Biology and Medicine*, 85, 75-85.

- Fan, J. L., Zhen, W. Z. and Xie, W. X. 2003. Suppressed fuzzy c-means clustering algorithm. *Pattern Recognition Letters*, 24(9): 1607-1612.
- Fan, Q. and Qi, C., 2016. Saliency detection based on global and local short-term sparse representation. *Neurocomputing*, 175, 81-89.
- Feng, D., Wenkang, S., Liangzhou, C., Yong, D. and Zhenfu, Z. 2005. Infrared image segmentation with 2-D maximum entropy method based on particle swarm optimization (PSO). *Pattern Recognition Letters*, 26(5): 597-603.
- Feng, J., Jiao, L., Zhang, X., Gong, M. and Sun, T. 2013. Robust non-local fuzzy c-means algorithm with edge preservation for SAR image segmentation. *Signal Processing*, 93(2): 487-499.
- Feng, Y., Shen, X., Chen, H. and Zhang, X. 2016. A weighted-ROC graph based metric for image segmentation evaluation. *Signal Processing*, 119, 43-55.
- Fernández-Vázquez, R., Stinco, C.M., Hernanz, D., Heredia, F.J. and Vicario, I.M., 2013. Colour training and colour differences thresholds in orange juice. *Food Quality and Preference*, 30(2): 320-327.
- Ferreira, M. R. and De Carvalho, F. D. A. 2014. Kernel fuzzy c-means with automatic variable weighting. *Fuzzy Sets and Systems*, 237, 1-46.
- Ferreira, M. R., de Carvalho, F. d. A. and Simões, E. C. 2016. Kernel-based hard clustering methods with kernelization of the metric and automatic weighting of the variables. *Pattern Recognition*, 51, 310-321.
- Fister, I., Yang, X. S. and Brest, J. 2013. A comprehensive review of firefly algorithms. *Swarm and Evolutionary Computation*, 13, 34-46.
- Flores, E. and Scharcanski, J. 2016. Segmentation of melanocytic skin lesions using feature learning and dictionaries. *Expert Systems with Applications*, 56, 300-309.
- Forgy, E. W., 1965. Cluster analysis of multivariate data: efficiency vs interpretability of classifications, *Biometrics*, 21, 768-769.

- Fränti, P. and Kivijärvi, J. 2000. Randomised local search algorithm for the clustering problem. *Pattern Analysis & Applications*, 3 (4): 358-369.
- Fränti, P., Kivijärvi, J. and Nevalainen, O. 1998. Tabu search algorithm for codebook generation in vector quantization. *Pattern recognition*, 31(8): 1139-1148.
- Gao, H., Xu, W., Sun, J. and Tang, Y. 2010. Multilevel thresholding for image segmentation through an improved quantum-behaved particle swarm algorithm. *IEEE Transactions on Instrumentation and Measurement*, 59(4): 934-946.
- García-Mateos, G., Hernández-Hernández, J., Escarabajal-Henarejos, D., Jaén-Terrones, S. and Molina-Martínez, J. 2015. Study and comparison of color models for automatic image analysis in irrigation management applications. *Agricultural Water Management*, 151, 158-166.
- Géraud, T., Strub, P. Y. and Darbon, J., 2001. Color image segmentation based on automatic morphological clustering, *Image Processing*, 3, 70-73.
- Ghinea, R., Pérez, M.M., Herrera, L.J., Rivas, M.J., Yebra, A. and Paravina, R.D., 2010. Color difference thresholds in dental ceramics. *Journal of Dentistry*, 38, e57-e64.
- Ghosh, S. and Dubey, S. K. 2013. Comparative analysis of k-means and fuzzy c-means algorithms. *International Journal of Advanced Computer Science and Applications*, 4(4): 34-39.
- Glasbey, C. A. 1993. An analysis of histogram-based thresholding algorithms. *CVGIP: Graphical models and image processing*, 55(6): 532-537.
- Goldberg, D. E. 1989. Genetic algorithms in search and machine learning. *Reading, Addison Wesley*, 102.
- Gonzales-Barron, U. and Butler, F. 2006. A comparison of seven thresholding techniques with the k-means clustering algorithm for measurement of bread-crumbs features by digital image analysis. *Journal of Food Engineering*, 74(2): 268-278.
- Gonzalez, C. I., Melin, P., Castro, J. R., Mendoza, O. and Castillo, O. 2016. An improved sobel edge detection method based on generalized type-2 fuzzy logic. *Soft Computing*, 20(2): 773-784.

Gudipalli, A. and Tirumala, R. 2012. Comprehensive infrared image edge detection algorithm. *International Journal of Image Processing*, 6(5): 297.

Güngör, Z. and Ünler, A. 2007. K-harmonic means data clustering with simulated annealing heuristic. *Applied Mathematics and Computation*, 184(2): 199-209.

Gutman, D., Codella, N. C., Celebi, E., Helba, B., Marchetti, M., Mishra, N. and Halpern, A. 2016. Skin lesion analysis toward melanoma detection: a challenge at the International Symposium on Biomedical Imaging (ISBI) 2016, hosted by the International Skin Imaging Collaboration (ISIC). *arXiv preprint arXiv:1605.01397*.

Hachouf, F. and Mezhoud, N. 2005. A clustering approach for color image segmentation. *Advanced Concepts for Intelligent Vision Systems*. 3708, 515-522.

Haifeng, S. and Lanlan, L. 2012. Clustering color image segmentation based on maximum entropy. *Computer Application and System Modeling*. 1466-1468.

Hammouche, K., Diaf, M. and Siarry, P. 2008. A multilevel automatic thresholding method based on a genetic algorithm for a fast image segmentation. *Computer Vision and Image Understanding*, 109(2): 163-175.

Hammouche, K., Diaf, M. and Siarry, P. 2010. A comparative study of various meta-heuristic techniques applied to the multilevel thresholding problem. *Engineering Applications of Artificial Intelligence*, 23(5): 676-688.

Hansen, P. and Mladenović, N. 2001. J-means: a new local search heuristic for minimum sum of squares clustering. *Pattern recognition*, 34(2): 405-413.

Haralick, R. M. and Shapiro, L. G. 1985. Image segmentation techniques. *Computer Vision, Graphics and Image Processing*, 29(1): 100-132.

Harrabi, R. and Ben Braiek, E. 2014. Color image segmentation using a modified Fuzzy C-Means technique and different color spaces: Application in the breast cancer cells images. *Advanced Technologies for Signal and Image Processing*, 231-236.

- Harrabi, R. and Braiek, E. B. 2012. Color image segmentation based on a modified fuzzy c-means technique and statistical features. *International Journal of Computational Engineering Research*, 2(1): 120-135.
- He, C., Xiong, R. and Dai, L. K. 2002. Fast segmentation and identification in vision system for soccer robots. *Intelligent Control and Automation*, 532-536.
- Hettiarachchi, R. and Peters, J. F. 2016. Voronoi Region-Based Adaptive Unsupervised Color Image Segmentation. *Pattern recognition*, 65, 119-135.
- Hornig, M. H. 2010. Multilevel minimum cross entropy threshold selection based on the honey bee mating optimization. *Expert Systems with Applications*, 37(6): 4580-4592.
- Hornig, M. H. 2011. Multilevel thresholding selection based on the artificial bee colony algorithm for image segmentation. *Expert Systems with Applications*, 38(11): 13785-13791.
- Hornig, M. H. and Liou, R. J. 2011. Multilevel minimum cross entropy threshold selection based on the firefly algorithm. *Expert Systems with Applications*, 38(12): 14805-14811.
- Hosseinpour, S., Rafiee, S., Mohtasebi, S.S. and Aghbashlo, M., 2013. Application of computer vision technique for on-line monitoring of shrimp color changes during drying. *Journal of Food Engineering*, 115(1): 99-114.
- Hoy, D. E. 1997. On the use of color imaging in experimental applications. *Experimental Techniques*, 21(4): 17-19.
- Huang, D. Y. and Wang, C. H. 2009. Optimal multi-level thresholding using a two-stage Otsu optimization approach. *Pattern Recognition Letters*, 30(3): 275-284.
- Huang, D. Y., Lin, T. W. and Hu, W. C. 2011. Automatic multilevel thresholding based on two-stage Otsu's method with cluster determination by valley estimation. *International Journal of Innovative Computing, Information and Control*, 7(10): 5631-5644.
- Huang, X. Q., Shi, J. S., Yang, J. and Yao, J. C. 2007. Study on color image quality evaluation by mse and psnr based on color difference. *Acta Photonica Sinica*, 36(S1): 295-298.

- Hung, M. H., Hsieh, C. H., Kuo, C. M. and Pan, J. S. 2011. Generalized playfield segmentation of sport videos using color features. *Pattern Recognition Letters*, 32(7): 987-1000.
- Hussein, W. A., Sahran, S. and Abdullah, S. N. H. S. 2016. A fast scheme for multilevel thresholding based on a modified bees algorithm. *Knowledge-Based Systems*, 101, 114-134.
- Ikonomakis, N., Plataniotis, K. N. and Venetsanopoulos, A. N. 2000. Color image segmentation for multimedia applications. *Journal of Intelligent and Robotic Systems*, 28(1-2): 5-20.
- Ingle, M. A. and Talmale, G. R. 2016. Respiratory mask selection and leakage detection system based on Canny edge detection operator. *Procedia Computer Science*, 78, 323-329.
- Ionita, M. C., Corcoran, P. and Buzuloiu, V. 2009. On color texture normalization for active appearance models. *IEEE Transactions on Image Processing*, 18(6): 1372-1378.
- Isa, N. A. M., Salamah, S. and Ngah, U. K. 2009. Adaptive fuzzy moving K-means clustering algorithm for image segmentation. *IEEE Transactions on Consumer Electronics*, 55(4): 2145-2153.
- ISIC Archive: The International Skin Imaging Collaboration: Melanoma Project. Available: <https://isic-archive.com/-90>.
- Jain, A. K. 2010. Data clustering: 50 years beyond K-means. *Pattern Recognition Letters*, 31(8): 651-666.
- Jain, A. K., Duin, R. P. and Mao, J. 2000. Statistical pattern recognition: A review. *IEEE Transactions on Pattern Analysis and Machine Intelligence*, 22(1): 4-37.
- James, C. B. 1981. *Pattern recognition with fuzzy objective function algorithms*: Kluwer Academic Publishers.
- Jancey, R.C., 1966. Multidimensional group analysis. *Australian Journal of Botany*, 14(1): 127-130.
- Jassim, F. A. and Altaani, F. H. 2013. Hybridization of Otsu method and median filter for color image segmentation. *arXiv preprint arXiv:1305.1052*.
- Ji, Z., Xia, Y., Chen, Q., Sun, Q., Xia, D. and Feng, D. D. 2012. Fuzzy c-means clustering with weighted image patch for image segmentation. *Applied Soft Computing*, 12(6): 1659-1667.

- Ji, Z.X., Sun, Q.S. and Xia, D.S., 2011. A modified possibilistic fuzzy c-means clustering algorithm for bias field estimation and segmentation of brain MR image. *Computerized Medical Imaging and Graphics*, 35(5): 383-397.
- Jiang, B., Zhang, L., Lu, H., Yang, C. and Yang, M.H., 2013. Saliency detection via absorbing Markov chain. *Computer Vision Foundation*, 1665-1672.
- Jiang, X. L., Wang, Q., He, B., Chen, S. J. and Li, B. L. 2016. Robust level set image segmentation algorithm using local correntropy-based fuzzy c-means clustering with spatial constraints. *Neurocomputing*, 207, 22-35.
- Jiang, Y., Hao, Z., Yang, Z., Wang, Y. and He, H. 2014. A cooperative honey bee mating algorithm and its application in multi-threshold image segmentation. *Evolutionary Computation*, 1579-1585.
- Jiang, Y., Tsai, P., Hao, Z. and Cao, L. 2015. Automatic multilevel thresholding for image segmentation using stratified sampling and Tabu Search. *Soft Computing*, 19(9): 2605-2617.
- John, N., Viswanath, A., Sowmya, V. and Soman, K. 2016. Analysis of various color space models on effective single image super resolution. *Intelligent Systems Technologies and Applications*. 384, 529-540.
- Johnson, B. and Xie, Z. 2011. Unsupervised image segmentation evaluation and refinement using a multi-scale approach. *ISPRS Journal of Photogrammetry and Remote Sensing*, 66(4): 473-483.
- Jumb, V., Sohani, M. and Shrivastava, A. 2014. Color image segmentation using K-means clustering and Otsu's adaptive thresholding. *International Journal Innovation Technology and Exploring Engineering*, 3(9): 72-76.
- Jurio, A., Pagola, M., Galar, M., Lopez-Molina, C. and Paternain, D. 2010. A comparison study of different color spaces in clustering based image segmentation. *Information Processing and Management of Uncertainty in Knowledge-Based Systems. Applications*, 81, 532-541.
- Kakumanu, P., Makrogiannis, S. and Bourbakis, N. 2007. A survey of skin-color modeling and detection methods. *Pattern Recognition*, 40(3): 1106-1122.
- Kang, B. Y., Kim, D. W. and Li, Q. 2005. Spatial homogeneity-based fuzzy c-means algorithm for image segmentation. *Fuzzy Systems and Knowledge Discovery*, 3613, 462-469.

- Kannan, S., Devi, R., Ramathilagam, S. and Takezawa, K. 2013. Effective FCM noise clustering algorithms in medical images. *Computers in Biology and Medicine*, 43(2): 73-83.
- Kapur, J. N., Sahoo, P. K. and Wong, A. K. 1985. A new method for gray-level picture thresholding using the entropy of the histogram. *Computer Vision, Graphics, and Image Processing*, 29(3): 273-285.
- Kasmi, R. and Mokrani, K., 2016. Classification of malignant melanoma and benign skin lesions: implementation of automatic ABCD rule. *IET Image Processing*, 10(6): 448-455.
- Khan, J., Malik, A. S., Kamel, N., Dass, S. C. and Affandi, A. M. 2015. Segmentation of acne lesion using fuzzy C-means technique with intelligent selection of the desired cluster. *Engineering in Medicine and Biology Society*, 3077-3080.
- Khan, S. S. and Ahmad, A. 2013. Cluster center initialization algorithm for K-modes clustering. *Expert Systems with Applications*, 40(18): 7444-7456.
- Khan, Z.F., Al Sayyari, A.S. and Quadri, S.U., 2017. Automated segmentation of lung images using textural echo state neural networks. *Informatics, Health & Technology*, 1-5.
- Khashayar, G., Bain, P.A., Salari, S., Dozic, A., Kleverlaan, C.J. and Feilzer, A.J., 2014. Perceptibility and acceptability thresholds for colour differences in dentistry. *Journal of Dentistry*, 42(6), 637-644.
- Khattab, D., Ebied, H. M., Hussein, A. S. and Tolba, M. F. 2014. Color image segmentation based on different color space models using automatic GrabCut. *The Scientific World Journal*, 1-10.
- Khattab, D., Ebied, H. M., Hussein, A. S. and Tolba, M. F. 2015. A comparative study of different color space models using FCM-Based automatic GrabCut for image segmentation. *Computational Science and Its Applications*, 9155, 489-501.
- Khelifi, L. and Mignotte, M., 2017. EFA-BMFM: A multi-criteria framework for the fusion of colour image segmentation. *Information Fusion*, 38, 104-121.
- Kim, D. W., Lee, K. H. and Lee, D. 2004. A novel initialization scheme for the fuzzy c-means algorithm for color clustering. *Pattern Recognition Letters*, 25(2): 227-237.

Kim, J., Han, D., Tai, Y.W. and Kim, J., 2014. Salient object detection via high-dimensional color transform. *Computer Vision and Pattern Recognition* , 883-890.

Kim, J., Han, D., Tai, Y.W. and Kim, J., 2016. Salient object detection via high-dimensional color transform and local spatial support. *IEEE Transactions on Image Processing*, 25(1), 9-23.

Kirkpatrick, S. and Vecchi, M. P. 1983. Optimization by simulated annealing. *Science*, 220(4598): 671-680.

Kittler, J. and Illingworth, J. 1986. Minimum error thresholding. *Pattern Recognition*, 19(1): 41-47.

Koch, C. and Ullman, S., 1987. Shifts in selective visual attention: towards the underlying neural circuitry. *Matters of Intelligence*, 115-141.

Kodagali, J. A. and Balaji, S. 2012. Computer vision and image analysis based techniques for automatic characterization of fruits—a review. *International Journal of Computer Applications*, 50(6).

Kolaman, A. and Yadid-Pecht, O. 2012. Quaternion structural similarity: a new quality index for color images. *IEEE Transactions on Image Processing*, 21(4): 1526-1536.

Krishnapuram, R. and Keller, J. M. 1993. A possibilistic approach to clustering. *IEEE Transactions on Fuzzy Systems*, 1(2): 98-110.

Kumar, S., Kumar, P., Sharma, T. K. and Pant, M. 2013. Bi-level thresholding using PSO, artificial bee colony and MRLDE embedded with Otsu method. *Memetic Computing*, 5(4): 323-334.

Kumar, V. and Wu, X. 2009. *The top ten algorithms in data mining*. CRC Press.

Kurban, T., Civicioglu, P., Kurban, R. and Besdok, E. 2014. Comparison of evolutionary and swarm based computational techniques for multilevel color image thresholding. *Applied Soft Computing*, 23, 128-143.

Kwok, N., Ha, Q. and Fang, G. 2009. Effect of color space on color image segmentation. *Image and Signal Processing*, 1-5.

- Le, H. M., Thi, B. T. N., Ta, M. T. and Le Thi, H. A. 2013. Image segmentation via feature weighted fuzzy clustering by a DCA based algorithm. *Advanced Computational Methods for Knowledge Engineering*, 479, 53-63.
- Lee, C. Y., Leou, J. J. and Hsiao, H. H. 2012. Saliency-directed color image segmentation using modified particle swarm optimization. *Signal Processing*, 92(1): 1-18.
- Lee, J., Coomes, D., Schonlieb, C.B., Cai, X., Lellmann, J., Dalponte, M., Malhi, Y., Butt, N. and Morecroft, M., 2017. A graph cut approach to 3D tree delineation, using integrated airborne LiDAR and hyperspectral imagery. *arXiv preprint arXiv:1701.06715*.
- Lei, J., Jiang, T., Wu, K., Du, H., Zhu, G. and Wang, Z. 2016. Robust K-means algorithm with automatically splitting and merging clusters and its applications for surveillance data. *Multimedia Tools and Applications*: 1-17.
- Leung, Y., Zhang, J.-S. and Xu, Z.-B. 2000. Clustering by scale-space filtering. *IEEE Transactions on Pattern Analysis and Machine Intelligence*, 22 (12): 1396-1410.
- Lezoray, O. and Charrier, C., 2009. Color image segmentation using morphological clustering and fusion with automatic scale selection. *Pattern Recognition Letters*, 30(4): 397-406.
- Li, C. H. and Lee, C. 1993. Minimum cross entropy thresholding. *Pattern recognition*, 26(4): 617-625.
- Li, J. Y., Zhao, Y. D., Li, J. H. and Liu, X. J. 2015. Artificial bee colony optimizer with bee-to-bee communication and multipopulation coevolution for multilevel threshold image segmentation. *Mathematical Problems in Engineering*, 1-23.
- Li, L., Xia, W., Fang, Y., Gu, K., Wu, J., Lin, W. and Qian, J. 2016a. Color image quality assessment based on sparse representation and reconstruction residual. *Journal of Visual Communication and Image Representation*, 38, 550-560.
- Li, L., Xia, W., Fang, Y., Gu, K., Wu, J., Lin, W. and Qian, J. 2016. Color image quality assessment based on sparse representation and reconstruction residual. *Journal of Visual Communication and Image Representation*, 38, 550-560.

- Li, M., Stein, A., Bijker, W. and Zhan, Q. 2016b. Region-based urban road extraction from VHR satellite images using binary partition tree. *International Journal of Applied Earth Observation and Geoinformation*, 44, 217-225.
- Li, Z., Liu, G., Zhang, D. and Xu, Y. 2016c. Robust single-object image segmentation based on salient transition region. *Pattern Recognition*, 52, 317-331.
- Liao, L., Lin, T. and Li, B. 2008. MRI brain image segmentation and bias field correction based on fast spatially constrained kernel clustering approach. *Pattern Recognition Letters*, 29(10): 1580-1588.
- Liao, P. S., Chen, T. S. and Chung, P. C. 2001. A fast algorithm for multilevel thresholding. *Journal of Information Science and Engineering*, 17 (5): 713-727.
- Lievers, W. and Pilkey, A. 2004. An evaluation of global thresholding techniques for the automatic image segmentation of automotive aluminum sheet alloys. *Materials Science and Engineering: A*, 381(1): 134-142.
- Liew, A. W.-C. and Yan, H. 2003. An adaptive spatial fuzzy clustering algorithm for 3-D MR image segmentation. *IEEE Transactions on Medical Imaging*, 22(9): 1063-1075.
- Lin, J. Y., Wu, C.-H., Katsavounidis, I., Li, Z., Aaron, A. and Kuo, C. C. J. 2015. EVQA: an ensemble-learning-based video quality assessment index. *Multimedia & Expo Workshops*, 1-6.
- Lin, W. and Kuo, C.-C. J. 2011. Perceptual visual quality metrics: A survey. *Journal of Visual Communication and Image Representation*, 22(4): 297-312.
- Litjens, G., Toth, R., van de Ven, W., Hoeks, C., Kerkstra, S., van Ginneken, B., Vincent, G., Guillard, G., Birbeck, N., Zhang, J. and Strand, R., 2014. Evaluation of prostate segmentation algorithms for MRI: the PROMISE12 challenge. *Medical image analysis*, 18(2): 359-373.
- Liu, L., Hua, Y., Zhao, Q., Huang, H. and Bovik, A. C. 2016a. Blind image quality assessment by relative gradient statistics and adaboosting neural network. *Signal Processing: Image Communication*, 40, 1-15.
- Liu, L., Sun, S. Z., Yu, H., Yue, X. and Zhang, D. 2016b. A modified fuzzy C-means (FCM) clustering algorithm and its application on carbonate fluid identification. *Journal of Applied Geophysics*, 129, 28-35.

- Liu, Y., Mu, C., Kou, W. and Liu, J. 2015. Modified particle swarm optimization-based multilevel thresholding for image segmentation. *Soft Computing*, 19(5): 1311-1327.
- Lloyd, S. P. 1982. Least squares quantization in PCM., *IEEE Transactions on Information Theory*, 28(2): 129-137.
- Lughofer, E. and Sayed-Mouchaweh, M. 2015. Autonomous data stream clustering implementing split-and-merge concepts—towards a plug-and-play approach. *Information Sciences*, 304, 54-79.
- Luszczkiewicz-Piatek, M. 2014. Which color space should be chosen for robust color image retrieval based on mixture modeling. *Image Processing and Communication Challenges*, 233, 55-64.
- MacQueen, J. 1967. Some methods for classification and analysis of multivariate observations. *Berkeley Symposium on Mathematical Statistics and Probability*, 281-297.
- Madooei, A. and Drew, M.S., 2016. Incorporating color information for computer-aided diagnosis of melanoma from dermoscopy images: A retrospective survey and critical analysis. *International Journal of Biomedical Imaging*, 1-18.
- Mahmood, M.H., Díez, Y., Salvi, J. and Lladó, X., 2017. A collection of challenging motion segmentation benchmark datasets. *Pattern Recognition*, 61, 1-14.
- Mahmud, M. S., Rahman, M. M. and Akhtar, M. N. 2012. Improvement of K-means clustering algorithm with better initial centroids based on weighted average. *Electrical & Computer Engineering*, 647-650.
- Maier, O., Menze, B.H., von der Gablentz, J., Häni, L., Heinrich, M.P., Liebrand, M., Winzeck, S., Basit, A., Bentley, P., Chen, L. and Christiaens, D., 2017. ISLES 2015-A public evaluation benchmark for ischemic stroke lesion segmentation from multispectral MRI. *Medical Image Analysis*, 35, 250-269.
- Maitra, M. and Chatterjee, A. 2008. A novel technique for multilevel optimal magnetic resonance brain image thresholding using bacterial foraging. *Measurement*, 41(10): 1124-1134.
- Makrogiannis, S., Economou, G. and Fotopoulos, S., 2005. A region dissimilarity relation that combines feature-space and spatial information for color image segmentation. *IEEE Transactions on Systems, Man and Cybernetics, Part B: Cybernetics*, 35(1): 44-53.

- Mala, C. and Sridevi, M. 2015. Multilevel threshold selection for image segmentation using soft computing techniques. *Soft Computing*: 1-18.
- Margolin, R., Tal, A. and Zelnik-Manor, L., 2013. What makes a patch distinct? *Computer Vision and Pattern Recognition*, 1139-1146.
- Martí, R., Glover, F. and Kochenberger, G. 2003. Handbook of metaheuristics. *Multi-Start Methods*. Kluwer Academic Publishers.
- Martin, D., Fowlkes, C., Tal, D. and Malik, J. 2001. A database of human segmented natural images and its application to evaluating segmentation algorithms and measuring ecological statistics. *Computer Vision*, 416-423.
- Martínez, G. E., Melin, P., Mendoza, O. D. and Castillo, O. 2015. Face Recognition with a Sobel Edge Detector and the Choquet Integral as Integration Method in a Modular Neural Networks. *Design of Intelligent Systems Based on Fuzzy Logic, Neural Networks and Nature-Inspired Optimization*. 59-70.
- Mashor, M. Y. 2000. Hybrid training algorithm for RBF network. *International Journal of the Computer, the Internet and Management*, 8(2): 50-65.
- McCann, M. T., Mixon, D. G., Fickus, M. C., Castro, C. A., Ozolek, J. A. and Kovacevic, J. 2014. Images as occlusions of textures: a framework for segmentation. *IEEE Transactions on Image Processing*, 23(5): 2033-2046.
- Menze, B.H., Jakab, A., Bauer, S., Kalpathy-Cramer, J., Farahani, K., Kirby, J., Burren, Y., Porz, N., Slotboom, J., Wiest, R. and Lanczi, L., 2015. The multimodal brain tumor image segmentation benchmark (BRATS). *IEEE Transactions on Medical Imaging*, 34(10): 1993-2024.
- Mesejo, P., Ibáñez, O., Cerdón, O. and Cagnoni, S. 2016. A survey on image segmentation using metaheuristic-based deformable models: state of the art and critical analysis. *Applied Soft Computing*, 44, 1-29.
- Miao, R. H., Tang, J.-L. and Chen, X.-Q. 2015. Classification of farmland images based on color features. *Journal of Visual Communication and Image Representation*, 29, 138-146.

- Mikut, R. and Reischl, M., 2015. A Benchmark Data Set to Evaluate the Illumination Robustness of Image Processing Algorithms for Object Segmentation and Classification. *PloS one*, 10(7), p.e0131098.
- Mizushima, A. and Lu, R. 2013. An image segmentation method for apple sorting and grading using support vector machine and Otsu's method. *Computers and Electronics in Agriculture*, 94, 29-37.
- Moghaddam, R. F. and Cheriet, M. 2012. AdOtsu: An adaptive and parameterless generalization of Otsu's method for document image binarization. *Pattern Recognition*, 45(6): 2419-2431.
- Mohan, B. C. and Baskaran, R. 2012. A survey: Ant colony optimization based recent research and implementation on several engineering domain. *Expert Systems with Applications*, 39(4): 4618-4627.
- Mohanty, A., Mir, Z. M., Rajkumar, S. and Bardhan, P. 2013. Analysis of color images using cluster based segmentation techniques. *Analysis*, 79(2), 42-47.
- Muthukannan, K. and Merlin Moses, M. 2010. Color image segmentation using k-means clustering and optimal fuzzy C-means clustering. *Communication and Computational Intelligence*, 229-234.
- Nakib, A., Oulhadj, H. and Siarry, P. 2007. Image histogram thresholding based on multiobjective optimization. *Signal Processing*, 87(11): 2516-2534.
- Naldi, M. C. and Campello, R. J. 2015. Comparison of distributed evolutionary k-means clustering algorithms. *Neurocomputing*, 163,78-93.
- Nazeer, K. A. and Sebastian, M. 2009. Improving the accuracy and efficiency of the k-means clustering algorithm. *World Congress on Engineering*. 1-3.
- Nilima, S., Dhanesh, P. and Anjali, J. 2013. Review on image segmentation, clustering and boundary encoding. *International Journal of Innovative Research in Science, Engineering and Technology*, 2(11): 6309-6314.
- Ninos, K., Kostopoulos, S., Kalatzis, I., Sidiropoulos, K., Ravazoula, P., Sakellaropoulos, G., Panayiotakis, G., Economou, G. and Cavouras, D., 2016. Microscopy image analysis of p63 immunohistochemically stained laryngeal cancer lesions for predicting patient 5-year survival. *European Archives of Oto-Rhino-Laryngology*, 273(1): 159-168.

- Noda, I., Suzuki, S. j., Matsubara, H., Asada, M. and Kitano, H. 1998. RoboCup-97: The first robot world cup soccer games and conferences. *AI magazine*, 19(3): 49.
- Norton, K. A., Iyatomi, H., Celebi, M. E., Ishizaki, S., Sawada, M., Suzaki, R., Kobayashi, K., Tanaka, M. and Ogawa, K., 2012. Three-phase general border detection method for dermoscopy images using non-uniform illumination correction. *Skin Research and Technology*, 18(3): 290-300.
- Oghaz, M. M., Maarof, M. A., Zainal, A., Rohani, M. F. and Yaghoubyan, S. H. 2015. A hybrid color space for skin detection using genetic algorithm heuristic search and principal component analysis technique. *PloS one*, 10(8): e0134828.
- Oh, K., Lee, M., Lee, Y. and Kim, S., 2017. Salient Object Detection using Recursive Regional Feature Clustering. *Information Sciences*, 387, 1-18.
- Oh, S., Hoogs, A., Perera, A., Cuntoor, N., Chen, C. C., Lee, J. T., Mukherjee, S., Aggarwal, J.K., Lee, H., Davis, L. and Swears, E., 2011. A large-scale benchmark dataset for event recognition in surveillance video. *Computer Vision and Pattern Recognition*, 3153-3160.
- Ohno, K., Tsubouchi, T., Maeyama, S. and Yuta, S. I. 2001. A mobile robot campus walkway following with daylight-change-proof walkway color image segmentation. *Intelligent Robots and Systems*, 77-83.
- Ohta, Y. I., Kanade, T. and Sakai, T. 1980. Color information for region segmentation. *Computer Graphics and Image Processing*, 13(3): 222-241.
- Ohyama, N., Suzuki, K., Honda, T., Tsujiuchi, J., Ono, R. and Ikeda, S. 1985. Digital processing of endoscopic color images. *Optics Communications*, 55(4): 242-247.
- Okuboyejo, D. A., Olugbara, O. O. and Odunaike, S. A. 2014. CLAHE inspired segmentation of dermoscopic images using mixture of methods. *Transactions on Engineering Technologies*, 355-365.
- Okuboyejo, D., Olugbara, O. O and Odunaike, S., 2013. Automating skin disease diagnosis using image classification. *Engineering and Computer Science*, 2, 850-854.
- Oliva, D., Cuevas, E., Pajares, G., Zaldivar, D. and Osuna, V. 2014. A multilevel thresholding algorithm using electromagnetism optimization. *Neurocomputing*, 139, 357-381.

- Olugbara, O. O. and Ndhlovu, B. N., 2014. Constructing frugal sales system for small enterprises. *The African Journal of Information Systems*, 6(4): 120-139.
- Olugbara, O. O., Ojo, S. O. and Mphahlele, M. I., 2010. Exploiting image content in location-based shopping recommender systems for mobile users. *International Journal of Information Technology & Decision Making*, 9(5): 759-778.
- Olugbara, O. O., Adetiba, E. and Oyewole, S. A. 2015. Pixel intensity clustering algorithm for multilevel image segmentation. *Mathematical Problems in Engineering*, 1-19.
- Olugbara, O. O., Joshi, M., Modiba, M. M. and Bhavsar, V. C. 2015. Automated Matchmaking to Improve Accuracy of Applicant Selection for University Education System. *arXiv preprint arXiv:1507.02439*,
- Olugbara, O. O., Ojo, S. O. and Mphahlele, M. 2010. Exploiting image content in location-based shopping recommender systems for mobile users. *International Journal of Information Technology & Decision Making*, 9(5): 759-778.
- Omran, M. G. 2004. Particle swarm optimization methods for pattern recognition and image processing. <http://hdl.handle.net/2263/29826>.
- Orchard, M. T. and Bouman, C. 1991. Color quantization of images. *IEEE Transactions on Signal Processing* , 39(12): 2677-2690.
- Osamor, V. C., Adebisi, E. F., Oyelade, J. O. and Doumbia, S. 2012. Reducing the Time Requirement of k-means Algorithm. *PloS one*, 7(12): e49946.
- Otsu, N. 1979. Thresholds selection method form grey-level histograms. *IEEE Transactions on Systems, Man and Cybernetics*, 9 (1): 1979.
- Oyewole, S., Olugbara, O., Adetiba, E. and Nepal, T. Classification of product images in different color models with customized kernel for support vector machine, 10.1109/AIMS.2015.33.
- Ozturk, C., Hancer, E. and Karaboga, D. 2015. Improved clustering criterion for image clustering with artificial bee colony algorithm. *Pattern Analysis and Applications*, 18(3): 587-599.

- Pal, N. R. and Pal, S. K. 1993. A review on image segmentation techniques. *Pattern Recognition*, 26 (9): 1277-1294.
- Pant, D.R. and Farup, I., 2010. Riemannian formulation of the CIEDE2000 color difference formula. *Society for Imaging Science and Technology*, 103-108.
- Pare, S., Kumar, A., Bajaj, V. and Singh, G. 2016. A multilevel color image segmentation technique based on cuckoo search algorithm and energy curve. *Applied Soft Computing*, 47, 76-102
- Patel, A., van Ginneken, B., Meijer, F.J., van Dijk, E.J., Prokop, M. and Manniesing, R., 2017. Robust cranial cavity segmentation in CT and CT perfusion images of trauma and suspected stroke patients. *Medical Image Analysis*, 36, 216-228.
- Pathak, D., Krahenbuhl, P., Donahue, J., Darrell, T. and Efros, A. A. 2016. Context Encoders: Feature Learning by Inpainting. *arXiv preprint arXiv:1604.07379*,
- Peng, B. and Li, T. 2013. A probabilistic measure for quantitative evaluation of image segmentation. *Signal Processing Letters*, 20(7): 689-692.
- Peng, B., Zhang, L. and Zhang, D. 2011. Automatic image segmentation by dynamic region merging. *IEEE Transactions on Image Processing*, 20(12): 3592-3605.
- Peng, H., Li, B., Ji, R., Hu, W., Xiong, W. and Lang, C., 2013. Salient Object Detection via Low-Rank and Structured Sparse Matrix Decomposition. *AAAI*, 796-802.
- Peng, Y., Zheng, W.L. and Lu, B.L., 2016. An unsupervised discriminative extreme learning machine and its applications to data clustering. *Neurocomputing*, 174, 250-264.
- Pennisi, A., Bloisi, D. D., Nardi, D., Giampetruzzi, A. R., Mondino, C. and Facchiano, A. 2016. Skin lesion image segmentation using delaunay triangulation for melanoma detection. *Computerized Medical Imaging and Graphics*, 52, 89-103.
- Pham, D. L. 2001. Spatial models for fuzzy clustering. *Computer Vision and Image Understanding*, 84 (2): 285-297.
- Pirnog, I., Oprea, C. and Paleologu, C. 2009. Image content extraction using a bottom-up visual attention model. *Digital Society*, 300-303.

Pont-Tuset, J., Arbelaez, P., Barron, J. T., Marques, F. and Malik, J., 2017. Multiscale combinatorial grouping for image segmentation and object proposal generation. *IEEE Transactions on Pattern Analysis and Machine Intelligence*, 39(1): 128-140.

Premaladha, J. and Ravichandran, K.S., 2016. Novel approaches for diagnosing melanoma skin lesions through supervised and deep learning algorithms. *Journal of Medical Systems*, 40(4): 1-12.

Purohit, P. and Joshi, R. 2013. A new Efficient Approach towards k-means Clustering Algorithm. *International Journal of Computer Applications*, 65 (11).

Qi, J., Dong, S., Huang, F. and Lu, H., 2017. Saliency detection via joint modeling global shape and local consistency. *Neurocomputing*, 222, 81-90.

Rahman, M. H. and Afrin, J. 2013. Human face detection in color images with complex background using triangular approach. *Global Journal of Computer Science and Technology*, 13(4),

Rahman, S., Rahman, M. M., Abdullah-Al-Wadud, M., Al-Quaderi, G. D. and Shoyaib, M., 2016. An adaptive gamma correction for image enhancement. *EURASIP Journal on Image and Video Processing*, 2016(1): 1-15.

Rajaby, E., Ahadi, S. and Aghaeinia, H. 2016. Robust color image segmentation using fuzzy c-means with weighted hue and intensity. *Digital Signal Processing*, 51, 170-183.

Rajinikanth, V. and Couceiro, M. 2015. RGB histogram based color image segmentation using firefly algorithm. *Procedia Computer Science*, 46, 1449-1457.

Randhawa, A. K. and Mahajan, R., 2014. An improved approach towards image segmentation using mean shift and FELICM. *International Journal of Advanced Research in Computer Science and Software Engineering*, 4(7): 197-202.

Reddy, E. V. and Reddy, E. 2014. Image segmentation for different color spaces using dynamic histogram based rough-fuzzy clustering algorithm. *International Journal of Computer Applications*, 85(14).

Riche, N., Mancas, M., Duvinage, M., Mibulumukini, M., Gosselin, B. and Dutoit, T., 2013. Rare2012: A multi-scale rarity-based saliency detection with its comparative statistical analysis. *Signal Processing: Image Communication*, 28(6): 642-658.

Rossel, R. V., Minasny, B., Roudier, P. and McBratney, A. 2006. Color space models for soil science. *Geoderma*, 133(3): 320-337.

Rouhi, R., Jafari, M., Kasaei, S. and Keshavarzian, P. 2015. Benign and malignant breast tumors classification based on region growing and CNN segmentation. *Expert Systems with Applications*, 42(3): 990-1002.

Rudyanto, R.D., Kerkstra, S., Van Rikxoort, E.M., Fetita, C., Brillet, P.Y., Lefevre, C., Xue, W., Zhu, X., Liang, J., Öksüz, I. and Ünay, D., 2014. Comparing algorithms for automated vessel segmentation in computed tomography scans of the lung: the VESSEL12 study. *Medical Image Analysis*, 18(7): 1217-1232.

Ruiz-Ruiz, G., Gómez-Gil, J. and Navas-Gracia, L. 2009. Testing different color spaces based on hue for the environmentally adaptive segmentation algorithm (EASA). *Computers and Electronics in Agriculture*, 68(1): 88-96.

Rujirapipat, S., McGarry, K. and Nelson, D., 2017. Bioinformatic Analysis Using Complex Networks and Clustering Proteins Linked with Alzheimer's Disease. *Advances in Computational Intelligence Systems*, 219-230.

Rungruangbaiyok, S., Duangsoithong, R. and Chetpattananondh, K. 2015. Ensemble Threshold Segmentation for hand detection. *Electrical Engineering/Electronics, Computer, Telecommunications and Information Technology*, 1-5.

Ruspini, E. H. 1969. A new approach to clustering. *Information and control*, 15 (1): 22-32.

Ruusuvuori, P., Lehmissola, A., Selinummi, J., Rajala, T., Huttunen, H. and Yli-Harja, O., 2008. Benchmark set of synthetic images for validating cell image analysis algorithms. *Signal Processing*, 1-5.

Sahoo, P. K., Soltani, S. and Wong, A. K. 1988. A survey of thresholding techniques. *Computer Vision, Graphics, and Image Processing*, 41(2): 233-260.

Sampat, M. P., Wang, Z., Gupta, S., Bovik, A. C. and Markey, M. K. 2009. Complex wavelet structural similarity: A new image similarity index. *IEEE Transactions on Image Processing*, 18 (11): 2385-2401.

Sathya, P. and Kayalvizhi, R. 2010. PSO-based Tsallis thresholding selection procedure for image segmentation. *International Journal of Computer Applications*, 5(4): 39-46.

Sathya, P. and Kayalvizhi, R. 2011. Modified bacterial foraging algorithm based multilevel thresholding for image segmentation. *Engineering Applications of Artificial Intelligence*, 24(4): 595-615.

Schikora, M. and Schikora, A. 2014. Image-based analysis to study plant infection with human pathogens. *Computational and structural biotechnology journal*, 12(20): 1-6.

Seghir, Z. A. and Hachouf, F. 2011. Edge-region information measure based on deformed and displaced pixel for image quality assessment. *Signal Processing: Image Communication*, 26(8): 534-549.

Seo, D., Hernández, D. C. and Jo, K.-H. 2015. Comparison of edge operators for detection of vanishing Points. *Computational Collective Intelligence*, 443-452.

Serapião, A. B., Corrêa, G. S., Gonçalves, F. B. and Carvalho, V. O. 2016. Combining K-Means and K-Harmonic with Fish School Search Algorithm for data clustering task on graphics processing units. *Applied Soft Computing*.

Setti, F., Conigliaro, D., Rota, P., Bassetti, C., Conci, N., Sebe, N. and Cristani, M., 2017. The S-Hock dataset: A new Benchmark for Spectator Crowd Analysis. *Computer Vision and Image Understanding*, 159, 47-58.

Sevara, C., Pregesbauer, M., Doneus, M., Verhoeven, G. and Trinks, I. 2016. Pixel versus object—A comparison of strategies for the semi-automated mapping of archaeological features using airborne laser scanning data. *Journal of Archaeological Science: Reports*, 5, 485-498.

Severino Jr, O. and Gonzaga, A. 2013. A new approach for color image segmentation based on color mixture. *Machine vision and applications*, 24(3): 607-618.

Sezgin, M. 2004. Survey over image thresholding techniques and quantitative performance evaluation. *Journal of Electronic Imaging*, 13(1): 146-168.

Sharma, G., Wu, W. and Dalal, E. N. 2005. The CIEDE2000 color-difference formula: implementation notes, supplementary test data, and mathematical observations. *Color Research & Application*, 30(1): 21-30.

Shaw, M.Q., Allebach, J.P. and Delp, E.J., 2015. Color difference weighted adaptive residual preprocessing using perceptual modeling for video compression. *Signal Processing: Image Communication*, 39, 355-368.

Shen, S., Sandham, W., Granat, M. and Sterr, A., 2005. MRI fuzzy segmentation of brain tissue using neighborhood attraction with neural-network optimization. *IEEE Transactions on Information Technology in Biomedicine*, 9(3): 459-467.

Shi, J. and Malik, J. 2000. Normalized cuts and image segmentation. *IEEE Transactions on Pattern Analysis and Machine Intelligence*, 22 (8): 888-905.

Shi, N. and Pan, J. 2016. An improved active contours model for image segmentation by level set method. *Optik-International Journal for Light and Electron Optics*, 127(3): 1037-1042.

Shi, X., Chen, Y., Fu, Y. Y. and Luo, J. H., 2009. Application of color difference meter in the quality inspection of food [J]. *Science and Technology of Food Industry*, 5, 117.

Shi, Y., 2010. Adaptive illumination correction considering ordinal characteristics. *Wireless Communications Networking and Mobile Computing*, 1-4.

Siddiqui, F. and Mat Isa, N. 2012. Optimized K-means (OKM) clustering algorithm for image segmentation. *Opto-Electronics Review*, 20 (3): 216-225.

Siddiqui, F. U. and Isa, N. A. M. 2011. Enhanced moving K-means (EMKM) algorithm for image segmentation. *IEEE Transactions on Consumer Electronics*, 57 (2): 833-841.

Skarbek, W., Koschan, A., Bericht, T. and Veröffentlichung, Z. 1994. Colour image segmentation-a survey, 1-81.

Smith, S. M. and Brady, J. M. 1997. SUSAN—a new approach to low level image processing. *International journal of computer vision*, 23(1): 45-78.

Smitha, P. and Junnarkar, A. A. 2013. Overview of colour image segmentation techniques. *International Journal of Advanced Research in Computer Science and Software Engineering*, 3(9).

Soundararajan, R. and Bovik, A. C. 2013. Video quality assessment by reduced reference spatio-temporal entropic differencing. *IEEE Transactions on Circuits and Systems for Video Technology*, 23(4): 684-694.

Stallkamp J, Schlipsing M, Salmen J, Igel C 2011. The German traffic sign recognition benchmark: A multi-class classification competition. *International Joint Conference on Neural Networks*, 1453–1460.

Steinhaus, H. 1956. Sur la division des corp materiels en parties. *Bull. Acad. Polon. Sci*, 1, 801-804.

Stetco, A., Zeng, X.-J. and Keane, J. 2015. Fuzzy C-means++: fuzzy C-means with effective seeding initialization. *Expert Systems with Applications*, 42(21): 7541-7548.

Storn, R. and Price, K. 1997. Differential evolution—a simple and efficient heuristic for global optimization over continuous spaces. *Journal of global optimization*, 11(4): 341-359.

Suganya, R. and Shanthi, R. 2012. Fuzzy C-Means Algorithm-A Review. *International Journal of Scientific and Research Publications*, 2(11): 1.

Sulaiman, S. N. and Isa, N. A. M. 2010. Adaptive fuzzy-K-means clustering algorithm for image segmentation. *IEEE Transactions on Consumer Electronics*, 56(4): 2661-2668.

Sumithra, R., Suhil, M. and Guru, D.S., 2015. Segmentation and classification of skin lesions for disease diagnosis. *Procedia Computer Science*, 45, 76-85.

Sun, G., Zhang, A., Yao, Y. and Wang, Z. 2016. A novel hybrid algorithm of gravitational search algorithm with genetic algorithm for multi-level thresholding. *Applied Soft Computing*, 46, 703-730

Sun, X., Young, J., Liu, J. H., Bachmeier, L., Somers, R. M., Chen, K. J. and Newman, D. 2016. Prediction of pork color attributes using computer vision system. *Meat science*, 113, 62-64.

Sural, S., Qian, G. and Pramanik, S., 2002. Segmentation and histogram generation using the HSV color space for image retrieval. *Image Processing*, 2, 589-592.

Szilágyi, L., Benyo, Z., Szilágyi, S. M. and Adam, H. 2003. MR brain image segmentation using an enhanced fuzzy c-means algorithm. *Medicine and Biology Society*, 724-726.

- Szilágyi, L., Szilágyi, S. M. and Benyó, Z. 2007. A modified FCM algorithm for fast segmentation of brain MR images. *Analysis and Design of Intelligent Systems using Soft Computing Techniques*, 119-127.
- Taherdangkoo, M., Bagheri, M. H., Yazdi, M. and Andriole, K. P. 2013. An effective method for segmentation of MR brain images using the ant colony optimization algorithm. *Journal of Digital Imaging*, 26(6): 1116-1123.
- Tan, K. S. and Isa, N. A. M. 2011. Color image segmentation using histogram thresholding–Fuzzy C-means hybrid approach. *Pattern Recognition*, 44(1): 1-15.
- Tan, K. S., Isa, N. A. M. and Lim, W. H. 2013. Color image segmentation using adaptive unsupervised clustering approach. *Applied Soft Computing*, 13(4): 2017-2036.
- Tan, K. S., Lim, W. H. and Isa, N. A. M. 2013. Novel initialization scheme for Fuzzy C-Means algorithm on color image segmentation. *Applied Soft Computing*, 13(4): 1832-1852.
- Tang, J. L., Chen, X. Q., Miao, R.-H. and Wang, D. 2016. Weed detection using image processing under different illumination for site-specific areas spraying. *Computers and Electronics in Agriculture*, 122, 103-111.
- Tang, K., Yuan, X., Sun, T., Yang, J. and Gao, S. 2011. An improved scheme for minimum cross entropy threshold selection based on genetic algorithm. *Knowledge-Based Systems*, 24(8): 1131-1138.
- Tao, W., Jin, H. and Zhang, Y. 2007. Color image segmentation based on mean shift and normalized cuts. *IEEE Transactions on Systems, Man, and Cybernetics, Part B: Cybernetics*, 37 (5): 1382-1389.
- Taubenböck, H., Wiesner, M., Felbier, A., Marconcini, M., Esch, T. and Dech, S. 2014. New dimensions of urban landscapes: The spatio-temporal evolution from a polynuclei area to a mega-region based on remote sensing data. *Applied Geography*, 47, 137-153.
- Thepade, S. D. and Bhondave, R. K. 2015. Multimodal identification technique using iris & palmprint traits with matching score level in various color Spaces with BTC of bit plane slices. *Industrial Instrumentation and Control*, 1469-1473.

Tian, J., Reinartz, P., d'Angelo, P. and Ehlers, M. 2013. Region-based automatic building and forest change detection on Cartosat-1 stereo imagery. *ISPRS Journal of Photogrammetry and Remote Sensing*, 79, 226-239.

Tillett, J., Rao, T., Sahin, F. and Rao, R. 2005. Darwinian particle swarm optimization. *International Conference on Artificial Intelligence*, <http://scholarworks.rit.edu/other/574>.

Tokmakov, P., Alahari, K. and Schmid, C., 2017. Learning Video Object Segmentation with Visual Memory. *arXiv preprint arXiv:1704.05737*.

Tripathy, B. and Mittal, D. 2016. Hadoop based uncertain possibilistic kernelized c-means algorithms for image segmentation and a comparative analysis. *Applied Soft Computing*, 46, 886-923.

Tsai, C. Y. and Liu, T.-Y. 2015. Real-time automatic multilevel color video thresholding using a novel class-variance criterion. *Machine Vision and Applications*, 26(2-3): 233-249.

Tsai, D. M. and Lin, C. C. 2011. Fuzzy C-means based clustering for linearly and nonlinearly separable data. *Pattern Recognition*, 44(8): 1750-1760.

Tuan, T. M. 2016. A cooperative semi-supervised fuzzy clustering framework for dental X-ray image segmentation. *Expert Systems with Applications*, 46, 380-393.

Tzortzis, G. and Likas, A. 2014. The MinMax k-Means clustering algorithm. *Pattern recognition*, 47(7): 2505-2516.

Uçar, A. 2014. Color face recognition based on steerable pyramid transform and extreme learning machines. *The Scientific World Journal*, 1-15.

Van Aken, J. R., 1984. An efficient ellipse-drawing algorithm. *Computer Graphics and Applications*, 4(9): 24-35.

Vojodi, H., Fakhari, A. and Moghadam, A. M. E. 2013. A new evaluation measure for color image segmentation based on genetic programming approach. *Image and Vision Computing*, 31(11): 877-886.

Wang, C.W., Huang, C.T., Lee, J.H., Li, C.H., Chang, S.W., Siao, M.J., Lai, T.M., Ibragimov, B., Vrtovec, T., Ronneberger, O. and Fischer, P., 2016. A benchmark for comparison of dental radiography analysis algorithms. *Medical image analysis*, 31, 63-76.

Wang, H. and Oliensis, J. 2010. Generalizing edge detection to contour detection for image segmentation. *Computer Vision and Image Understanding*, 114(7): 731-744.

Wang, H., Moss, R.H., Chen, X., Stanley, R.J., Stoecker, W.V., Celebi, M.E., Malters, J.M., Grichnik, J.M., Marghoob, A.A., Rabinovitz, H.S. and Menzies, S.W., 2011. Modified watershed technique and post-processing for segmentation of skin lesions in dermoscopy images. *Computerized Medical Imaging and Graphics*, 35(2): 116-120.

Wang, J., Deng, Z., Choi, K.-S., Jiang, Y., Luo, X., Chung, F. L. and Wang, S. 2016a. Distance metric learning for soft subspace clustering in composite kernel space. *Pattern recognition*, 52: 113-134.

Wang, J., Kong, J., Lu, Y., Qi, M. and Zhang, B. 2008. A modified FCM algorithm for MRI brain image segmentation using both local and non-local spatial constraints. *Computerized Medical Imaging and Graphics*, 32(8): 685-698.

Wang, Q., Chu, J., Xu, L. and Chen, Q. 2016b. A new blind image quality framework based on natural color statistic. *Neurocomputing*, 173, 1798-1810.

Wang, T., Sun, Q., Ji, Z., Chen, Q. and Fu, P. 2016c. Multi-layer graph constraints for interactive image segmentation via game theory. *Pattern Recognition*, 55, 28-44.

Wang, X. Y. and Bu, J. 2010. A fast and robust image segmentation using FCM with spatial information. *Digital Signal Processing*, 20(4): 1173-1182.

Wang, X. Y., Sun, W., Wu, Z. F., Yang, H. Y. and Wang, Q. Y. 2015. Color image segmentation using PDTDFB domain hidden Markov tree model. *Applied Soft Computing*, 29, 138-152.

Wang, X. Y., Wang, Q. Y., Yang, H. Y. and Bu, J. 2011. Color image segmentation using automatic pixel classification with support vector machine. *Neurocomputing*, 74(18): 3898-3911.

Wang, X. Y., Wu, Z. F., Chen, L., Zheng, H. L. and Yang, H. Y. 2016d. Pixel classification based color image segmentation using quaternion exponent moments. *Neural Networks*, 74, 1-13.

- Wang, X. Y., Wang, T. and Bu, J. 2011. Color image segmentation using pixel wise support vector machine classification. *Pattern Recognition*, 44(4): 777-787.
- Wang, Y. and Yuan, B. 2001. A novel approach for human face detection from color images under complex background. *Pattern Recognition*, 34(10): 1983-1992.
- Wang, Z. and Li, Q. 2011. Information content weighting for perceptual image quality assessment. *IEEE Transactions on Image Processing*, 20(5): 1185-1198.
- Wang, Z., Bovik, A. C., Sheikh, H. R. and Simoncelli, E. P. 2004. Image quality assessment: from error visibility to structural similarity. *IEEE Transactions on Image Processing*, 13(4): 600-612.
- Wang, Z., Simoncelli, E. P. and Bovik, A. C. 2003. Multiscale structural similarity for image quality assessment. *Signals, Systems and Computers*, 1398-1402.
- Welch, E., Moorhead, R. and Owens, J. 1991. Image processing using the HSI color space. *IEEE Proceedings of Southeastcon'91*, 722-725.
- Wighton, P., Lee, T. K., Lui, H., McLean, D. I. and Atkins, M. S. 2011. Generalizing common tasks in automated skin lesion diagnosis. *IEEE Transactions on Information Technology in Biomedicine*, 15(4): 622-629.
- Wu, J., Lin, W. and Shi, G. 2014. Image quality assessment with degradation on spatial structure. *IEEE Signal Processing Letters*, 21(4): 437-440.
- Wu, Y., Liang, J., Yin, J. and Nie, J. 2016. Extraction of golden area in image based on region growing. *Advanced Graphic Communications, Packaging Technology and Materials*, 295-302.
- Xie, F. and Bovik, A. C. 2013. Automatic segmentation of dermoscopy images using self-generating neural networks seeded by genetic algorithm. *Pattern Recognition*, 46(3): 1012-1019.
- Xu, X., Xu, S., Jin, L. and Song, E. 2011. Characteristic analysis of Otsu threshold and its applications. *Pattern Recognition Letters*, 32(7): 956-961.
- Xue, H., Géraud, T. and Lutz, A. D., 2003. Multiband segmentation using morphological clustering and fusion application to color image segmentation. *Image Processing*, 1, 353-356.

- Yang, C. C. and Kwok, S. H. 2003. Efficient gamut clipping for color image processing using LHS and YIQ. *Optical engineering*, 42(3): 701-711.
- Yang, C., Ji, J., Liu, J., Liu, J. and Yin, B. 2016. Structural learning of Bayesian networks by bacterial foraging optimization. *International Journal of Approximate Reasoning*, 69, 147-167.
- Yang, J., Liu, C. and Zhang, L. 2010. Color space normalization: enhancing the discriminating power of color spaces for face recognition. *Pattern Recognition*, 43(4): 1454-1466.
- Yang, W., Li, D., Wang, S., Lu, S. and Yang, J. 2013. Saliency-based colour image segmentation in foreign fiber detection. *Mathematical and Computer Modelling*, 58(3): 852-858.
- Yang, X. S. 2010. A new metaheuristic bat-inspired algorithm. *Nature Inspired Cooperative Strategies for Optimization*, 284, 65-74.
- Ye, Z. W., Wang, M. W., Liu, W. and Chen, S. B. 2015. Fuzzy entropy based optimal thresholding using bat algorithm. *Applied Soft Computing*, 31, 381-395
- Ye, Z., Zheng, Z., Yu, X. and Ning, X. 2005. Automatic threshold selection based on ant colony optimization algorithm. *Neural Networks and Brain*. 728-732.
- Yu, M., Zheng, K., Jiang, G., Shao, F. and Peng, Z. 2016. Binocular perception based reduced-reference stereo video quality assessment method. *Journal of Visual Communication and Image Representation*, 38, 246-255.
- Yu, Z., Au, O. C., Zou, R., Yu, W. and Tian, J. 2010. An adaptive unsupervised approach toward pixel clustering and color image segmentation. *Pattern recognition*, 43(5): 1889-1906.
- Yuan, F., Meng, Z. H., Zhang, H. X. and Dong, C. R. 2004. A new algorithm to get the initial centroids. *Machine Learning and Cybernetics*, 1191-1193.
- Zadeh, L. A. 1965. Fuzzy sets. *Information and Control*, 8(3): 338-353.
- Zahara, E., Fan, S. K. S. and Tsai, D. M. 2005. Optimal multi-thresholding using a hybrid optimization approach. *Pattern Recognition Letters*, 26(8): 1082-1095.

- Zhang, B., Hsu, M. and Dayal, U. 1999. K-harmonic means-a data clustering algorithm. *Hewlett-Packard Labs Technical Report HPL-1999-124*,
- Zhang, C. and Wang, P. 2000. A new method of color image segmentation based on intensity and hue clustering. *Pattern Recognition*, 613-616.
- Zhang, C., Pan, J., Chen, S., Wang, T. and Sun, D. 2016. No reference image quality assessment using sparse feature representation in two dimensions spatial correlation. *Neurocomputing*, 173, 462-470.
- Zhang, C., Xiao, X., Li, X., Chen, Y. J., Zhen, W., Chang, J., Zheng, C. and Liu, Z. 2014a. White blood cell segmentation by color-space-based K-Means clustering. *Sensors*, 14(9): 16128-16147.
- Zhang, H., Fritts, J. E. and Goldman, S. A. 2008. Image segmentation evaluation: A survey of unsupervised methods. *Computer Vision and Image Understanding*, 110(2): 260-280.
- Zhang, J., Li, H., Tang, Z., Lu, Q., Zheng, X. and Zhou, J. 2014b. An improved quantum-inspired genetic algorithm for image multilevel thresholding segmentation. *Mathematical Problems in Engineering*, 1-12.
- Zhang, L., Zhang, L., Mou, X. and Zhang, D. 2011. FSIM: a feature similarity index for image quality assessment., *IEEE Transactions of Image Processing* , 20(8): 2378-2386.
- Zhang, X., Wang, S., Gu, K., Jiang, T., Ma, S. and Gao, W. 2015. Sparse structural similarity for objective image quality assessment. *Systems, Man and Cybernetics*, 1561-1566.
- Zhang, Y. and Wu, L. 2011. Fast document image binarization based on an improved adaptive Otsu's method and destination word accumulation. *Journal of Computational Information Systems*, 7(6): 1886-1892.
- Zhang, Y. J. 2006. An overview of image and video segmentation in the last 40 years. *Advances in Image and Video Segmentation*, 1-15.
- Zhao, F., Jiao, L. and Liu, H. 2013. Kernel generalized fuzzy c-means clustering with spatial information for image segmentation. *Digital Signal Processing*, 23(1): 184-199.
- Zhao, F., Jiao, L., Liu, H. and Gao, X. 2011. A novel fuzzy clustering algorithm with non local adaptive spatial constraint for image segmentation. *Signal Processing*, 91(4): 988-999.

Zhao, X., Li, Y. and Zhao, Q. 2015. Mahalanobis distance based on fuzzy clustering algorithm for image segmentation. *Digital Signal Processing*, 43, 8-16.

Zheng, J. and Hryciw, R. D. 2016. Segmentation of contacting soil particles in images by modified watershed analysis. *Computers and Geotechnics*, 73, 142-152.

Zhu, G. and Kwong, S. 2010. Gbest-guided artificial bee colony algorithm for numerical function optimization. *Applied Mathematics and Computation*, 217(7): 3166-3173.

Zortea, M., Flores, E. and Scharcanski, J., 2017. A simple weighted thresholding method for the segmentation of pigmented skin lesions in macroscopic images. *Pattern Recognition*, 64, 92-104.

Zuva, T., Olugbara, O. O., Ojo, S. O. and Ngwira, S. M. 2011. Image segmentation, available techniques, developments and open issues. *Image Processing and Computer Vision*, 2(3): 20-29.